SSC-122

BEHAVIOR OF RIVETED AND WELDED CRACK ARRESTORS

by

R. J. Mosborg

SHIP STRUCTURE COMMITTEE

SHIP STRUCTURE COMMITTEE

MEMBER AGENCIES:

BUREAU OF SHIPS, DEPT. OF NAVY
MILITARY SEA TRANSPORTATION SERVICE, DEPT. OF NAVY
UNITED STATES COAST GUARD, TREASURY DEPT.
MARITIME ADMINISTRATION, DEPT. OF COMMERCE
AMERICAN BUREAU OF SHIPPING

ADDRESS CORRESPONDENCE TO:

SECRETARY
SHIP STRUCTURE COMMITTEE
U. S. COAST GUARD HEADQUARTERS
WASHINGTON 25, D. C.

August 31, 1960

Dear Sir:

As part of its program related to the improvement of hull structures of ships, the Ship Structure Committee has sponsored a study of crack arrestors at the University of Illinois. Herewith is a copy of this project's Final Report, SSC-122, Behavior of Riveted and Welded Crack Arrestors, by R. J. Mosborg.

This project has been conducted under the advisory guidance of the Ship Structure Subcommittee.

This report is being distributed to individuals and groups associated with or interested in the work of the Ship Structure Committee. Comments concerning this report are solicited.

Sincerely yours,

E. H. Thiele
Rear Admiral, U. S. Coast Guard
Chairman, Ship Structure Committee

Serial No. SSC-122

Final Report
of
Project SR-134

to the

SHIP STRUCTURE COMMITTEE

on

BEHAVIOR OF RIVETED AND WELDED CRACK ARRESTORS

by

R. J. Mosborg

University of Illinois
Urbana, Illinois

under

Department of the Navy
Bureau of Ships Contract NObs-65789
BuShips Index No. NS-021-201

Washington, D. C.
National Academy of Sciences-National Research Council
August 31, 1960

ABSTRACT

This report describes the laboratory work undertaken 1) to investigate the feasibility of developing a welded crack arrestor and 2) to observe the behavior of various crack arresting devices. The study was accomplished by propagating a brittle crack, initiated by driving a wedge into a notch at the edge of the specimen, into 2-ft and 6-ft wide steel plates containing either (a) welded inserts of T-1 steel (b) riveted doubler plates or (c) welded inserts of ABS Class C normalized steel, which were located at various distances from the edge of the plate. Most of the tests were conducted at nominal stresses between 20 and 30 ksi and at temperatures between -25 and 40 F. Some of the specimens were instrumented with strain gages to provide information on crack speed and strain pattern.

The progress of the crack and the extent of its penetration in the T-1 steel insert depended primarily on the severity of the resulting eccentric load and the width of the arrestor material. Strain gage measurements indicated that the average speed of brittle crack propagation was generally between 2800 and 3800 fps and that little change occurred in the strain across the uncracked portion of the plate beyond the localized influence of the crack front.

A riveted doubler plate was shown to be an excellent form of arrestor if the discontinuity produced by the slot in the main plate beneath was present. However, the rivet holes did not necessarily attract propagating cracks.

In tests of specimens with ABS Class C normalized steel as the arrestor material, a brittle crack which had propagated 12 in. was either completely accepted or refused by the strake of killed and normalized steel; this transition in behavior occurred between 10 and 35 F.

Drop-weight and explosion-bulge test results plus data from various Charpy V-notch criteria (absorbed energy, per cent shear, lateral expansion) are compared with the results from the large-scale tests of crack-arrestor specimens.

CONTENTS

SR-134 PROJECT ADVISORY COMMITTEE

"Crack Arrestors"

for the

SHIP STRUCTURE SUBCOMMITTEE

Chairman:

J. B. Robertson, Jr.
Office of Merchant Marine Safety
U. S. Coast Guard Headquarters

Members:

D. B. Bannerman, Jr.
Chief Surveyor - Hull
American Bureau of Shipping

T. J. Griffin
Head, Metals Fabrication Branch
Bureau of Ships

A. M. Johnson
Bureau of Ships

R. W. Vanderbeck
Applied Research Laboratory
U. S. Steel Corporation

Edward Wenk, Jr.
Legislative Reference
Library of Congress

INTRODUCTION

General

Although we now know that brittle failures may occur in structures such as pipelines, storage tanks, and bridges, this phenomenon in normally ductile steels was not fully appreciated until the outbreak of brittle failures in many of our welded merchant ships during and after World War II. An immediate study of the problem revealed that the initiation of some of these brittle failures was a result of poorly chosen design and fabrication details. A review of these brittle failures also showed that ships with riveted shell seams suffered fewer failures and that in many instances propagating cracks were stopped by the discontinuity introduced by the riveted sections. Therefore, welded ships were required to have riveted crack arrestors in areas where cracks were likely to develop.

Subsequently, extensive research on the problem of brittle fracture has demonstrated that proper consideration for materials, geometry, and fabrication techniques can reduce the probability of brittle fracture. However, brittle fractures are potentially dangerous and catastrophic, and the adequate protection of a structure against severe failure is necessary. Until a thorough understanding of the mechanics of brittle fracture is available, a system that can effectively restrict a propagating crack to a partial fracture in a structure is a requirement.

Object and Scope

Although the above-mentioned riveted crack arrestors proved to be effective in preventing a complete failure in many of the cases where a crack developed,[1] the elimination of riveting as a means of fabricating crack arrestors was considered desirable since it could simplify shipyard organization and, in the case of tankers, could also simplify maintenance.[2] Hence, the concept of halting a brittle fracture with a strake of notch-tough steel welded between strakes of standard structural steel was conceived.

This report describes a laboratory investigation of crack-arresting devices that was conducted during the period from July 1954 to September 1958.

The objectives of the program were to investigate the feasibility of developing a welded crack arrestor and to observe the behavior of various possible crack-arresting devices.

The initial phase of this program consisted of development work and was a joint effort with a related program concerned with Brittle-Fracture Mechanics (Ship Structure Committee Project SR-137). The development work that relates to the Crack-Arrestor Program is summarized briefly below.

When a reliable test procedure had been developed, tests of relatively small-scale (3/4 in. thick by 2-ft wide by 6 ft long), rimmed-steel specimens were conducted as part of Project SR-137. These plain plate tests provided information on the conditions necessary to initiate a brittle crack and on the behavior of material during brittle-fracture propagation in the type of laboratory specimen under consideration.

In the Arrestor Program, a few tests were first conducted on 2-ft wide, rimmed-steel, crack-arrestor specimens containing a doubler plate. However, this specimen detail was abandoned in favor of one in which a strake of tough steel was butt-welded in the same plane as the other strakes making up the specimen so that the undesirable doubler plate and main-plate slot were eliminated.

Preliminary studies (Tests 1-3) were conducted on 3/4-in. thick by 2-ft wide specimens containing a strake of notch-tough steel. The results of this series were encouraging and warranted the extension of this work to 3/4-in. thick by 6-ft wide specimens, since it was felt that specimens of this larger size would relate more readily to service conditions.

Tests 4-18 comprise the first series of large-scale (3/4 in. thick by 6-ft wide by about 18-ft long) welded arrestor specimens. These specimens consisted of long pull-plates welded to an insert that contained a heat-treated, high-strength steel (USS T-1 Steel--designated as T-steel hereafter) as the arrestor material. Brittle cracks were permitted to propagate as far as 4 ft before encountering the strake of tough steel. The influence of various widths of T-steel (4--36 in.), as well as that of an E12015 butt weld alone, on a propa-

gating crack was observed at temperatures ranging from -54 to 8 F and at average stresses from 25 to 33 ksi. All of the specimens in this series were instrumented with crack speed detectors and/or strain gages to provide information on the speed of propagating cracks and on the strain pattern in the vicinity of the running crack as well as in the arrestor material beyond the end of the crack.

In order to provide a basis of comparison between the welded and riveted arrestor specimens, a few 6-ft wide plates were fitted with doubler plates riveted to one side. The riveted arrestor specimens were fabricated by a qualified ship builder according to a detail that had been widely used in service. Instrumented with strain gages and/or crack speed detectors, these specimens provided laboratory test data on a riveted arrestor detail that had proved satisfactory under service conditions. Tests (19-23) of these specimens were conducted at temperatures ranging from -20 to 1 F at a stress of 26.8 ksi.

The other steel whose crack-arresting behavior was observed in 6-ft wide welded arrestor specimens was a fully killed and normalized ABS Class C Steel (designated as C-steel hereafter). The arresting ability of this steel in widths of 6, 18 and 60 in. was investigated under the influence of a 1-ft long crack in Tests 24-45, where the average stress was generally 20.0 or 28.0 ksi and most testing temperatures were in the 10 to 39 F range. In addition, the results from these tests of 6-ft wide crack-arrestor specimens were compared with various criteria obtained from tests of Charpy V-notch specimens and also with results from drop-weight and explosion-bulge tests.

Brief Reference to Published Work

Following the numerous merchant-ship failures in the early 1940's, research programs were initiated to study various phases of the brittle-fracture problem. Some of the earliest tests on wide-plate specimens were conducted in 1944-46 by Wilson, Hechtman, and Bruckner[3] and involved static tests of internally notched steel plates of various widths. In 1953, the Standard Oil Company undertook an extensive brittle fracture test program on steel plates from 10 to 72 in. wide where the effects of temperature, stress, material, impact, and specimen geometry were studied.[4] Other experimental

and analytical work in the brittle-fracture field has been reported by E. Orowan,[5] G. R. Irwin,[6] A. A. Wells,[7] and T. S. Robertson.[8] These references comprise only a small part of the available literature in the brittle-fracture field; other important work may be found in the extensive bibliographies of the references cited.

On work dealing with the arrest of propagating brittle cracks, however, only two references were found. Hunter's work[9] was on rather small specimens, but it indicated the possibility of arresting brittle cracks by introducing a narrow strip of Austerritic Stainless Steel. Wells, Lane, and Coates[10] investigated, in a limited number of tests, the crack arresting ability of 36-in. wide specimens containing riveted straps and welded notch-tough steel arrestors. These tests are those most closely related to the program described here.

The service performance of World War II ship plates has already been analyzed and related to Charpy V-notch test data. In addition, these results have been compared with the findings from other tests that have been subsequently investigated as a possible indicator of the tendency for brittle fracture.[11—13]

The development work and preliminary tests, as well as some of the 6-ft wide plate tests conducted under Project SR-137 have been previously reported.[14—16] Some of this work was a joint effort of Projects SR-134 and SR-137. A summary of some of the work on the Crack-Arrestor Program has already been presented.[17] In addition, studies of the energy-absorption capacity of some of the welds used in the crack-arrestor specimens have been published.[18]

Acknowledgment

The work described here, sponsored by the Ship Structure Committee, was conducted in the Structural Research Laboratory of the Department of Civil Engineering, University of Illinois. The members of the Crack Arrestor Advisory Committee of the Ship Structure Subcommittee have acted in an advisory capacity in the planning of this program.

The project was under the general direction of N. M. Newmark,

Professor and Head of the Department of Civil Engineering, and under the immediate supervision of R. J. Mosborg, Associate Professor of Civil Engineering. The author wishes to thank W. H. Munse, Research Professor of Civil Engineering, W. J. Hall, Associate Professor of Civil Engineering (supervisor of Project SR-137, "Brittle Fracture Mechanics") and V. J. McDonald, Research Associate Professor of Civil Engineering (in charge of instrumentation) for their helpful advice. The writer also wishes to acknowledge the valuable assistance of K. Hayashi, T. J. Hall, J. N. Chopy, W. H. Walker, J. N. Kirk, and H. A. R. de Paiva, Research Assistants in Civil Engineering, who carried on various phases of the program.[19—22]

The large riveted arrestor specimens were fabricated through the courtesy of Manitowoc Shipbuilding, Incorporated. The drop-weight tests were conducted by the United States Steel Corporation and the explosion-bulge tests by the Naval Research Laboratory.

Nomenclature

The following terms are commonly used throughout the text:

Dynamic Strain Gage--An SR-4 strain gage whose signal is monitored on an oscilloscope during the fracture test.

Static Strain Gage--An SR-4 strain gage read at specified loads by means of a portable strain indicator.

Crack Detector--A device (in most cases, a single wire, SR-4 Type A-9 strain gage with a 6-in. gage length) that is mounted on the plate surface perpendicular to the expected crack path and breaks as the crack passes, thus interrupting an electrical circuit.

Starter Material--A steel which readily initiates and propagates a brittle crack under selected laboratory conditions of stress, temperature, and lateral impact.

Arrestor Material--A strake of steel that possesses improved strength and ductility properties and is used to arrest a propagating brittle crack.

Notch Line--An imaginary horizontal line connecting the notches on opposite edges of the specimen insert.

Submerged Crack--A relatively short, arrested crack that does not cleave through the plate surface and is characterized by a clearly defined depression of the plate surface.

INITIAL DEVELOPMENT WORK

General Description of Testing Apparatus, Equipment, and Specimens

The initial development work on this program was a joint effort with a companion program on Brittle Fracture Mechanics (SR-137) and included the consideration of (a) a dependable method of crack initiation, (b) a means of cooling the test specimen satisfactorily with dry ice, (c) instrumentation techniques, and (d) a suitable specimen geometry. A detailed explanation (including complete figures, drawings, and photographs) of the initial development work associated with these various items has been given previously,[14] and therefore, only a brief summary of this work will be given here.

The initial development work was performed with flat-plate specimens 3/4 in. thick by 2 ft wide by 6 ft long (clear distance between pull heads). In general, these specimens were made from rimmed E-steel (Lukens Heat No. 20279). The check analysis and mechanical properties of this steel are presented in Fig. 1.

The method of fracture initiation that was finally developed and used throughout this program (hereafter referred to as the notch-wedge-impact method) employs a gas-operated piston device to drive a wedge into a prepared saw-cut notch at the edge of a plate specimen. The pressure of the gas (bottled commercial nitrogen) and the stroke of the piston can be varied so that a theoretical external impact up to 3000 ft-lb can be provided by the piston device.

The reaction that occurs during acceleration of the piston is absorbed by a weight (approximately 120 lb) which bears against the far edge of the specimen and is tied to the piston device. The impact device and the reac-

TENSILE TEST DATA

DIRECTION OF ROLLING	YIELD STRENGTH KSI	ULTIMATE STRENGTH KSI	ELONGATION IN 2 IN %	REDUCTION OF AREA %
PARALLEL	34.7	68.1	36	58
NORMAL	35.2	68.7	31	52

CHECK ANALYSIS

C	Mn	P	S	Si	Cu	Cr	Ni	Al
0.18	0.42	0.013	0.031	0.02	0.23	0.07	0.14	0.003

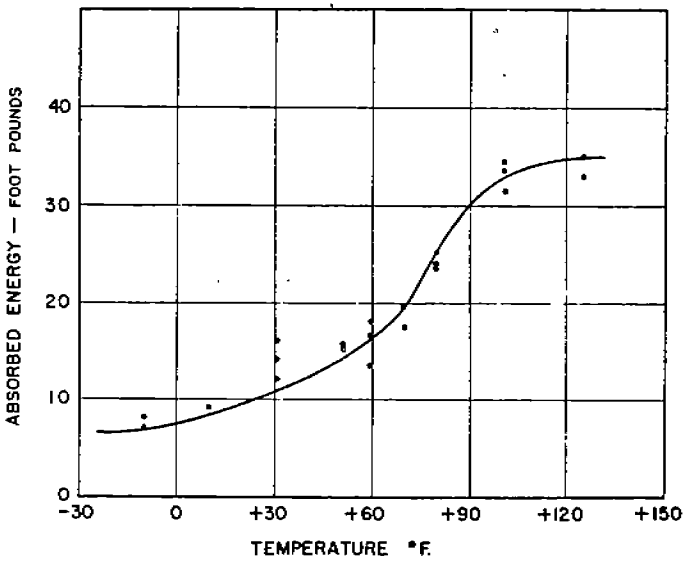

CHARPY V-NOTCH IMPACT RESULTS

(a) Z - STEEL, HEAT NO. 16 445

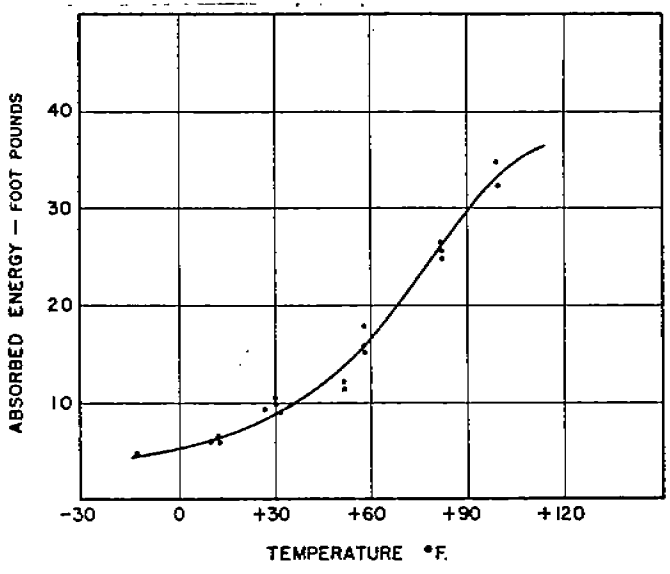

CHARPY V-NOTCH IMPACT RESULTS

CHECK ANALYSIS

C	Mn	P	S	Si	Cu	Cr	Ni	Al
0.21	0.34	0.019	0.030	0.01	0.18	0.12	0.19	0.003

TENSILE TEST DATA

DIRECTION OF ROLLING	YIELD STRENGTH KSI	ULTIMATE STRENGTH KSI	ELONGATION IN 2 IN. %	REDUCTION OF AREA %
PARALLEL	32.1	64.9	36	57
NORMAL	31.8	64.4	31	54

(b) E - STEEL, HEAT NO. 20279

Fig. 1. Properties of Lukens Rimmed Steels.

tion weight are supported from the top pull-plate and thus are semi-isolated from the specimen.

The cooling agent for these tests and all subsequent tests in this program was crushed dry ice. In these development tests, the dry ice was placed in trays hung on each side of the specimen and the specimen was then wrapped with insulating material and cloth.

Plain Plate Tests

From the initial development tests on 2-ft wide plain plate specimens made of E-steel,[14] a theoretical lateral impact of 1200 ft-lb was found to be sufficient to produce (with the notch-wedge-impact method) brittle fracture for the type of specimen, material, and test conditions under consideration. It was found that with this impact a brittle crack could be initiated and propagated across a plain-plate specimen of E-steel under an average stress on the net section of 15.0 ksi at an average temperature of 0°F, or under an average stress of 16.5 ksi at an average temperature of 30 F.

Subsequently, preliminary tests were carried out on plain plates of Lukens rimmed Z-steel (see Fig. 1 for check analysis and mechanical properties). With a lateral impact of 1200 ft-lb, a brittle crack was consistently initiated and propagated across specimens of this steel under an average stress of 18.0 ksi at an average temperature of 0°F.[14]

2-Ft Wide Doubler-Type Specimens

After the initial development tests on 2-ft wide plain plate specimens had determined the proper combination of average stress, average temperature, and lateral impact to consistently initiate and propagate brittle fracture in the materials available, this program was directed toward the consideration of suitable crack-arrestor specimens.

The first type of 2-ft wide welded arrestor specimen considered was an imitation of the conventional riveted doubler-type crack arrestor and consisted of a 3/4-in. by 18-in by 24-in. slotted E-steel insert plate with a single doubler plate of varying size and mode of attachment placed over the slot. Detailed drawings of the four specimens in this series, Specimens E-5, E-6, E-7 and E-8,

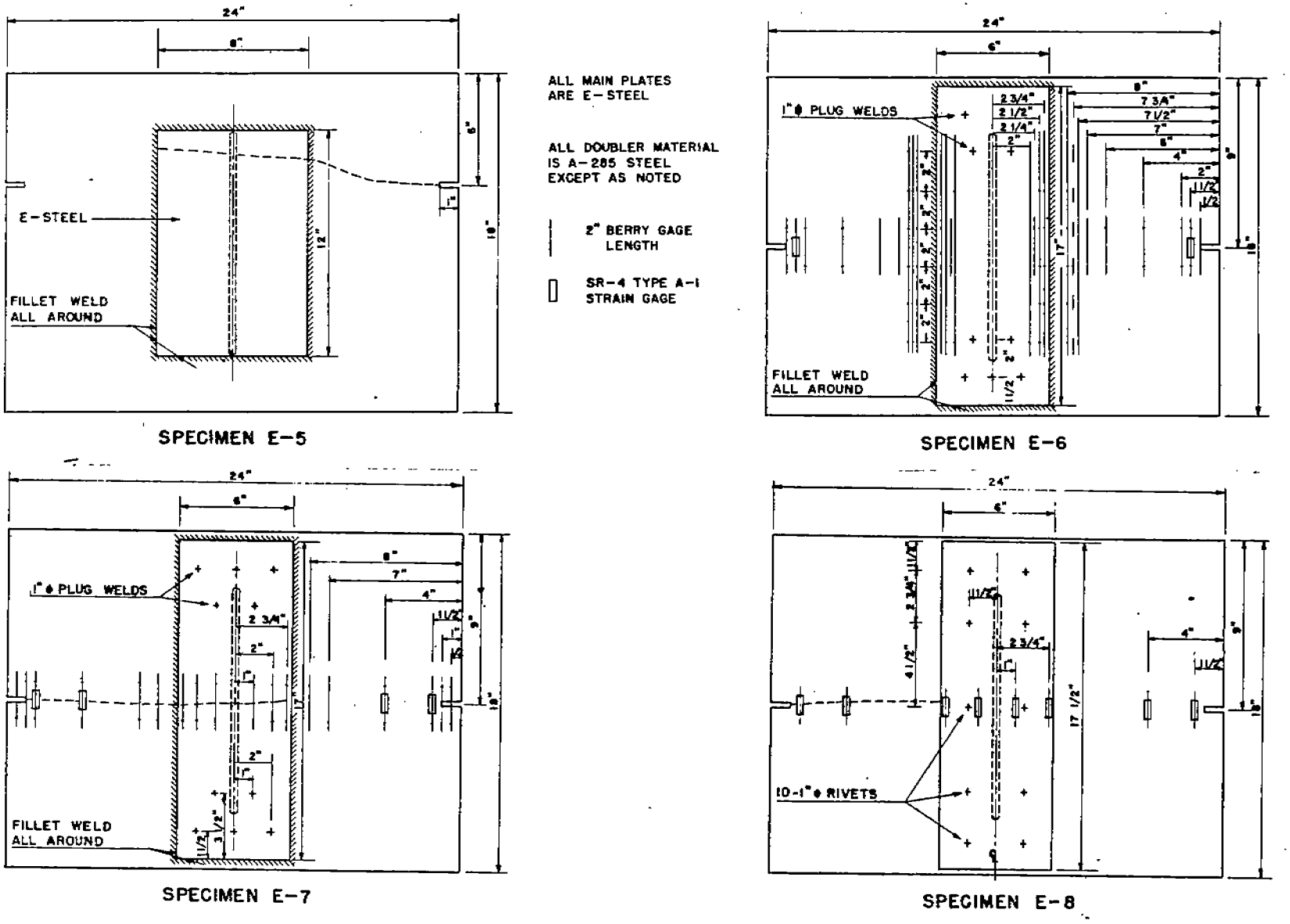

Fig. 2. Details of Two-Foot Wide Doubler Type Specimen, E-5, E-6, E-7, and E-8.

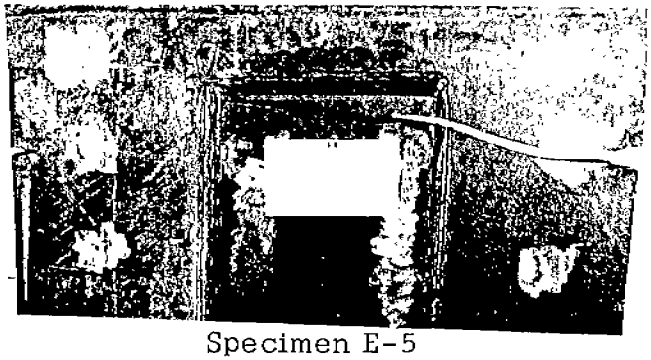

Specimen E-5

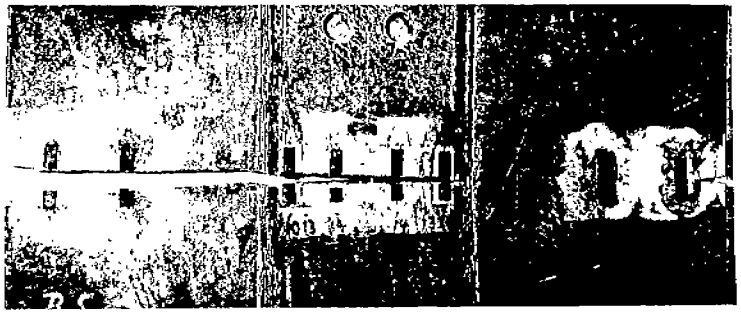

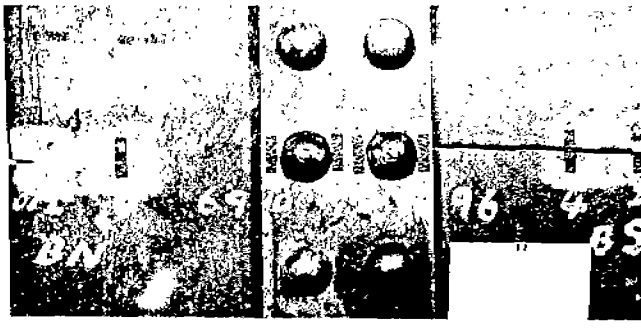

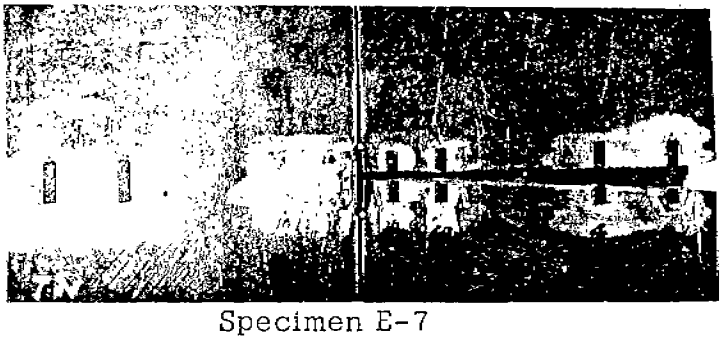

Specimen E-7

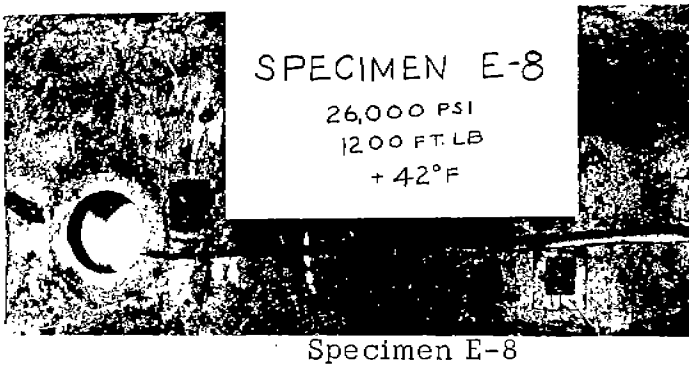

Specimen E-8

Fig. 3. Fracture Paths for Specimens E-5, E-7, and E-8.

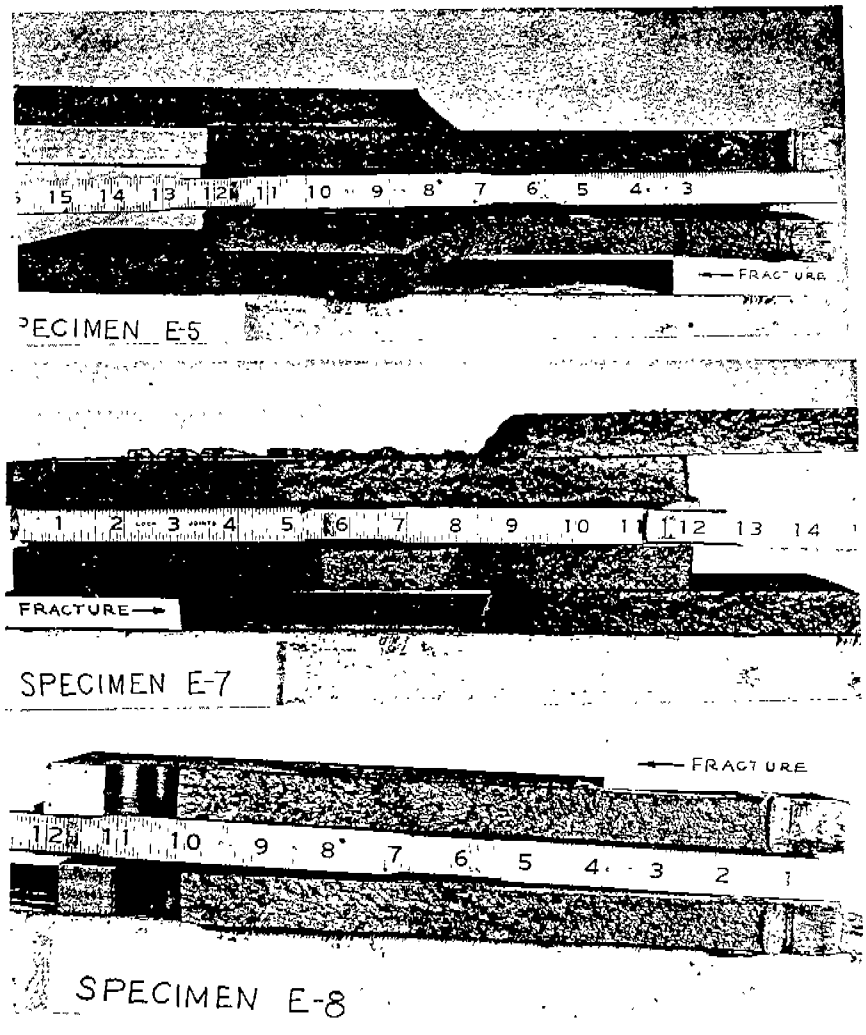

Specimen E-5

Specimen E-7

Specimen E-8

Fig. 4. Fracture Surfaces for Specimens E-5, E-7, and E-8.

are shown in Fig. 2, and the sequence of tests on each of these specimens is summarized in Table 1.

In the fabrication of the first specimen, E-5, the 3/4-in. by 12-in. by 8-in. E-steel doubler plate was fillet-welded to the insert plate at each end and then along both sides. As shown in Table 1, by applying a second impact at each notch, four attempts (each with a somewhat higher stress) were made to fracture this specimen. An average effective stress of 22.5 ksi and a temperature of 24 F (combined with a 1200 ft-lb impact) were required to initiate and propagate a brittle fracture in this specimen. The crack propagated to the central slot in the main plate and, at the same time, through the fillet weld and almost completely across the attached doubler, as shown in Fig. 3. The fractured surface of this specimen can be seen in Fig. 4.

TABLE 1

SUMMARY OF TESTS ON 2-FT WIDE WELDED DOUBLER-TYPE ARRESTOR SPECIMENS

Specimen Designation	Doubler-Plate Description	Impact Location	Avg. Stress on Net Section (ksi)	Avg. Temp. (°F)	Remarks
These tests were conducted on 2-ft wide specimens in a 600,000 lb screw-type testing machine. The test specimen is a 3/4 x 18 x 24 in. E steel insert plate (containing a 12-in. long vertical slot at the center) with a doubler plate of varying size and mode of attachment placed over the slot. The insert is welded to 3/4 in. pull-plates, using double "V" butt welds - E7016 electrodes, to provide a test piece 2-ft wide x 6 ft long. The notch used consists of a slot which is four hacksaw blades wide (approx. 0.141 in.) for the first 7/8 in., one hacksaw blade wide (approx. 0.034 in.) for the next 1/16 in., and one jeweler's-saw cut wide (approx. 0.012 in.) for the remaining 1/16 in. Two notches are cut, one at each edge of the specimen, and are referred to in the following table as notch 1 or notch 2. Theoretical lateral impact from the gas-operated piston device was 1?00 ft-lb. Repetition of the notch number in the column headed "Impact Location" signifies a second impact on that notch.					
E-5	3/4 x 12 x 8 in. E steel doubler with fillet welds all around.	1	15.0	17	No initiation.
		2	16.5	20	No initiation.
		2	18.0	20	Slight submerged crack.
		1	22.5	24	Crack propagated to slot in main plate and to far side of doubler.
E-6	3/4 x 17 x 6 in. A-285 steel doubler with five 1-in. dia. plug welds top and bottom and fillet welds all around.	1	18.3	20	No initiation.
		1	20.6	20	3 in. submerged crack.
		2	20.6	27	No initiation.
		2	20.6	27	No initiation.
E-7*	3/4 x 17 x 6 in. A-285 steel doubler with five 1-in. dia. plug welds top and bottom and fillet welds all around.	1	21.0	24	1 in. submerged crack.
		2	26.0	29	Crack propagated to slot in main plate and to far side of doubler.
E-8	3/4 x 17 x 6 in. A-285 steel doubler with ten 1-in. dia. button head rivets.	1	20.0	35	3 1/2 in. submerged crack.
		1	26.0	42	Crack propagated to first rivet line in main plate.

*Mechanically stress relieved to 20.0 ksi.

The stress of 22.5 ksi required to initiate and propagate a brittle crack in this specimen was considerably more than the stress required to break a plain plate specimen of the same material (E-steel), indicating the possible development of unfavorable residual strains in the specimen during the welding of the doubler plate to the main plate.

From a very limited number of Berry gage readings on Specimen E-5, it was apparent that the strain in the doubler plate was substantially less than that in the main insert plate. A method of developing greater strain in the doubler plate was needed, and it seemed that the participation of the doubler plate might be improved by making it longer and plug-welding it at both ends to the main insert plate. This would provide more opportunity for the doubler to pick up load.

In view of the previous comments on Specimen E-5, Specimen E-6 was fabricated with a longer doubler plate which contained five plug welds at each end. In addition, several 2-in. Berry gage holes and four SR-4, Type A-1 strain gages were located on the specimen as shown in Fig. 2. These strain measurements provided information on both the residual strains across the specimen resulting from welding and on the strain history at a point 1/2 in. from the base of the notch as the series of tests on this specimen progressed.

These strain data are presented in Fig. 5 for Specimen E-6 and indicate that compressive residual strains of almost yield point magnitude were present in the region at the end of the notch. As a result, strain in this region remained compressive with respect to the original zero reading until considerable load was applied to the specimen or until a lateral impact (which, although unsuccessful in initiating a brittle crack, could result in substantial plastic deformation) was applied to the notch. This compressive strain would help to explain why the applied stress required to initiate and propagate a brittle crack in this type of specimen was considerably higher than that needed in a plain plate specimen of the same material.

In general, the mechanical strain gage readings, measured with a 2-in. Berry gage across a transverse section on both sides of the specimen, showed

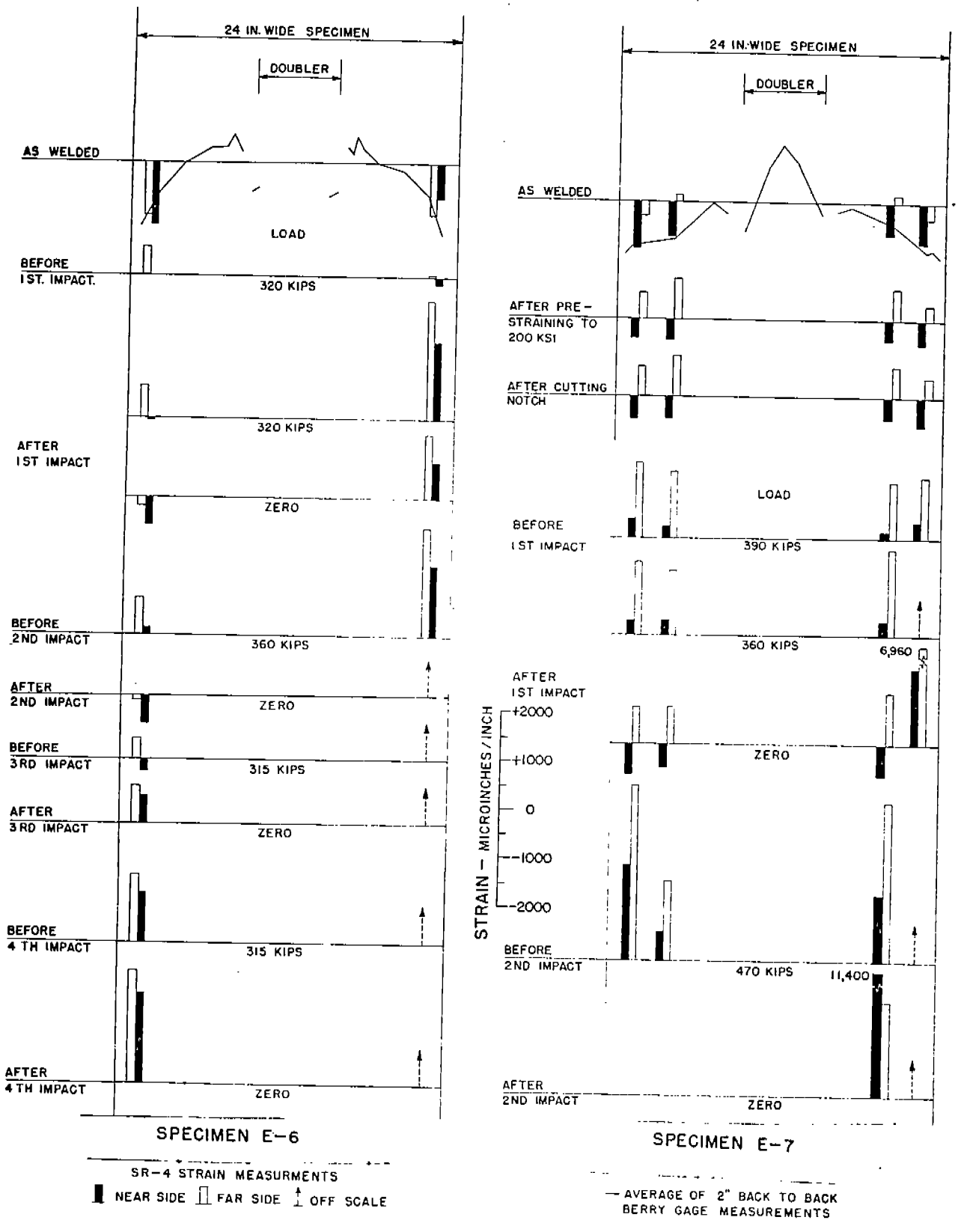

Fig. 5. Strain Variation during Successive Impacts--Specimens E-6 and E-7.

for each pair of back-to-back strain readings that the strain on the side opposite the doubler was usually larger (tension-positive and compression-negative). The residual strains on the side of the insert on which the doubler was welded were primarily compressive, whereas the residual strains on the opposite side of the insert were usually tensile. These strains are consistent with what might be expected as the weld metal connecting the doubler plate to one side of the insert plate cools and shrinks.

The 2-in. Berry gage readings that were taken along a vertical line adjacent to the 3/4-in. fillet-weld on both the insert plate and the doubler plate did not indicate any consistent pattern. In a transverse direction, the strain in the doubler plate was approximately one-fourth of that developed in the main insert plate of this specimen. As shown in Table 1, four tests were conducted on Specimen E-6 and no brittle fracture was obtained under the conditions selected.

The dimensions of Specimen E-7 were exactly the same as those of Specimen E-6 except that a much heavier end-fillet-weld was made to improve the end connection of the doubler plate to the insert plate. Because of the high compressive residual strains developed near the end of the notch of Specimen E-6, modifications in the fabrication procedure of Specimen E-7 were made also. In welding the doubler to the main plate, the longitudinal fillet-welds were back-stepped from the center and gradually built up so as to introduce a minimum amount of residual strain in the specimen. In addition, the specimen was preloaded to an average effective stress of 20.0 ksi before the edge notches were cut.

Strain measurements were made at the locations shown in Fig. 2 with SR-4, Type A-1 strain gages and a 2-in. Berry gage during the fabrication and testing of Specimen E-7. The distribution of residual strains in Specimen E-7 is shown in Fig. 5, where it can be seen that they are somewhat less in this specimen than they were in Specimen E-6, probably because of the modification of the welding procedure used in preparing the specimen. Also shown in the figure is the strain history at selected points in the specimen as the specimen was preloaded, notched, and impacted.

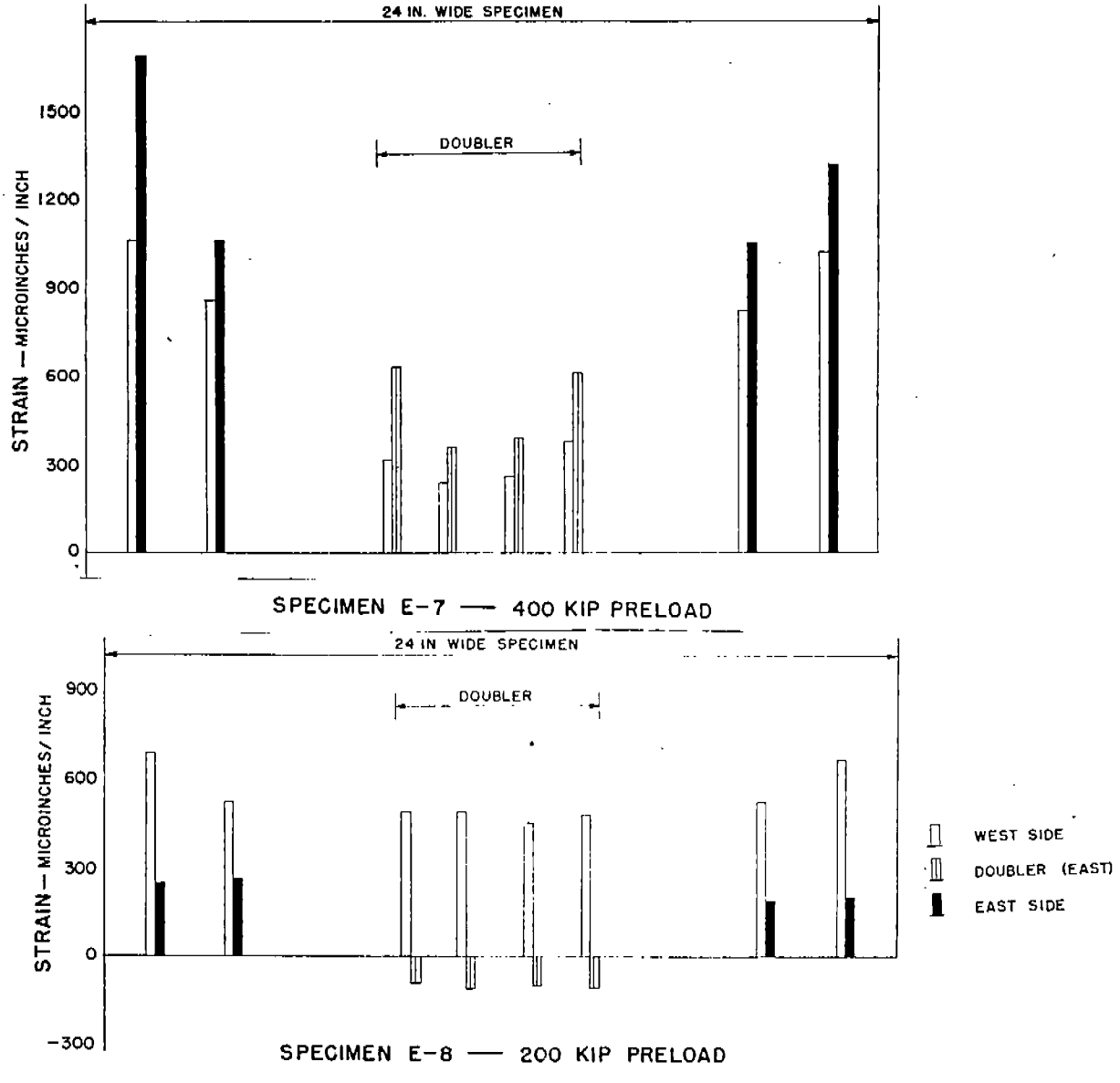

Fig. 6. Strain Increment Across Specimens E-7 and E-8 for Preload Indicated.

After the doubler plate had been completely welded to one side of the main insert plate, additional SR-4, Type A-1 strain gages were mounted in a back-to-back manner on the doubler and insert plate. These eight gages, together with the eight gages that were originally mounted on the main insert plate before the beginning of the fabrication of the specimen, provided a complete picture of the strain distribution across a transverse section of the specimen under load. From these strain gages, the strain increments shown in Fig. 6

were obtained in Specimen E-7 under a 400-kip preload. In this specimen, the participation of the doubler plate was much better than in any of the previous welded doubler-plate specimens.

The two tests on this specimen are summarized in Table 1, where it is shown that at an average effective stress of 26.0 ksi and a temperature of 29 F the brittle crack propagated across the main plate to the flame-cut slot, through the fillet-weld, and across to the opposite edge of the attached doubler plate. The extent of crack propagation on both sides of this specimen can be seen in Fig. 3. The fractured surfaces of the main plate and the doubler plate, indicating the characteristic chevron pattern pointing in the direction of the fracture initiation, is shown in Fig. 4.

Specimen E-8 was similar to Specimen E-7 except that a doubler plate of A-285-steel was riveted with two rows of 1-in. diam. button-head rivets to one side of the insert plate as shown in Fig. 2. This model was similar to the riveted doubler-type crack arrestors that had been used under service conditions. After the specimen was riveted, SR-4, Type A-1 strain gages were mounted on the specimen as shown in Fig. 2 to provide a record of the distribution of strain throughout the doubler and insert plates during preparation and loading.

The strain increments shown by these gages under a preload of 200 kips are plotted in Fig. 6. Comparing the back-to-back strain gage readings on the insert plate, it is evident that the strains on the side of the plate on which the doubler is fastened are considerably less. In addition, the strains on the surface of the doubler plate in this specimen are compressive, indicating the load carried by the doubler in this case is extremely small. The almost negligible participation by the doubler in this specimen was entirely unsatisfactory and indicated that special provisions must be made in future tests so that the doubler in riveted doubler specimens would take more of the applied load.

As shown in Table 1, two tests were conducted on this specimen. An average effective stress of 20.0 ksi and a temperature of 35 F, together with a theoretical impact of 1200 ft-lb, created a 3 1/2-in. submerged crack. A second impact on the same notch at an average effective stress of 26.0 ksi

and a temperature of 42 F succeeded in initiating a crack that propagated to the rivet hole but was not evident in the doubler plate. The facture path in this specimen can be seen in Fig. 3, and the fractured surface from the main plate is shown in Fig. 4.

DESCRIPTION OF TEST SPECIMENS AND EQUIPMENT

Specimens and Materials

All of the specimens tested in this investigation were 3/4 in. thick and consisted of an insert butt-welded with E7016 electrodes to the pulling plates of the testing machines. In Tests 1-3, the 18-in. long insert, when welded to the 3/4-in. thick pull-plates, provided a test piece 2-ft wide by 6-ft long in plan dimension (exclusive of the pull heads of the 200,000-lb screw-type testing machine).

In the remaining tests, the depth of the insert varied between 16 and 60 in., some of the longer inserts being used for more than one test. For the tests in the 3,000,000-lb hydraulic testing machine, the 6-ft wide pull-plates were 1 in. thick for Tests 4-31 and 3/4 in. thick for Tests 32-45. In this program, the length of each pull-plate varied from 3 1/4 to almost 9 ft. Therefore the overall length of the specimens tested varied from approximately 8 to 19 ft, depending upon the depth of the insert and the length of the pull-plates. The majority of the specimens, however, had an overall length of approximately 18 ft. A typical test set-up is shown in Fig. 7. Depending upon the depth of the notch at each edge of the plate, the net width of the specimen on the notch line was 2 or 2 1/4 in. less than the gross width.

The welded arrestor specimens were fabricated with two or more types of steel, which were welded together with double-V butt-welds in such a manner as to introduce a minimum amount of residual stress. The welded arrestor specimens were composed of certain widths of starter and arrestor material and, in some cases, another material to complete the 72-in. wide specimen. In all of the tests in this investigation, Lukens

(a) Six-Foot Wide Specimen in 3,000,000 lb machine

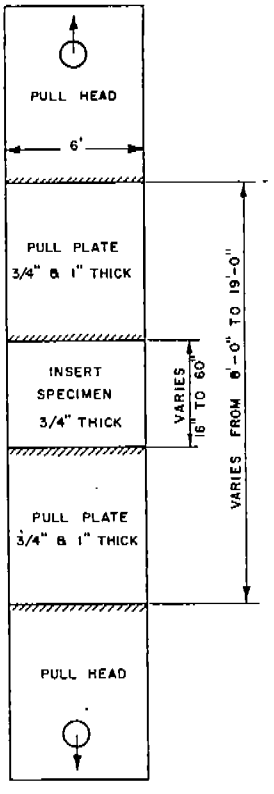

(b) Line Diagram of Plate Specimen

Fig. 7. Typical Test Setup.

rimmed steels (designated as E- or Z-steel) were used as the starter material, USS T-1 and ABS-Class C normalized steels (designated as T- and C-steel) were used as the arresting materials, and USS semikilled steel (designated as X-steel) was used to make up the necessary specimen width. The main plate and doubler plate of the riveted arrestor specimens were made of Z-steel. All of the specimens were oriented so that the direction of rolling was parallel to the specimen axis and transverse to the direction of crack propagation.

The mechanical properties and chemical compositions for all of these steels, together with the Charpy V-notch impact results, are presented in Figs. 1, 8, and 9.

Crack Initiation

After a considerable amount of initial development work, summarized briefly in the preceding section and completely described elsewhere[14] a satis-

TENSILE TEST DATA

DIRECTION OF ROLLING	YIELD STRENGTH KSI	ULTIMATE STRENGTH KSI	ELONGATION IN 2 IN. %	REDUCTION OF AREA %
PARALLEL	34.9	66.7	39.	65
NORMAL	34.3	60.1	39.	59

CHECK ANALYSIS

C	Mn	P	S	Si	Cu	Cr	Ni	Al
0.20	0.76	0.019	0.040	0.03	0.04	0.02	0.16	0.002

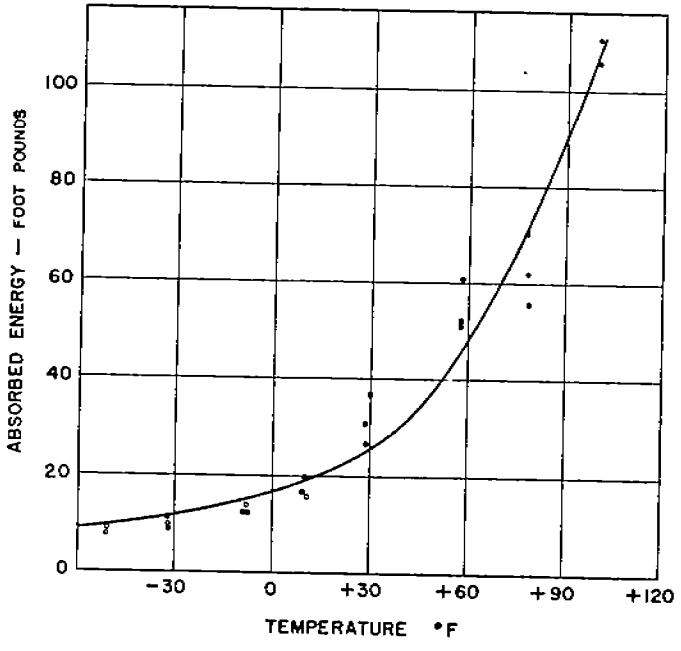

CHARPY V-NOTCH IMPACT RESULTS

(a) X — STEEL, HEAT NO. 64 M 487

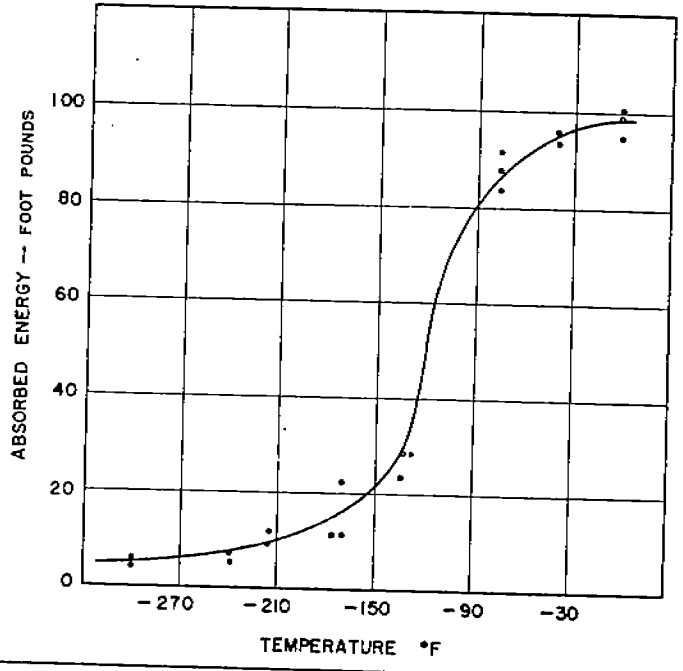

CHECK ANALYSIS

C.	Mn.	P.	S.	Si.	Cu.	Cr.	Ni.	Al.	Mo.	V.
0.11	0.84	0.036	0.015	0.28	0.32	0.50	0.99	0.09	0.53	0.095

TENSILE TEST DATA

DIRECTION OF ROLLING	YIELD STRENGTH KSI	ULTIMATE STRENGTH KSI	ELONGATION IN 2 IN. %	REDUCTION OF AREA %
PARALLEL	111.9*	126.6	22	69
NORMAL	—	128.9	15	46

* Based on 0.2 per cent offset

CHARPY V-NOTCH IMPACT RESULTS

(b) T — STEEL

Fig. 8. Properties of USS Semikilled and T-1 Steels.

TENSILE TEST DATA

DIRECTION OF ROLLING	YIELD STRENGTH KSI	ULTIMATE STRENGTH KSI	ELONGATION IN 2 IN. %	REDUCTION OF AREA %
PARALLEL	48.0	71.9	33	62
NORMAL	47.3	71.1	.32	57

CHECK ANALYSIS

C	Mn	P	S	Si	Cu	Cr	Ni	Al
0.24	0.69	0.022	0.030	0.20	0.22	0.08	0.015	0.034

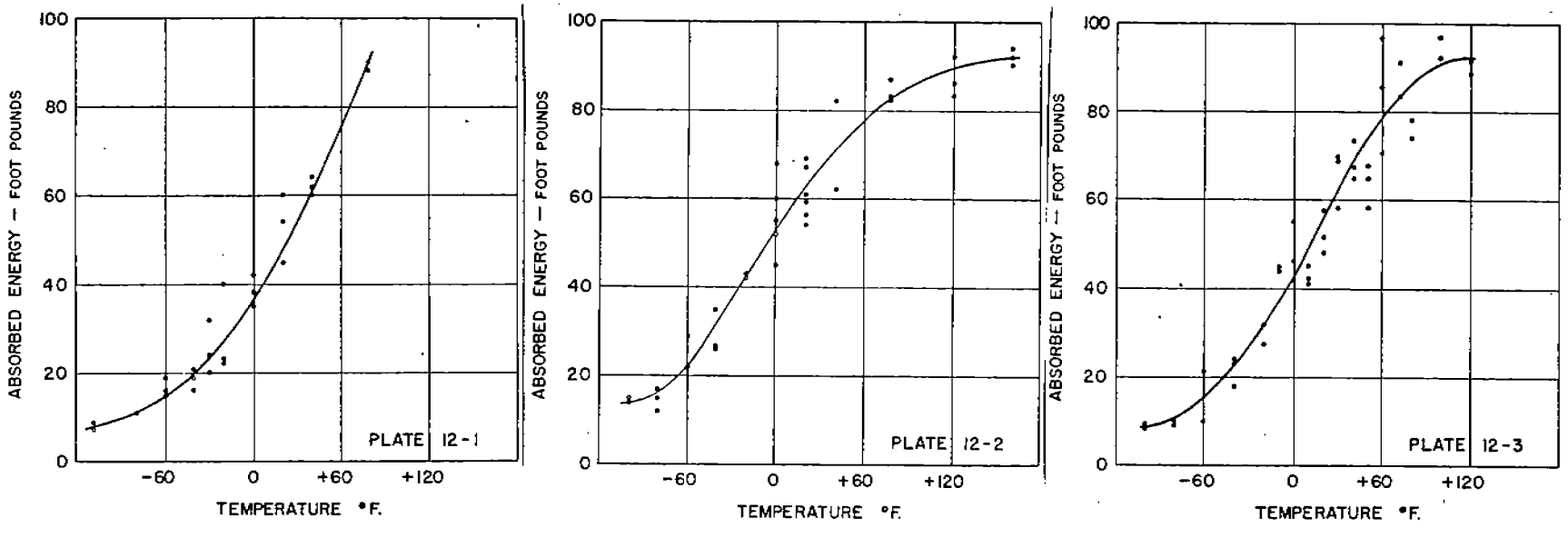

CHARPY V-NOTCH IMPACT RESULTS

C-STEEL, HEAT NO. 24883

Fig. 9. Properties of Lukens ABS-Class C Normalized Steel.

factory method of initiating a brittle fracture consistently under laboratory conditions in the type of specimen under consideration was developed and used in all tests of the program. This "notch-wedge-impact method" consists of driving a tapered wedge into a prepared notch at the edge of the plate. The driving of the wedge provides a high rate of local strain, commonly recognized as one of the factors that may contribute to the initiation of brittle fracture in steel. This procedure is a modification of the initiation method used by the Standard Oil Development Company in conducting its wide plate tests.[4]

The prepared notch used in the specimens of Tests 1-10 and 19-21 had a total depth of 1 in. The first 7/8 in. was made with four hacksaw blades (approximately 0.141 in. wide), extended 1/16 in. with one hacksaw blade (approximately 0.034 in. wide), and ended with a 1/16-in. jeweler's saw-cut (approximately 0.012 in. wide). For the remaining tests (11-18 and 22-45), the depth of the notch was changed to 1 1/8 in. by increasing the depth of cut of the four hacksaw blades to 1 in. The notch was then hand-filled to fit a standard 1-in. octagonal cold chisel (included angle of approximately 16°) which was cut to a length of 4 3/4 in. and weighed 1.0 lb.

To provide the impact required to advance the wedge, a gas-operated piston device capable of providing a theoretical impact as high as 3000 ft-lb was used. Generally, the theoretical lateral impact was 1200 ft-lb (obtained with a 5-in. stroke and a pressure of 280 psi), but values as high as 1600 ft-lb were used in the latter part of the program. To absorb the reaction of the piston device during acceleration of the piston, the device was tied to a weight (approximately 120 lb) which bore against the far side of the specimen at the notch line.

Several attempts were made to investigate the reliability and output of the gas-operated impact device. The method adopted, which gives satisfactory results, is based on the deformation of round (1 1/2-in. diameter) brass cylinders. This method involves (1) the making of tests to obtain the relationship between the deformation of the brass cylinders and the energy input from a drop-weight testing machine, and (2) the making of corresponding tests on similar brass cylinders made with the gas-operated impact device

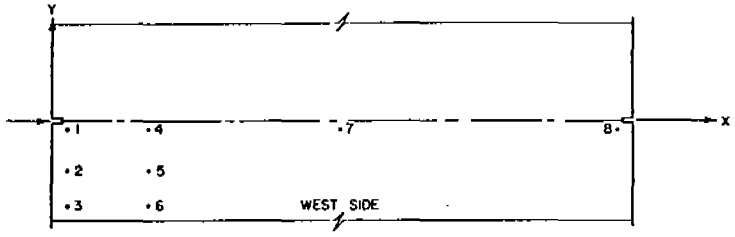

TESTS 4 – 10

NO.	X IN.	Y IN.	TEMP. AT TIME OF TEST 9
1	2	- 2	- 54
2	2	- 6	- 54
3	2	- 10	- 56
4	12	- 2	- 54
5	12	- 6	- 53
6	12	- 10	- 53
7	36	- 2	- 51
8	70	- 2	- 53

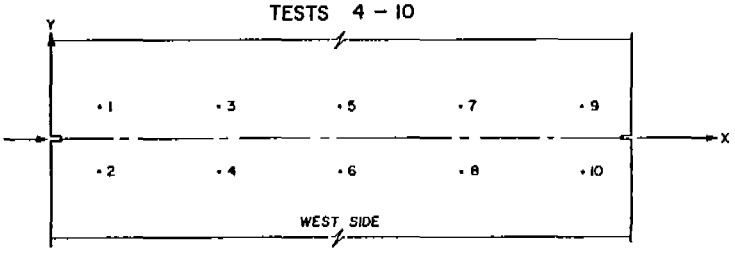

TESTS 11-18, 22, AND 23

NO.	X IN.	Y IN.	TEMP. AT TIME OF TEST 11
1	6	+ 4	- 25
2	6	- 4	- 22
3	21	+ 4	- 25
4	21	- 4	- 25
5	36	+ 4	- 27
6	36	- 4	- 25
7	51	+ 4	- 26
8	51	- 4	- 30
9	66	+ 4	- 28
10	66	- 4	- 24

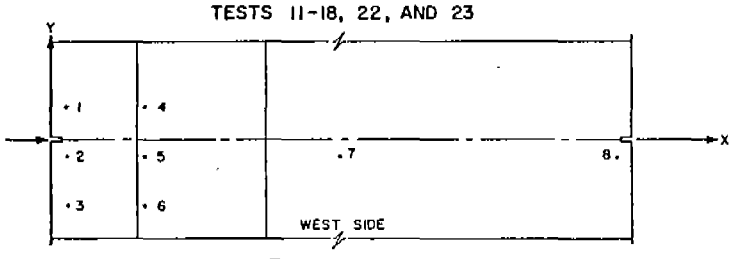

TESTS 19 – 21

NO.	X IN.	Y IN.	TEMP. AT TIME OF TEST 20
1	2	+ 4	+ 23
2	2	- 2	—
3	2	- 8	+ 21
4	12	+ 4	+ 18
5	12	- 2	+ 19
6	12	- 8	+ 19
7	36	- 2	+ 17
8	71	- 2	—

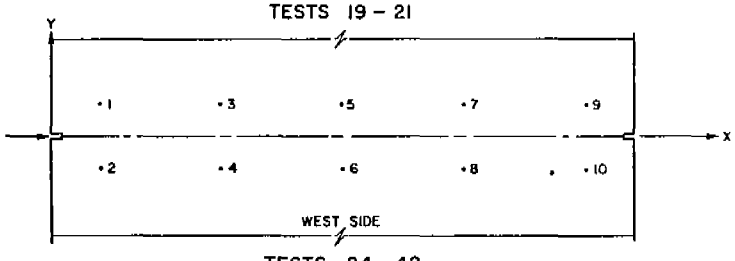

TESTS 24 – 42

NO.	X IN.	Y IN.	TEMP. AT TIME OF TEST 31
1	6	+ 4	+ 14
2	6	- 4	+ 18
3	21	+ 4	+ 15
4	21	- 4	+ 18
5	36	+ 4	+ 17
6	36	- 4	+ 20
7	51	+ 4	+ 17
8	51	- 4	+ 20
9	66	+ 4	+ 18
10	66	- 4	+ 19

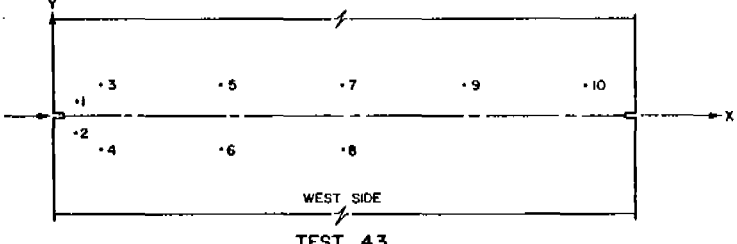

TEST 43

NO.	X IN.	Y IN	TEMP. AT TIME OF TEST
1	3	+ 2	+ 35
2	3	- 2	+ 38
3	6	+ 4	+ 38
4	6	- 4	+ 37
5	21	+ 4	+ 38
6	21	- 4	+ 36
7	36	+ 4	+ 36
8	36	- 4	+ 35
9	51	+ 4	+ 36
10	66	+ 4	+ 36

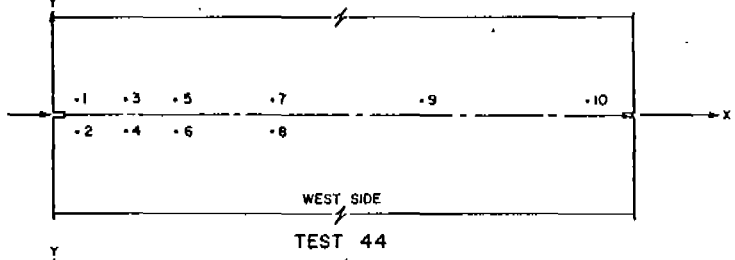

TEST 44

NO.	X IN.	Y IN.	TEMP. AT TIME OF SUBCOOLING NOTCH
1	3	+ 2	+ 27
2	3	- 2	+ 28
3	9	+ 2	+ 27
4	9	- 2	+ 28
5	15	+ 2	+ 28
6	15	- 2	+ 27
7	27	+ 2	+ 27
8	27	- 2	+ 28
9	46	+ 2	+ 27
10	66	+ 2	+ 26

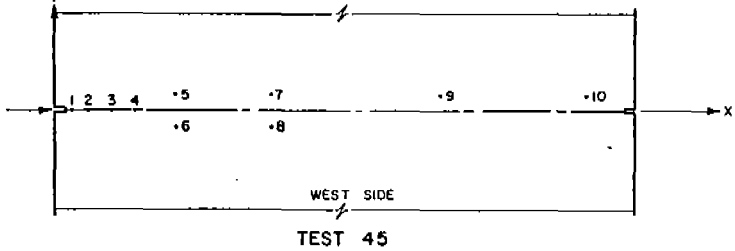

TEST 45

NO.	X IN.	Y IN.	TEMP. AT TIME OF SUBCOOLING NOTCH
1	2	0	+ 39
2	4	0	+ 39
3	7	0	+ 39
4	10	0	+ 39
5	15	+2	+ 39
6	15	-2	+ 39
7	27	+2	+ 39
8	27	-2	+ 39
9	48	+2	+ 39
10	66	+2	+ 39

Fig. 10. Typical Thermocouple Locations and Temperature Variations throughout the Plate.

set at various theoretical energy outputs, particularly at the stroke and pressure combinations used in the test program.

Cooling Method and Supporting Apparatus

The cooling of the specimen to the desired temperature was accomplished by placing crushed dry ice in specially made, approximately 3-in thick containers hung against each side of the specimen. For the 2-ft wide specimens, each container is 2 ft wide and almost 6 ft long, thus extending more than 2 ft above and below the insert. For the 6-ft wide specimens, a set of 3 containers (each 2 ft high by 6 ft wide) was hung on each side of the specimen so that the area covered on one side is about 6 ft by 6 ft, more than sufficient to cover the entire insert. In all tests, the container is recessed on both sides at the center so that neither the container nor the dry ice comes in contact with the instrumentation on the surface of the plate. The space around the perimeter of the tanks is sealed with rock wool insulation.

In general, this method of cooling provided the desired test temperatures satisfactorily and gave a fairly uniform temperature across the plate at the notch line. Many of the specimens were tested at a temperature between zero and -20 F, and these temperatures were usually attained within 60 to 90 min. after the dry ice was placed in the containers. In Fig. 10 are shown the thermocouple layouts used for all of the tests in this program, together with typical temperature variation across the plate at the time of the test.

The cooling tanks, impact device, and reaction weight were suspended from the upper pull-plate. The impact device and reaction weight were also tied together at each edge of the specimen. The horizontal channels that accomplished this in the 6-ft wide specimen can be seen in Fig. 7.

Instrumentation

Sensing Devices. Strain measurements were made with Baldwin SR-4, Type A-1 strain gages (13/16-in. gage length) in Tests 2-5 and Baldwin SR-4, Type A-7 strain gages (1/4-in. gage length) in Tests 6-23. These gages were used to obtain both static and dynamic strain measurements. They were attached to the specimen with a thin layer of Duco cement, dried as specified,

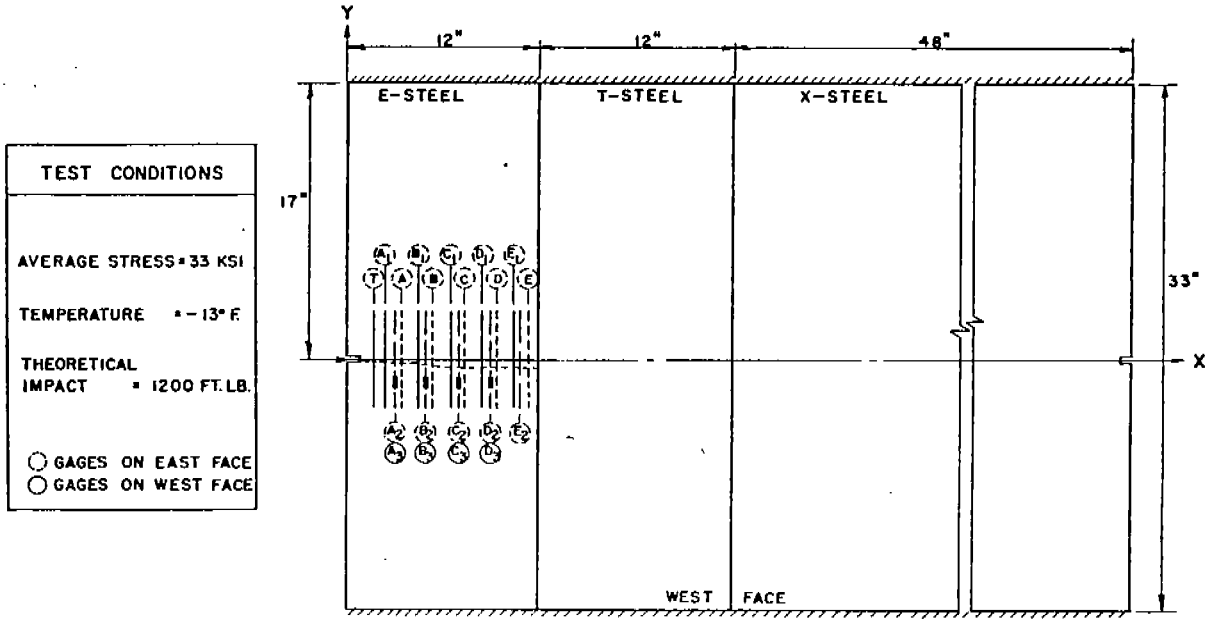

DETECTORS (A-9 STRAIN GAGES)		
NO.	X in	SPEED ft/sec.
A	3.4	
		2350
B	5.3	
		2600
C	7.3	
		2100
D	9.2	
		2400
E	11.1	

DETECTORS (PAPER)		
NO.	X in	SPEED ft/sec.
A_1	2.4	
		4200
B_1	4.5	
		2000
C_1	6.5	
		1550
D_1	8.4	
		2750
E_1	10.4	

DETECTORS (BISMUTH WIRE)		
NO.	X in	SPEED ft/sec.
A_2	3.0	
		2100
B_2	5.0	
		1800
C_2	6.9	
		4200
D_2	8.9	
		2550
E_2	10.7	

DETECTORS (A-7 STRAIN BRIDGE)			
NO	X in	Y in	SPEED ft/sec
A_3	2.8	−1.5	
			2000
B_3	5.0	−1.5	
			2300
C_3	7.0	−1.5	
			1500
D_3	9.0	−1.5	

CRACK PATH	
X in	Y in
3.0	−0.10
5.0	−0.25
7.0	−0.30
9.0	−0.30
11.0	−0.35

Fig. 11. Instrumentation and Calculated Speeds for Various Types of Detectors -- Test 6.

and covered with a moisture-proofing material. To minimize temperature-induced errors, approximately equal lengths of lead wire were used and cooled for all gages.

The crack speed was measured with a system of surface crack detectors. As the crack passed and broke a given detector, an electrical circuit was interrupted. From the spacing between detectors and the elapsed time between successive interruptions of the circuit, the average speed of the fracture was computed. After experimenting with various types of detectors[14] (Test 6), the single-wire Baldwin SR-4, Type A-9 strain gage (6-in. gage length) was selected as the detector for subsequent tests. The results of Test 6 (Fig. 11) show

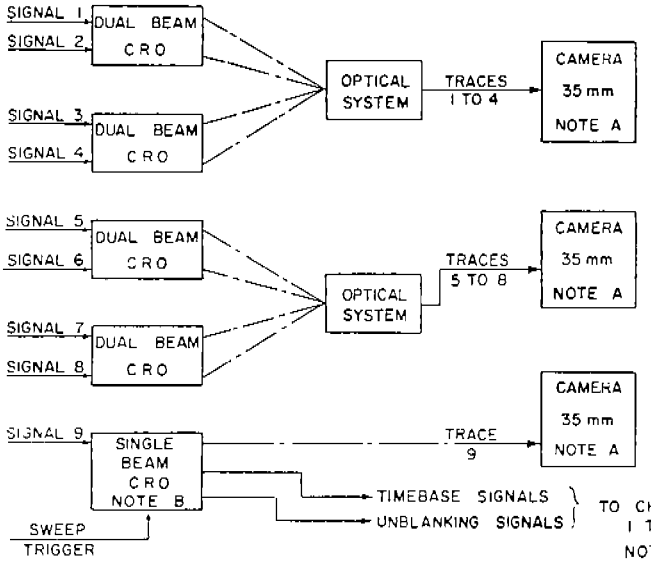

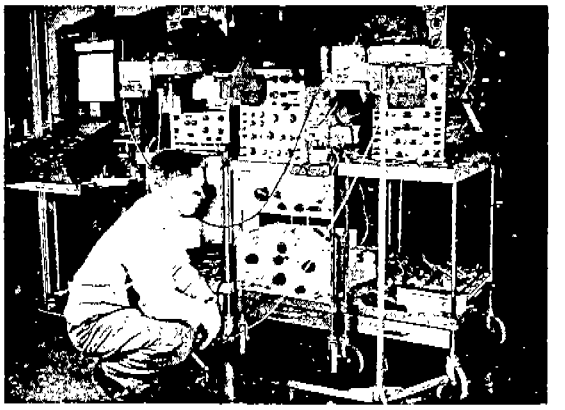

GENERAL VIEW OF RECORDING INSTRUMENTATION

NOTES

A CAMERA SHUTTERS MANUALLY OPERATED PRIOR TO AND FOLLOWING TEST.

B UNIT MODIFIED TO ALLOW ONE SWEEP WHEN TRIGGERED. MUST BE MANUALLY RESET BEFORE RETRIGGERING

C. ALL HORIZONTAL DEFLECTION PLATES DRIVEN BY A COMMON AMPLIFIER.

BLOCK DIAGRAM OF RECORDING EQUIPMENT

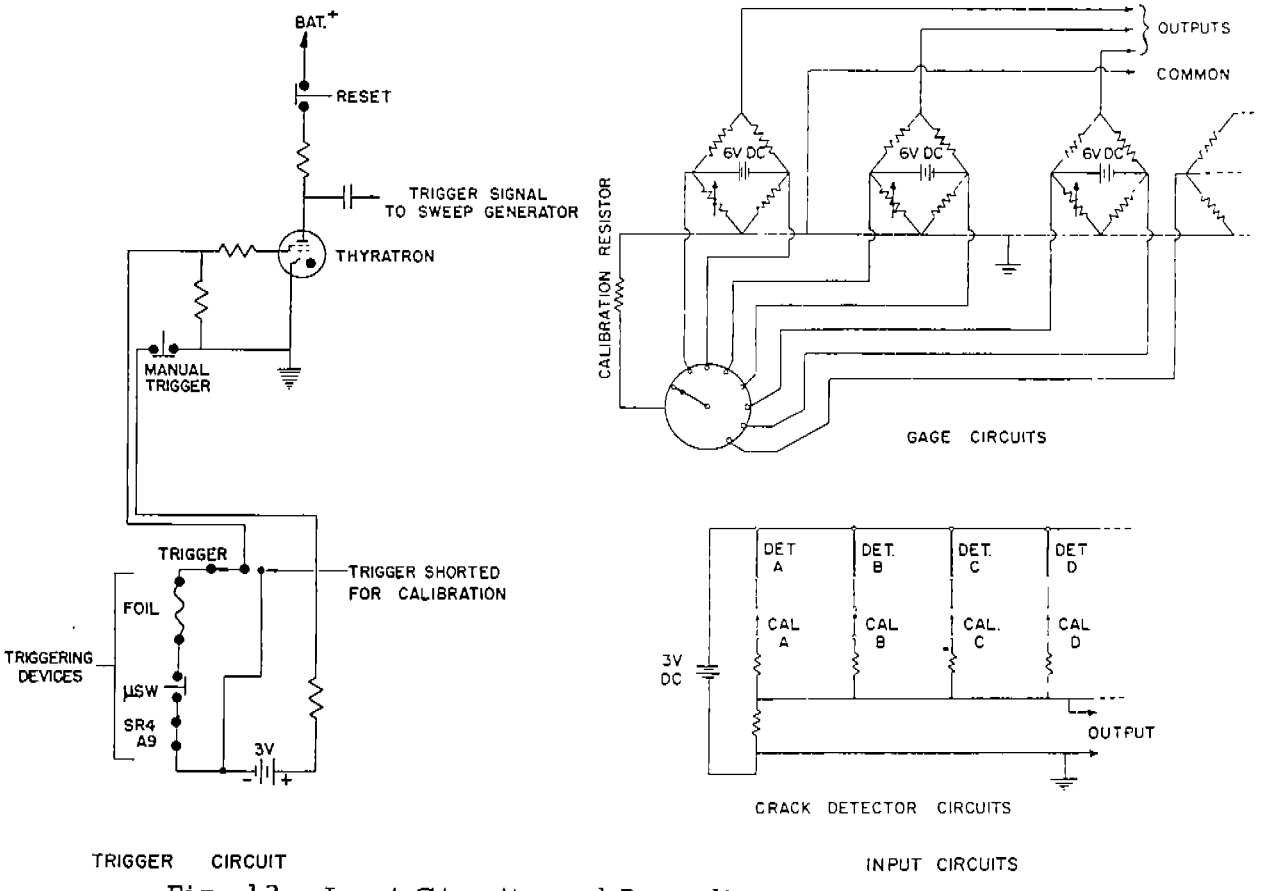

TRIGGER CIRCUIT

INPUT CIRCUITS

Fig. 12. Input Circuits and Recording Instrumentation.

the speed measurements obtained using various methods of speed detection. These techniques include sets of 0.015-in. diameter bismuth wires, 1/8 in. by 6 in. printed silver circuits on charred paper, SR-4, Type A-9 strain gages, and a strain-gage bridge composed of SR-4, Type A-7 gages. On the premise that the strain signal peaked at the instant the crack passed the gage, speed calculations were made from the time intervals between peaks on the recorded trace from the strain-gage bridge. The results from Test 6 indicated that the SR-4, Type A-9 detectors gave results as consistent as did the other types of detectors and that they are more uniform and easier to apply.

It must be emphasized that this system provides a surface measurement only and may not give the true speed of the crack front. At the instant the detector breaks, the exact position of the surface failure and of the interior portion of the crack is not known. This method of speed determination was employed as the best available approximation at the time. Because of the equipment limitations, the difficulty in defining the crack front, and the possible strain gage inconsistencies, all calculated speeds were rounded off to the nearest 50 fps.

All recording equipment was started by the action of a triggering device. For Tests 2-12 and 19-23, the trigger was an SR-4, Type A-9 strain gage (denoted by T in the diagrams of the specimens) mounted about 1 in. beyond the tip of the edge notch. The breaking of this gage by the propagating crack started the recording equipment. For Tests 13-18, an external trigger (a strip of aluminum foil denoted by ET in the diagrams) was placed so that the movement of the piston would start the recording equipment and thus begin the record before the fracture was initiated. Figure 12 shows the trigger circuit. In this diagram the triggering devices shown are an SR-4, Type A-9 strain gage (plate-surface trigger), a microswitch (μSW), and a strip of aluminum foil (external triggers). These triggers were electrically connected in series so that the first one that opened the circuit or was in some way grounded activated the time-base generator.

Copper-constantan thermocouples were located at various points across the specimen to provide a temperature profile during cooling of the

specimen. These thermocouples were installed in No. 54 drill holes about 1/4 in. deep, located as shown in Fig. 10.

Recording Devices. As the program continued, the number of available channels was increased until a maximum of nine channels of high-speed cathode-ray oscilloscope equipment with photographic recording was available for strain and crack-speed signals. Four dual beam cathode-ray oscilloscopes provide eight of these channels and the ninth channel is a single beam unit. Shown in Fig. 12 are nine channels of oscilloscope equipment, the temperature recorder, and calibrating oscillators.

In the tests where dynamic strain records are taken for 8 millisec. or less, all signals were recorded photographically as a function of a common time-base supplied from the single-channel oscilloscope. This same oscilloscope provides all beams with the desired unblanking and intensifying signals used to minimize fogging of the record before and after the test period.

For dynamic strain records longer than 8 millisec., the time base is supplied mechanically in the dual-beam-unit cameras by continuous motion of the film and is generated electrically in the single-channel display tube because this image is photographed with a single-frame camera. The circuits that generate this time base electrically after receiving a signal from the trigger also supply pulses which are fed to all the dual beam units. These provide synchronizing pulses for the moving film so that the various traces can be synchronized with respect to time when the data are reduced.

Four traces from two dual-beam oscilloscopes were optically superimposed on a single frame in the interest of maximum photographic definition. Strip-film 35-mm cameras were employed with the dual-beam equipment (they were used as single-frame cameras for records as long as 8 millisec.) and a 35-mm single-frame camera was used with the single-channel oscilloscope. This equipment is shown in the block diagram in Fig. 12.

Six of the oscilloscope channels were sufficiently sensitive to allow at least 1 1/2 in. of trace deflection for 1000 μin./in. of strain. The

other three channels had about one-third this sensitivity. Whenever possible the latter channels were used to record the highest electrical magnitudes. The frequency response of the single-channel oscilloscope is flat from 0 to 1000 kc. The response of the dual-beam units is flat from 0 to 100 kc and decreases not more than fifty per cent at 300 kc. The response of the cathode-ray equipment considerably exceeds the limits imposed by spot size and photographic techniques when either the tube face is photographed as a single frame exposure or when the maximum film speed of 180 in./sec is used. In general, the records obtained did not include frequency components approaching the photographic limit of resolution. For these reasons the system used was considered adequate. The bandwidth, or frequency response, of the measuring gage and its associated wiring has been assumed to be in excess of any of these values.

The temperature was recorded during the cooling process in order that the cooling rate and the temperature gradient could be observed before the test. For this purpose, an automatic recorder which provides a sensitivity of about 1°F per 0.1 in. on the record was used. The various thermocouples are sequentially sampled by a motor-driven switch and directly recorded in degree Fahrenheit.

Input Circuit. The signals fed to the cathode-ray recording equipment consist of a sweep triggering pulse followed by strain and crack-location signals. The detectors, which fail as the crack crosses the plate, open an electrical circuit and feed step voltages to the recorder whose amplitudes are in the ratio of 1:2:4:8:16. Since each step has a different magnitude, a given step can be identified with the particular detector to which it is connected, thereby providing a positive identification of sequence.

The electrical time-base is initiated by the trigger. Opening the trigger circuit removes the bias signal from a triggering thyratron and allows it to start conducting. The step voltage, which results at the start of conduction, is fed into the standard circuits of the single oscilloscope unit. Reinitiation cannot occur until the thyratron is reset manually. This prevents subsequent multiple sweeps which may be triggered by such things as chatter

of the initiating wedge or accidental grounding of the broken wire which obscure the trace of interest on the single recorded frame.

The strain gages are connected in the customary Wheatstone bridge circuit. Dummy gages which complete the bridge circuit are mounted externally with respect to the specimen. These bridges are excited by direct current, and their outputs are fed to the recording channels. Typical input circuits are shown in Fig. 12.

Measurement Procedure and Calibration. The strain measuring channels are calibrated by shunting gages with a resistance whose equivalent strain value is known or measurable. Both the active arm and the adjacent dummy gage are shunted successively to obtain compression and tension calibrations. Only one calibrating value was used in these tests because other tests have indicated that the linearity of the recording system was adequate within the limit of resolution of the record. Crack-detector calibration was obtained by successively opening switches in series with the various detectors and recording the trace steps. In all tests without moving film, the time axis was calibrated by putting a time signal of known frequency on all channels simultaneously and photographing one sweep. This was done immediately after the test was completed. When moving film was used, the time axis was calibrated by putting a square-wave time signal of known frequency on all channels simultaneously by intensity modulations of the electron beams. Thus time calibrations are included with the test data, and, since all beams are modulated, relative shifts in base-time position as well as specific time on all traces can be observed.

Although the deflection plates are connected in parallel, individual construction of the various guns and deflection systems results in slight horizontal displacements between the traces, and some measure of this offset must be made on the eight traces in the moving film cameras. As noted earlier, pulses are inserted from the single frame sweep generator to show the trigger failure on each trace. These pulses provide a cross-check on the trace offsets as well as a specific time on all traces.

Data Reduction. A feature of the reduction of data for tests without

moving film (Tests 3-12 and 19-23) that may not be a standard procedure is the method of synchronizing the various traces with respect to time and the significance of the numerical time values. In general, some arbitrary point is called zero time. This may or may not correspond to the earliest point on the recorded traces. This point is selected near the early portion of the sweep at the first peak of the time-calibration sine wave. This provides a convenient and definite reference point common to all traces. The record is reduced in the customary manner of reading signal amplitude against time, each trace being read with an individual calibration on both the time and signal axis. The earliest time noted for any record is some finite but unknown period of time after the breaking of the sweep trigger wire, approximately 20 μ sec.

General Test Procedure

The specimen insert was welded between the pull-plates of the testing machine and the notches were cut in the edges of the specimen at the desired location. The strain gages and crack detectors were then mounted on those specimens on which instrumentation was to be included. Then the thermocouples were installed. The strain gages were checked at room temperatures by cycling (loading and unloading) the specimen to the test load. This was done to check the behavior of the gages and the strain distribution in the specimen. Occasionally it was necessary to replace faulty or questionable gages. Since many of the inserts were slightly warped, the strain gages usually recorded residual strains following the first load cycle. To reduce these residuals, the specimen was cycled until little or no residual strain was observed in any gage. The specimen, however, was never stressed higher than the test load.

All the wiring exposed to the cooled specimen was sprayed with a plastic compound to improve the insulation. As an additional precaution, the gages and wiring were covered with a plastic envelope to minimize the amount of condensation and to prevent stray pieces of dry ice from coming in contact with the instrumentation.

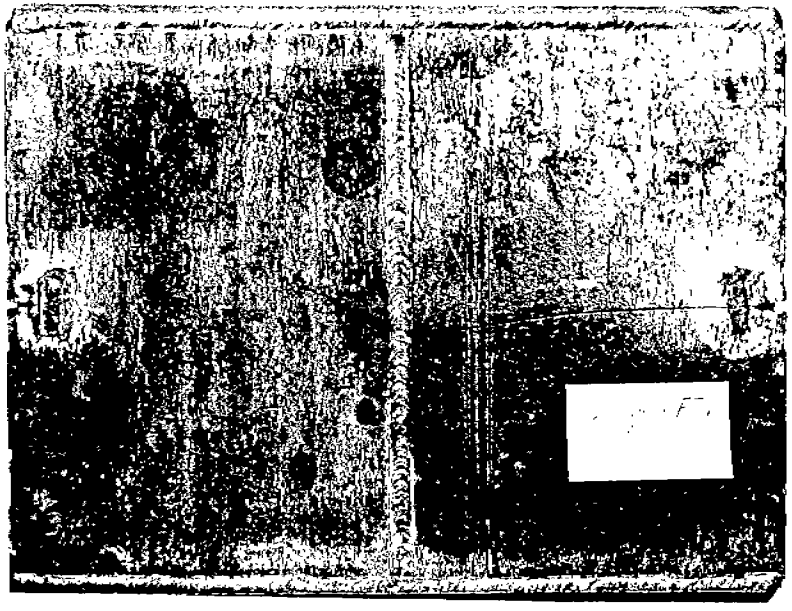

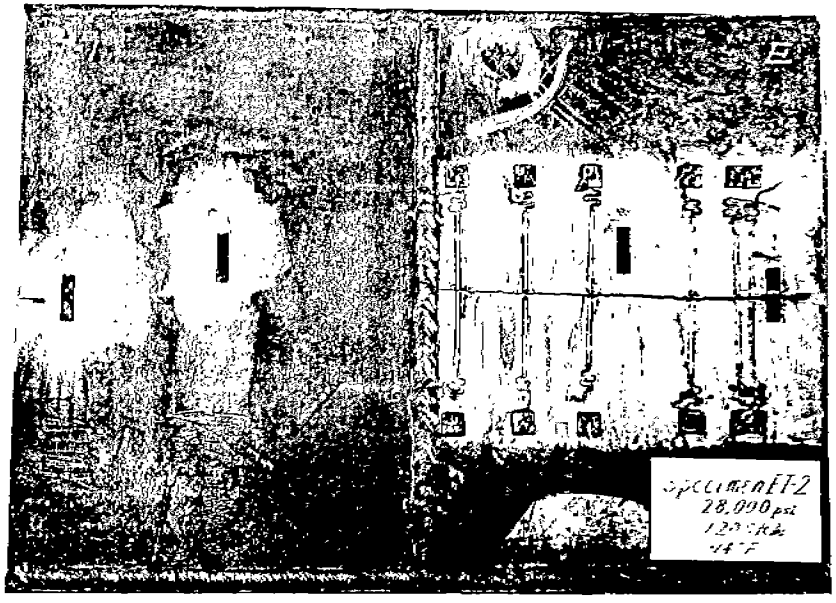

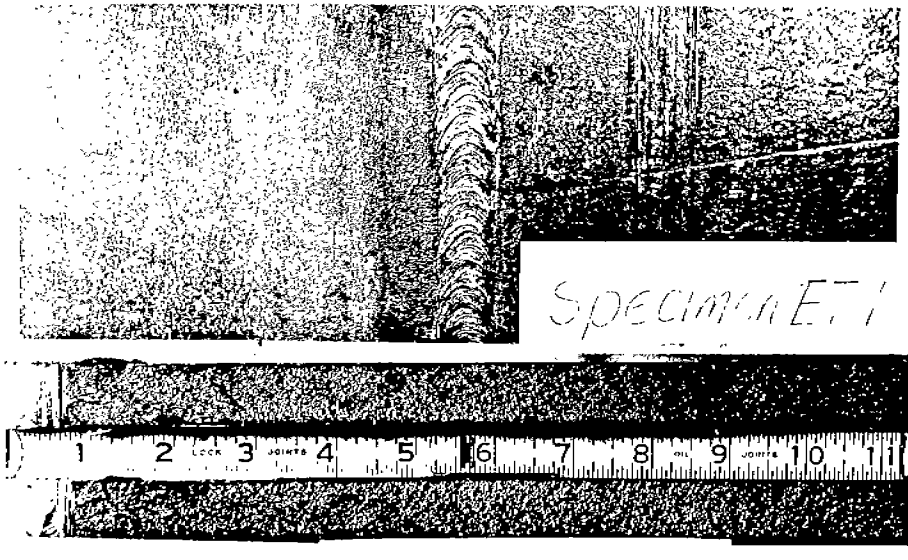

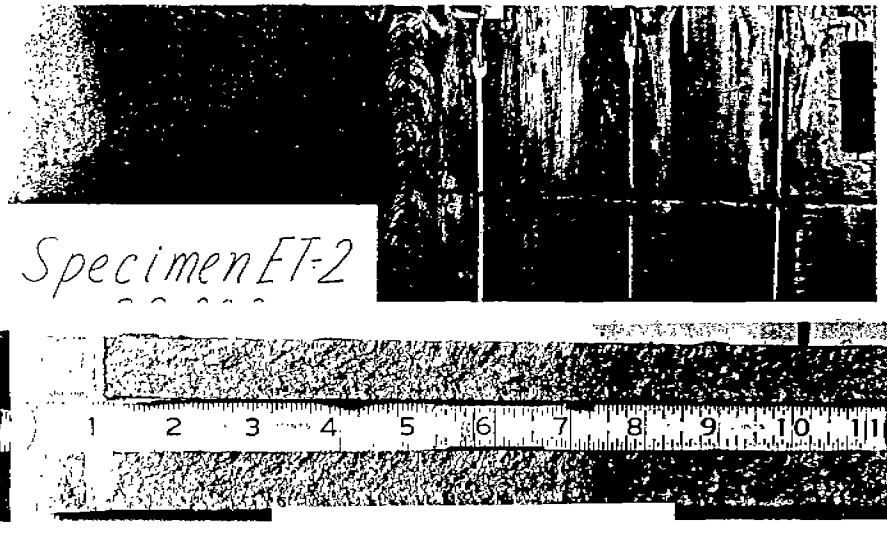

Fig. 13. Fracture Path and Surface--Test 1.

Fig. 14. Fracture Path and Surface--Test 2.

After the cooling tanks, gas-operated piston device, and reaction weight were suspended from the upper pull-plate, the instrumentation was connected and checked. The dry ice containers were filled and, as the desired test temperature was approached, the test load was applied to the specimen and the recording devices were calibrated. When the specimen reached the desired test temperature, the gas-operated piston device was pressured and fired.

The static strain gages were read immediately after the test. In the event that the fracture was arrested, the remaining load was recorded and the static gages were read at this load. Then the specimen was unloaded and the gages were read again so that the permanent set could be determined.

PRESENTATION AND DISCUSSION OF DATA

Preliminary 2-Ft Wide Welded Arrestor Specimens

In order to investigate the feasibility of arresting a propagating brittle crack with a butt-welded strake of tough steel, a few preliminary 2-ft wide specimens of this type were tested. It was felt that one of the best quality steels available at that time should be used for the tough steel and, for this purpose, T-steel was selected.

The specimens for Tests 1 and 2 consisted of a 12-in. wide plate of E- and T-steels butt-welded together with E12015 electrodes, and the specimen for Test 3 consisted of two 12-in. wide plates of E-steel butt-welded together with E12015 electrodes. A summary of this preliminary series of tests is presented in Table 2. In Tests 1 and 2 (at an average temperature of 15 F) a lateral impact of 1200 ft-lb initiated and propagated a brittle crack across the E-steel plate to the longitudinal butt-weld under average stresses on the net section of 17.0 and 28.0 ksi. In both cases the final load was slightly less than 80 per cent of the original value.

The fracture path and surface of the fracture for Tests 1 and 2 can be seen in Figs. 13 and 14. In both cases a separation is evident on the surface

TABLE 2

SUMMARY OF PRELIMINARY TESTS ON 2-FT WIDE WELDED ARRESTOR SPECIMENS

Test (Plate No.)	Width of Starter Material (in.)	Initial Load (kips)	Avg. Stress on Net Section (ksi)	Avg. Temp. (°F)	Remarks
These tests were conducted on two-ft wide specimens in a 600,000 lb screw-type testing machine. The test specimen is a 3/4 x 18 x 24 in. insert (fabricated from two 12 in.-wide strakes of steel) welded to 3/4 in. pull-plates, using double "V" butt welds - E7016 electrodes, to provide a test piece 2-ft wide x 6-ft long. The vertical weld within the specimen is a double "V" butt weld made with E12015 electrodes. A 1 in. long notch (see Table 1) and theoretical impact of 1200 ft-lb were used.					
The 3/4 x 18 x 24 in. inserts consisted of 12 in. of E-steel and 12 in. of T-steel.					
1 (ET-1)	12	280	17.0	16	Final load - 222 kips. Crack propagated 12 in. to near side of weld. No instrumentation.
2 (ET-2)	12	462	28.0	14	Final load - 357 kips. Crack propagated 12 in. to near side of weld, visible reduction in thickness of weld. Record lost.
The 3/4 x 18 x 24 in. insert consisted of two 12 in. E-steel strakes.					
3 (EE-1)	12	412.5	25.0	30	Complete brittle fracture with velocity reduction through weld. Partial dynamic record, good quality.

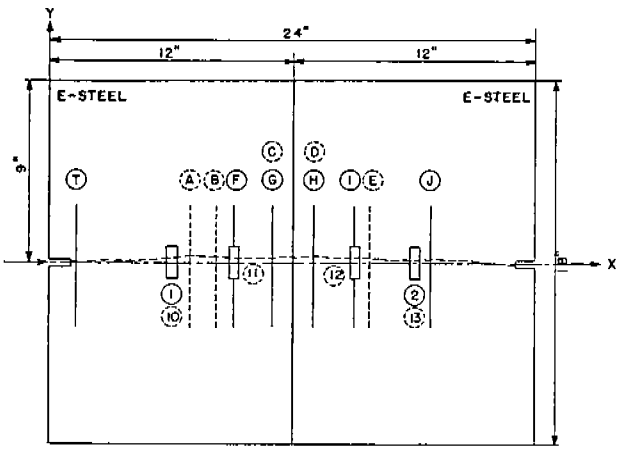

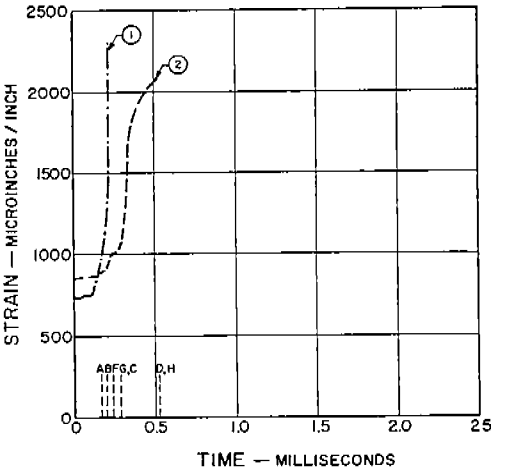

TEST CONDITIONS
AVERAGE STRESS = 25 KSI
TEMPERATURE = + 30° F.
THEORETICAL IMPACT = 1200 FT. LB.
◯ GAGES ON EAST FACE
◯ GAGES ON WEST FACE

STATIC STRAIN GAGES			
NO	X in.	Y in	INITIAL STRAIN
10	6	0	705
11	9	0	730
12	15	0	745
13	18	0	710

DYNAMIC STRAIN GAGES			
NO	X in	Y in.	INITIAL STRAIN
1	6	0	730
2	18	0	850

DETECTORS PAPER		
NO.	X In.	SPEED ft./sec.
F	9.0	4750
G	11.0	700
H	13.0	
I	15.0	
J	18.8	

DETECTORS BISMUTH WIRE		
NO.	X in.	SPEED ft./sec.
A	7.0	2900
B	8.3	2850
C	11.0	700
D	13.0	
E	15.8	

CRACK PATH	
X in.	Y in.
6	0.18
9	0.20
10	0.18
14	0.25
15	0.18
18	0.22

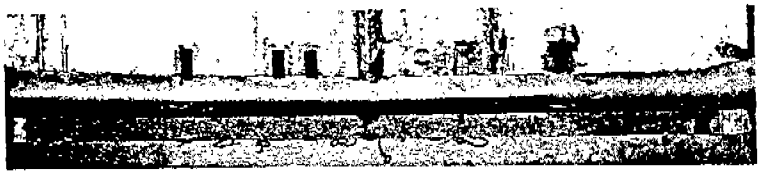

Fig. 15. Instrumentation, Record, and Fracture Surface -- Test 3.

of the E-steel to the butt-weld. In Test 2, there is also a significant reduction of area through the butt weld, probably caused by the combination of initially high stress and severe eccentricity. Although crack detectors and dynamic strain gages were mounted on the specimen of Test 2, a record was not obtained because of mechanical difficulties.

The portion of the plate around the end of the arrested crack in the specimen from Test 2 was removed for metallurgical examination. This metallurgical sample was sectioned along its midthickness. On this plane, the crack had traversed the weld metal, the heat-affected zone of the base metal, and had progressed about 0.1 in. into the unaffected parent metal, indicating a thumbnail-type shape for the contour of the arrested crack.

Test 3 was conducted in order to observe the effect of an E12015 butt-

weld (without an adjacent strake of tough steel) on the propagation of a brittle crack. Speed detectors and dynamic strain gages were mounted on the specimen as shown in Fig. 15. Also presented in Fig. 15 are the dynamic records obtained and the crack speeds calculated for this specimen when tested at a stress of 25,000 psi and at a temperature of 30 F. A sweep time of about 1 millisec. was set on the oscilloscope, but, since the weld apparently slowed down or stopped the crack temporarily, the detectors mounted on the far side of the weld were not broken before the total sweep time elapsed. Crack speeds as high as 4750 fps were measured in the E-steel, but an average speed of only 700 fps was indicated by the detectors on each side of the butt-weld. The photograph of the fractured specimen shows a ductile type of failure across part of the longitudinal butt-weld, and this might explain the slow-down or momentary arrest of the brittle crack.

6-Ft Wide Welded Arrestor Specimens with T-Steel

In these specimens, 4-, 12-, 24- and 36-in. wide strakes of T-steel (butt-welded with E12015 electrodes) constituted the arresting material. These arrestor strakes were combined with 1-4 ft widths of starter material (usually rimmed steel E or Z) and sufficient X-steel to fill out a 6-ft wide specimen. Strain gages and crack detectors were mounted on all specimens in this series and, as shown in Table 3 where these tests are summarized, a record was obtained in almost every case. Specimens tested in this series were subjected to a theoretical lateral impact of 1200 ft-lb, an average stress between 25.0 and 33.0 ksi, and a testing temperature between 10 and -54 F.

Test Records. The results of the instrumented tests are shown in Figs. 11 and 16—28. Each figure provides a detailed drawing of the insert, the location of the instrumentation and crack path with reference to a set of X and Y coordinates, the strain level for each strain gage at test load, the crack speeds as determined from the detectors, the stress-temperature conditions of the test, and a record of the strain-time relationships obtained

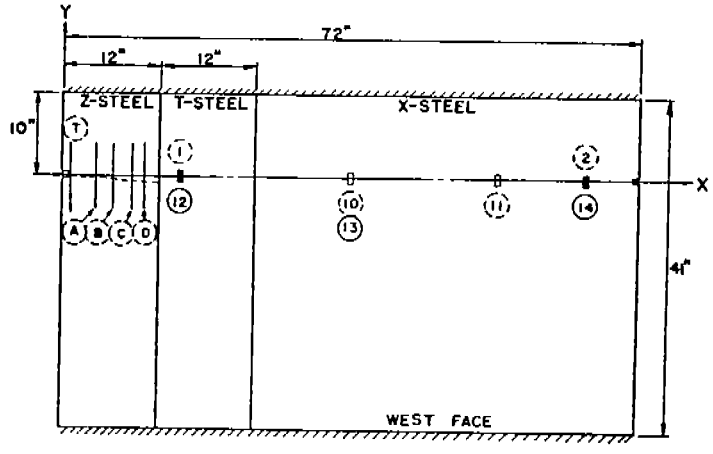

TEST CONDITIONS
AVERAGE STRESS = 25 KSI
TEMPERATURE = +10°F
THEORETICAL IMPACT = 1200 FT.LB.
◯ GAGES ON EAST FACE
◯ GAGES ON WEST FACE

DYNAMIC STRAIN GAGES			
NO.	X in.	Y in.	INITIAL STRAIN
1	15.0	0	+ 700
2	65.0	0	+ 700

STATIC STRAIN GAGES			
NO.	X in.	Y in.	INITIAL STRAIN
10	36.0	0	+ 730
11	54.0	0	+ 670
12	15.0	0	+1000
13	36.0	0	+1000
14	65.0	0	+ 970

DETECTORS (BISMUTH WIRE)		
NO.	X In.	SPEED ft./sec.
A	4.4	
B	6.5	2000
C	8.9	4050
D	10.4	2700

CRACK PATH	
X in.	Y in.
3	0
6	-0.25
9	-0.65
10.9	-0.85
11.8	-0.80

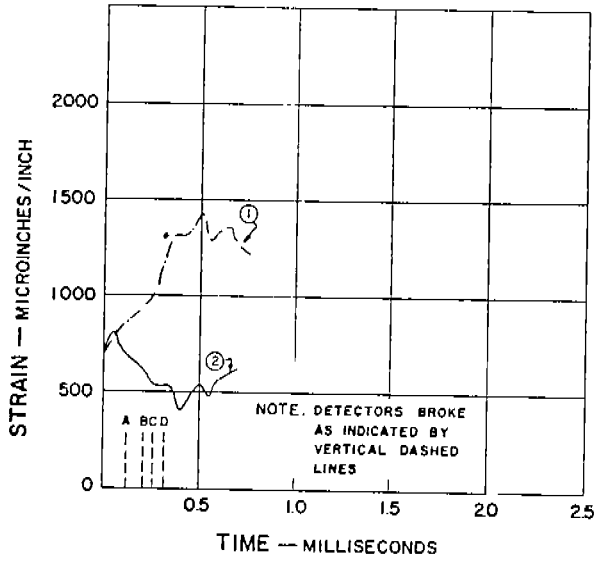

Fig. 16. Instrumentation and Record--Test 5.

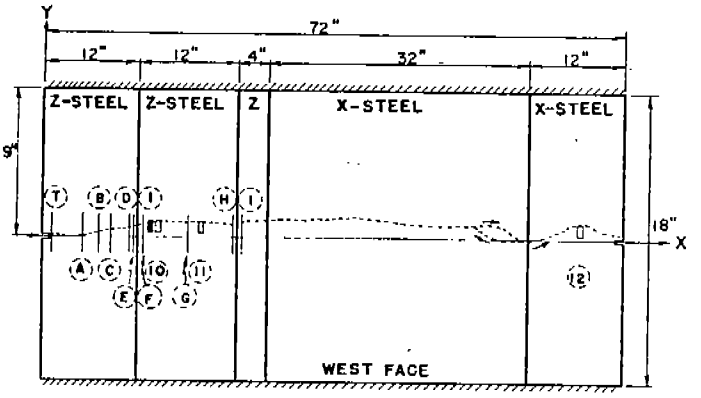

TEST CONDITIONS
AVERAGE STRESS = 30 KSI
TEMPERATURE = −10°F
THEORETICAL IMPACT = 1200 FT. LB.
○ GAGES ON EAST FACE
○ GAGES ON WEST FACE

DYNAMIC STRAIN GAGES			
NO.	X in	Y in	INITIAL STRAIN
1	13.1	+1	+1070

STATIC STRAIN GAGES			
NO.	X in	Y in	INITIAL STRAIN
10	13.5	+1	+1070
11	18.5	+1	+840
12	66.0	+1	+820

DETECTORS		
NO.	X in	SPEED ft./sec.
A	5.0	
B	7.0	2150
C	9.1	2300
D	11.1	3150
E	11.5	
F	12.8	2550
G	17.5	5200
H	23.4	4600
I	24.7	500

CRACK PATH	
X in	Y in
6	+0.35
12	+1.60
24	+2.23
30	+2.86
36	+3.03
42	+2.84
48	+2.57
54	+1.80
60	+0.30
66	+1.24
72	+0.60

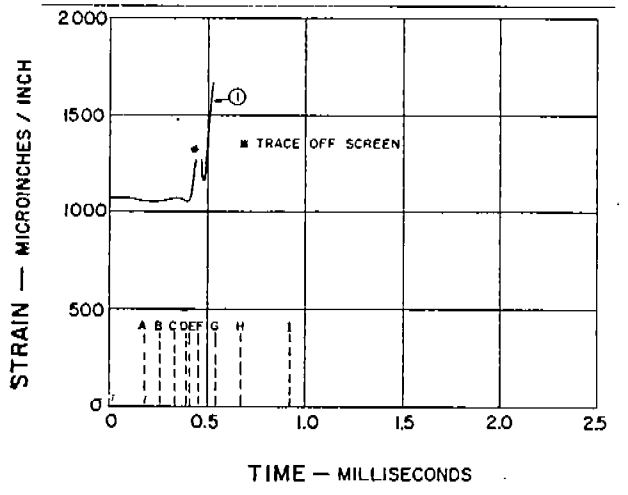

Fig. 17. Instrumentation and Record--Test 7.

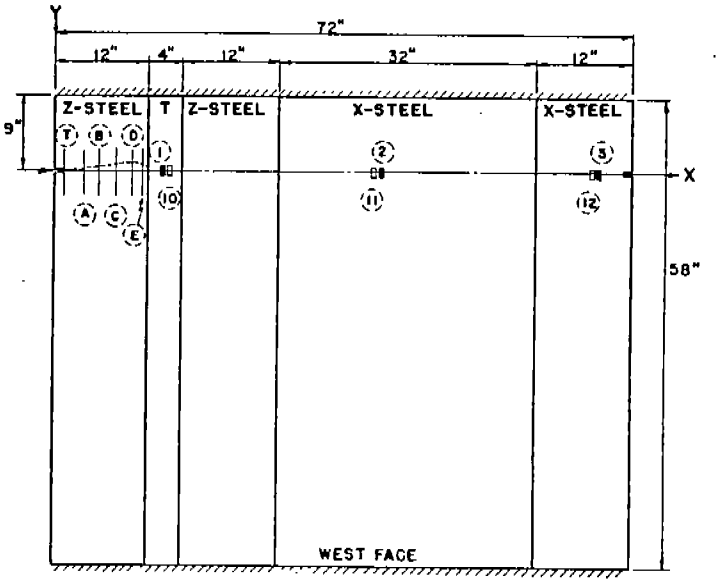

TEST CONDITIONS
AVERAGE STRESS = 33 KSI
TEMPERATURE = −5° F
THEORETICAL IMPACT = 1200 FT. LB.
○ GAGES ON EAST FACE
○ GAGES ON WEST FACE

DYNAMIC STRAIN GAGES			
NO.	X in	Y in	INITIAL STRAIN
1	14.0	0	+ 925
2	41.0	0	+1090
3	68.0	0	+1190

STATIC STRAIN GAGES			
NO	X in	Y in	INITIAL STRAIN
10	14 3	0	+ 925
11	40.6	0	+1090
12	67.7	0	+1190

DETECTORS		
NO.	X in	SPEED ft./sec.
A	3.75	5600
B	5.75	
C	7.75	3050
D	9.75	3600
E	11.50	

CRACK PATH	
X in	Y in
3	+0.06
6	+0.15
9	+0.21
12	+0.28

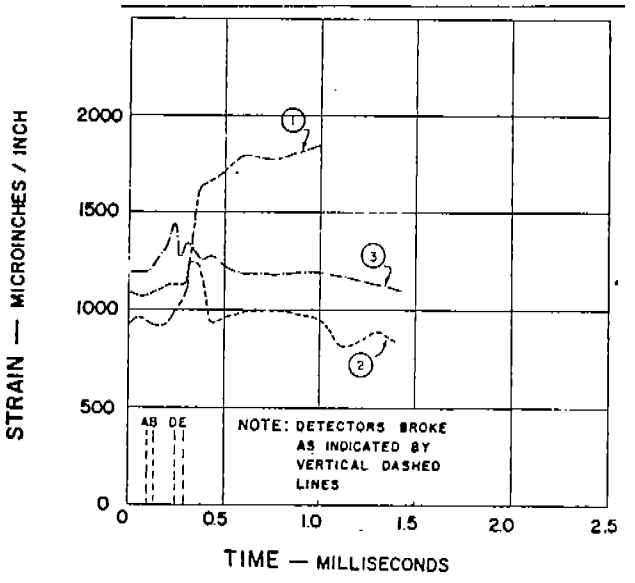

Fig. 18. Instrumentation and Record--Test 8.

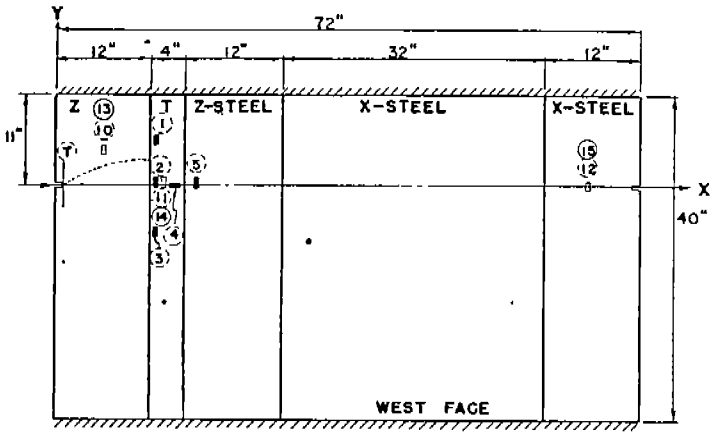

TEST CONDITIONS
AVERAGE STRESS = 29 KSI
TEMPERATURE = −54°F
THEORETICAL IMPACT = 1200 FT. LB.
○ GAGES ON EAST FACE
○ GAGES ON WEST FACE

DYNAMIC STRAIN GAGES			
NO.	X in	Y in	INITIAL STRAIN
1	13.0	+3.0	+1050
2	13.0	0	+1100
3	13.0	−3.0	+1100
4	15.0	0	− 300
5	17.5	0	+1050

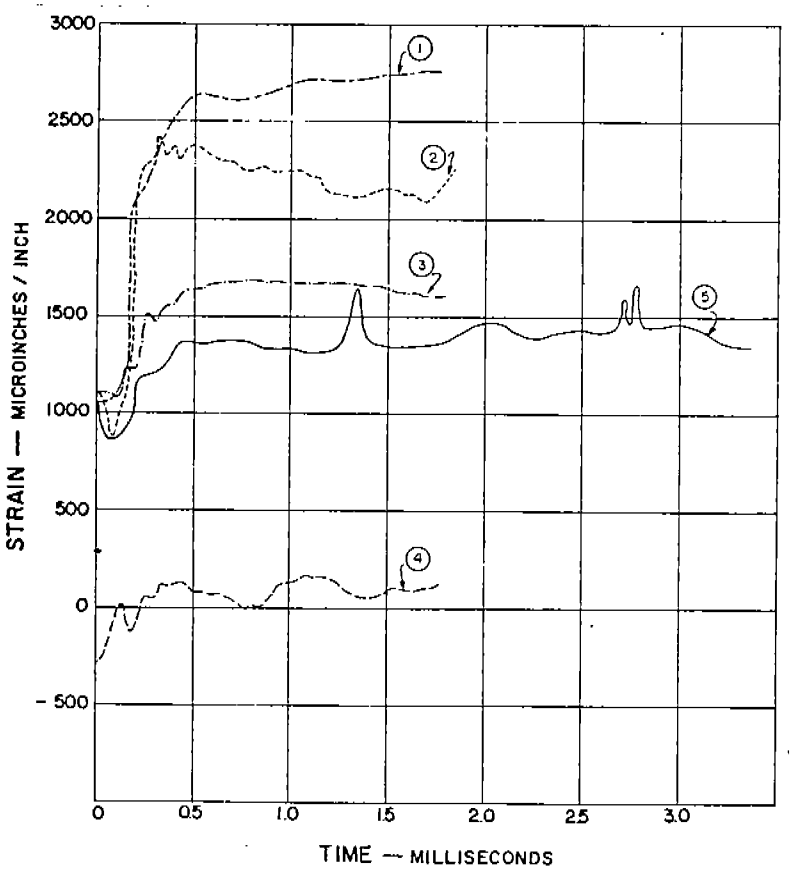

STATIC STRAIN GAGES			
NO.	X in	Y in	INITIAL STRAIN
10	6.0	+2	+1170
11	13.5	0	+1055
12	66.0	0	+1120
13	6.0	+2	+800
14	13.5	0	+ 935
15	66.0	0	+ 935

CRACK PATH	
X in	Y in
3	+0.55
6	+1.00
9	+1.36
12	+1.71
12.8	+1.85

Fig. 19. Instrumentation and Record--Test 9.

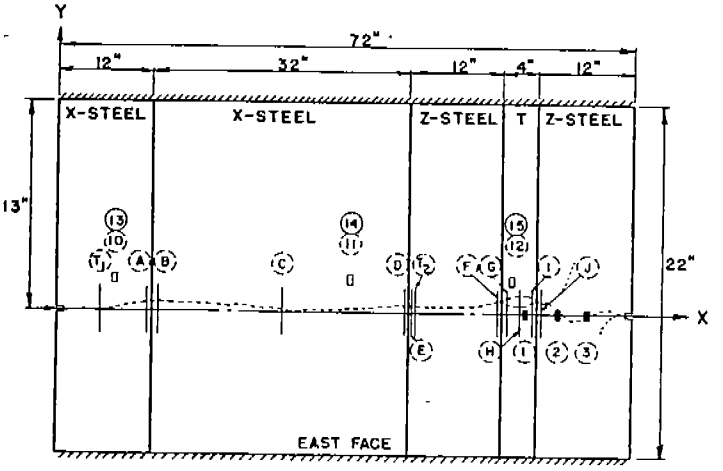

TEST CONDITIONS
AVERAGE STRESS = 27 KSI
TEMPERATURE = -39°F
THEORETICAL IMPACT = 1200 FT. LB.
○ GAGES ON EAST FACE
○ GAGES ON WEST FACE

DYNAMIC STRAIN GAGES			
NO.	X in.	Y in	INITIAL STRAIN
1	58.5	0	+ 850
2	61.5	0	+ 830
3	66.0	0	+ 830

STATIC STRAIN GAGES			
NO.	X in.	Y in.	INITIAL STRAIN
10	7.0	+2	+ 840
11	36.0	+2	+ 850
12	57.2	+2	+ 850
13	7.0	+2	+ 830
14	36.0	+2	+ 800
15	57.2	+2	+ 860

DETECTORS		
NO.	X in.	SPEED ft/sec.
A	11.3	
B	12.8	1900
C	28.1	3300
D	43.2	3200
E	44.7	1800
T_2	45.3	
F	55.3	700
G	56.9	100
H	58.2	
I	59.5	
J	61.1	

CRACK PATH	
X in.	Y in.
12	+0.84
18	+0.50
30	+0.15
44	+0.35
50	+0.55
56	+0.72
66	-0.50
72	0

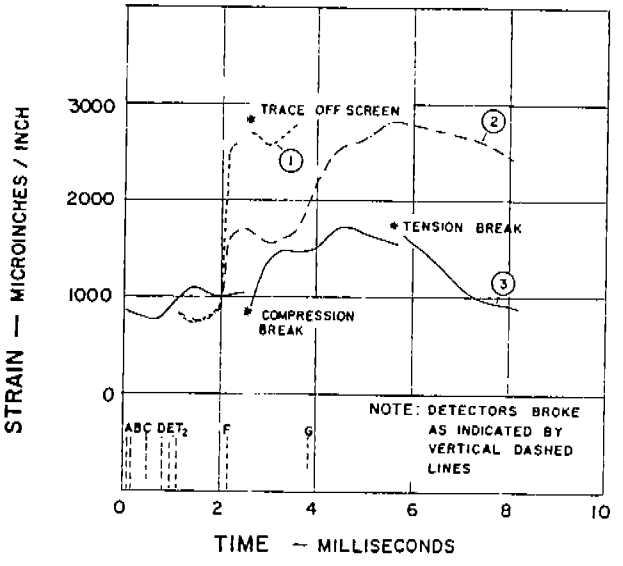

Fig. 20. Instrumentation and Record--Test 10.

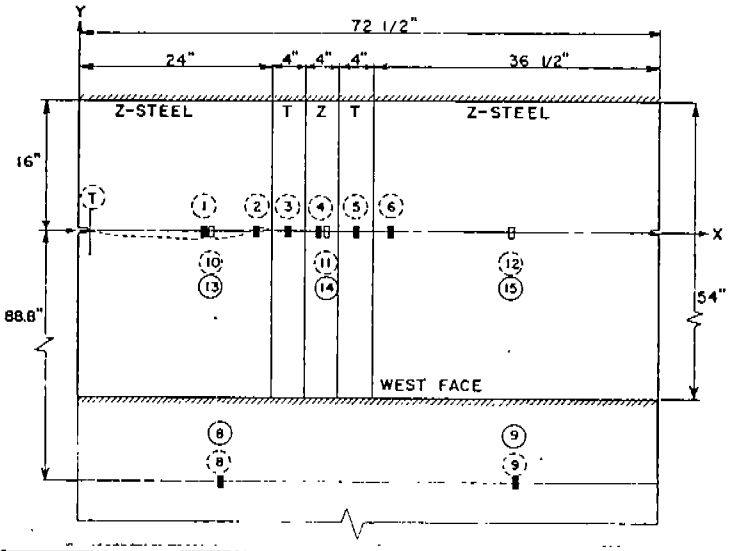

TEST CONDITIONS
AVERAGE STRESS = 28 KSI
TEMPERATURE = -25° F.
THEORETICAL IMPACT = 1200 FT. LB.
◌ GAGES ON EAST FACE
○ GAGES ON WEST FACE

DYNAMIC STRAIN GAGES			
NO.	X in	Y in	INITIAL STRAIN
1	18.0	0	+ 880
2	22.0	0	+ 770
3	26.0	0	+ 880
4	30.5	0	+ 870
5	34.5	0	+ 880
6	38.5	0	+ 890
8	18.0	-88.8	+ 670
9	54.0	-88.8	+ 675

STATIC STRAIN GAGES			
NO.	X in	Y in	INITIAL STRAIN
10	18.5	0	+ 850
11	31.0	0	+ 860
12	54.0	0	+ 860
13	18.5	0	+ 940
14	31.0	0	+ 990
15	54.0	0	+1010

CRACK PATH	
X in.	Y in.
6	-0.30
12	-0.42
18	-0.24
21.5	0
24	+0.15

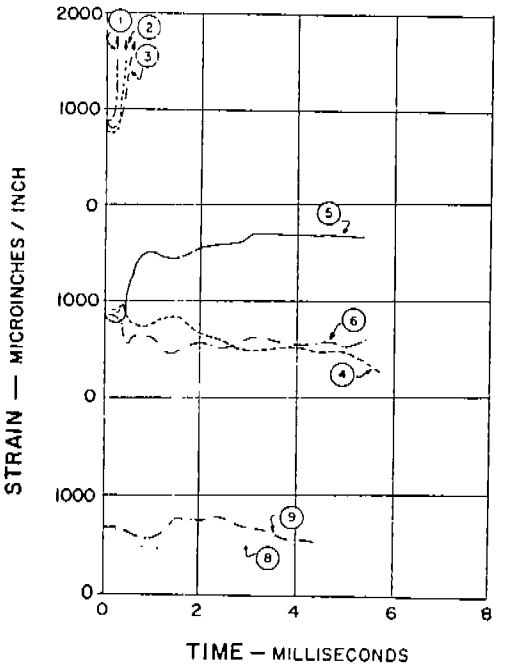

Fig. 21. Instrumentation and Record--Test 11.

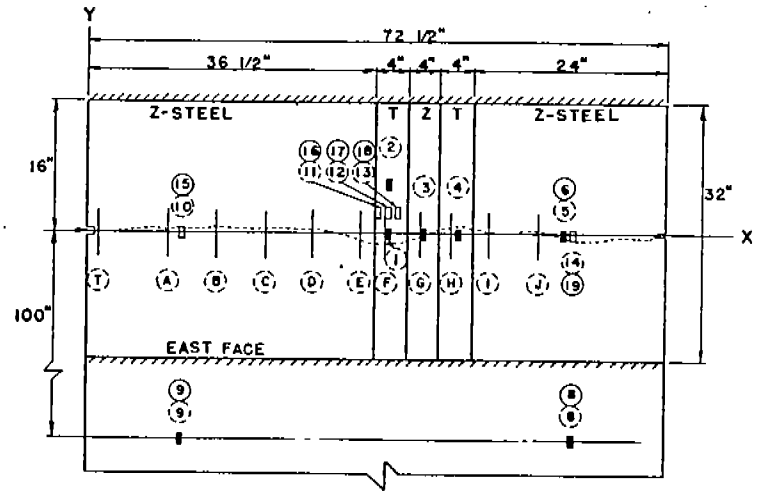

TEST CONDITIONS
AVERAGE STRESS = 28KSI
TEMPERATURE = -18°F
THEORETICAL IMPACT = 1200 FT. LB.
○ GAGES ON EAST FACE
○ GAGES ON WEST FACE

DYNAMIC STRAIN GAGES			
NO.	X in.	Y in.	INITIAL STRAIN
1	38.0	0	+840
2	38.0	+ 6	+940
3	42.3	0	+810
4	46.3	0	+810
5	60.0	0	+770
6	60.0	0	+675
8	54.0	-100	+670
9	12.0	-100	+675

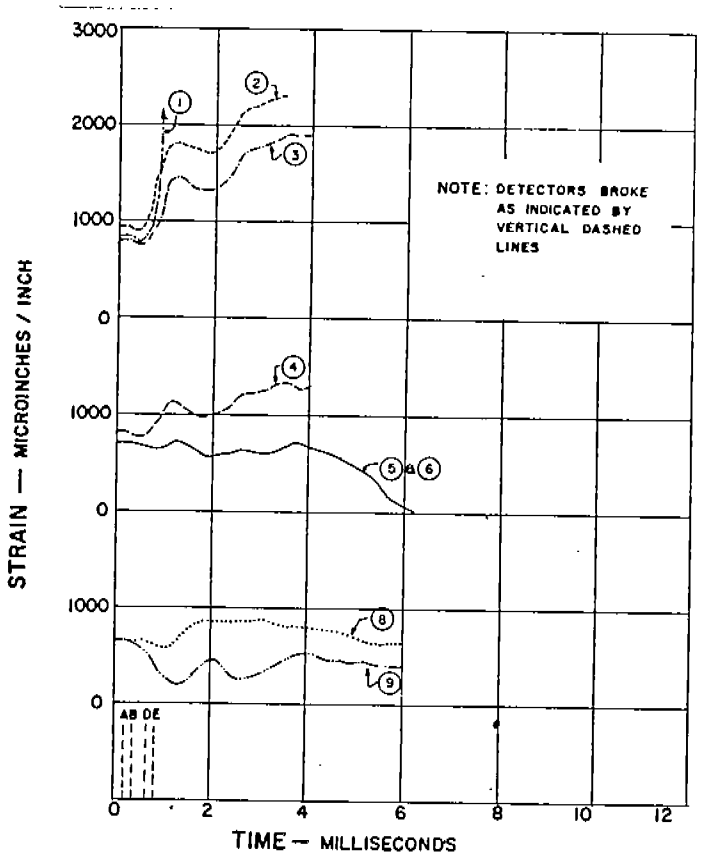

STATIC STRAIN GAGES			
NO.	X in.	Y in.	INITIAL STRAIN
10	12.0	0	+890
11	37.0	+2	+860
12	38.0	+2	+790
13	39.0	+2	+810
14	60.0	0	+780
15	12.0	0	+830
16	37.0	+2	+920
17	38.0	+2	+900
18	39.0	+2	+890
19	60.0	0	+830

DETECTORS		
NO.	X in.	SPEED ft./sec.
A	10.0	
B	16.0	3300
C	22.0	
D	28.0	3350
E	34.0	
F	37.5	2950
G	41.8	
H	45.8	
I	50.5	
J	56.5	

CRACK PATH	
X in.	Y in.
6	+0.40
24	+0.50
31.5	0
36	-0.70
40	-0.70
44	0
46	-0.75
60	0
65	-0.65
72	0

Fig. 22. Instrumentation and Record--Test 12.

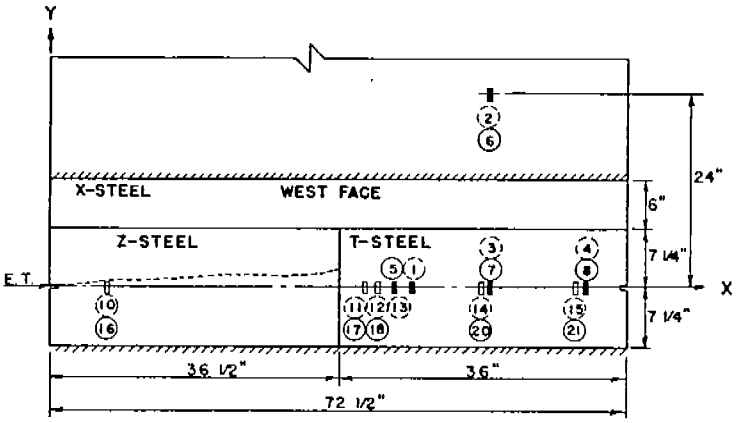

TEST CONDITIONS
AVERAGE STRESS = 28 KSI
TEMPERATURE = −21°F
THEORETICAL IMPACT = 1200 FT LB.
◌ GAGES ON EAST FACE
○ GAGES ON WEST FACE

DYNAMIC STRAIN GAGES			
NO.	X in.	Y In.	INITIAL STRAIN
1	45.5	0	+ 815
2	54.5	+24	+ 650
3	54.5	0	+ 770
4	66.5	0	+ 730
5	43.5	0	+ 995
6	54.5	+24	+ 665
7	54.5	0	+1060
8	66.5	0	+1055

STATIC STRAIN GAGES			
NO.	X in.	Y in.	INITIAL STRAIN
10	6.5	0	+ 770
11	39.5	0	+ 790
12	41.5	0	+ 795
13	43.5	0	+ 795
14	54.0	0	+ 740
15	66.0	0	+ 635
16	6.5	0	+ 985
17	39.5	0	+1000
18	41.5	0	+ 975
20	54.0	0	+1030
21	66.0	0	+ 970

CRACK PATH	
X in.	Y in.
6	+ 0.47
12	+ 0.90
18	+ 1.25
24	+ 1.30
30	+ 1.55
36	+ 2.05

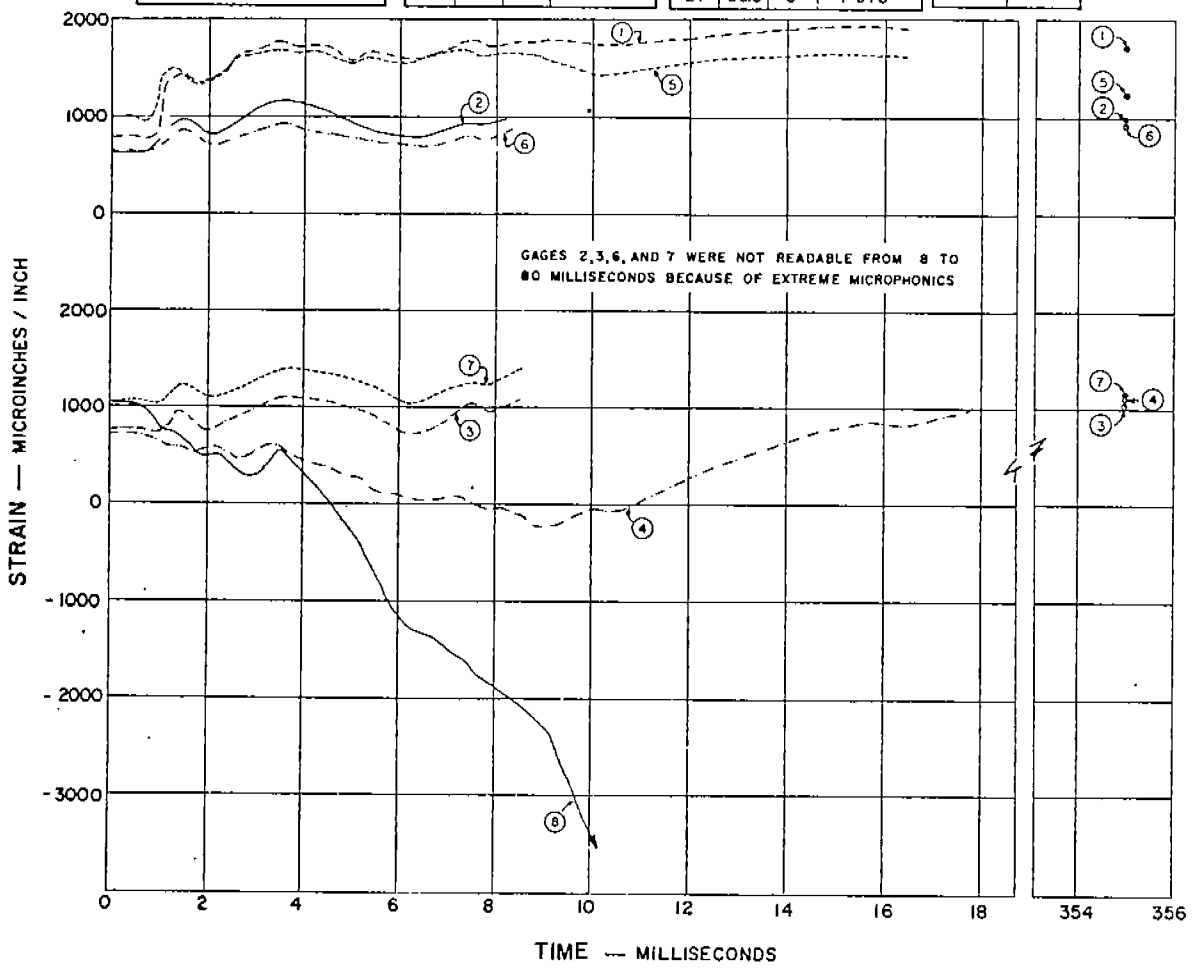

Fig. 23. Instrumentation and Record--Test 14.

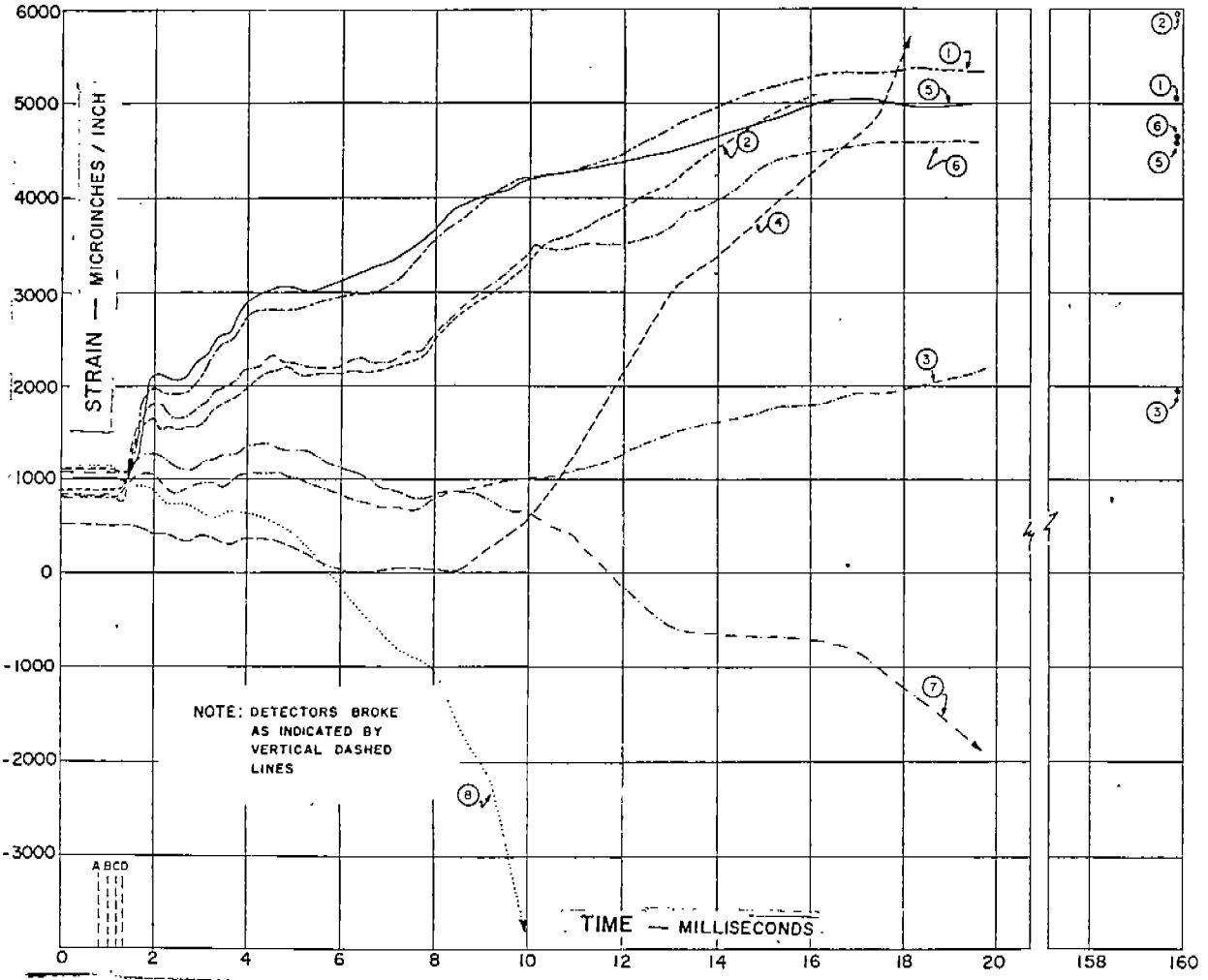

TEST CONDITIONS
AVERAGE STRESS = 28 KSI
TEMPERATURE = -24°F
THEORETICAL IMPACT = 1200 FT LB
○ GAGES ON EAST FACE
○ GAGES ON WEST FACE

DYNAMIC STRAIN GAGES			
NO.	X in.	Y in.	INITIAL STRAIN
1	40.0	0	+ 830
2	44.0	0	+ 875
3	54.5	0	+ 815
4	66.5	0	+ 505
5	40.0	0	+ 990
6	44.0	0	+1070
7	54.5	0	+1110
8	66.5	0	+1150

STATIC STRAIN GAGES			
NO.	X in.	Y in.	INITIAL STRAIN
10	6.5	0	+ 685
12	40.5	0	+ 910
13	43.5	0	+ 730
14	54.0	0	+ 880
15	66.0	0	+ 530
16	6.5	0	+1100
17	38.0	0	+ 970
18	40.5	0	+1030
19	43.5	0	+1010
20	54.0	0	+ 910
21	66.0	0	+1265

DETECTORS		
NO.	X in.	SPEED ft./sec.
A	6.0	
B	13.0	3600
C	20.0	3450
D	27.0	3500
E	34.0	

CRACK PATH	
X in.	Y in.
6	+0.60
12	+1.30
18	+2.00
24	+2.85
30	+3.65
36	+4.20
37	+4.90

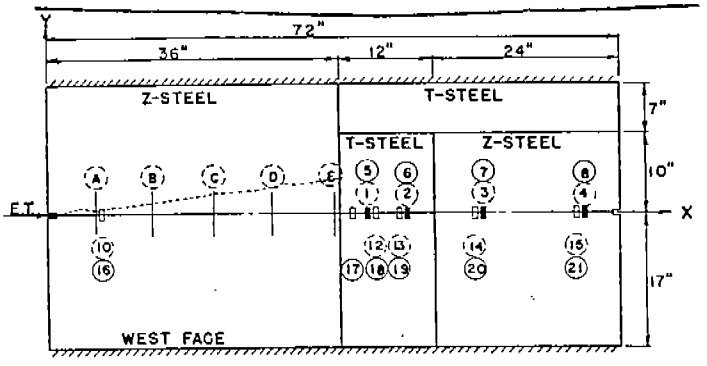

Fig. 24. Instrumentation and Record--Test 15.

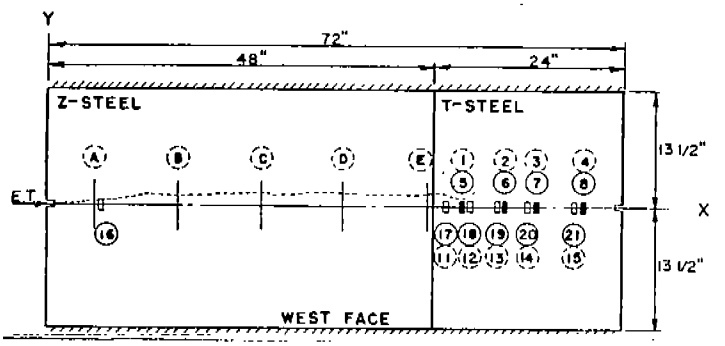

CRACK PATH	
X in.	Y in.
6	+0.60
12	+1.25
18	+1.32
24	+1.50
36	+1.45
42	+1.40
48	+1.40
51	+0.95
54	+1.48

TEST CONDITIONS
AVERAGE STRESS = 28 KSI
TEMPERATURE = -22°F.
THEORETICAL IMPACT = 1200 FT. LB.
◌ GAGES ON EAST FACE
○ GAGES ON WEST FACE

DYNAMIC STRAIN GAGES			
NO.	X in.	Y in.	INITIAL STRAIN
1	52.0	0	+ 905
2	56.0	0	+ 930
3	60.0	0	+ 920
4	66.5	0	+ 940
5	52.0	0	+ 965
6	56.0	0	+ 920
7	60.0	0	+ 900
8	66.5	0	+ 895

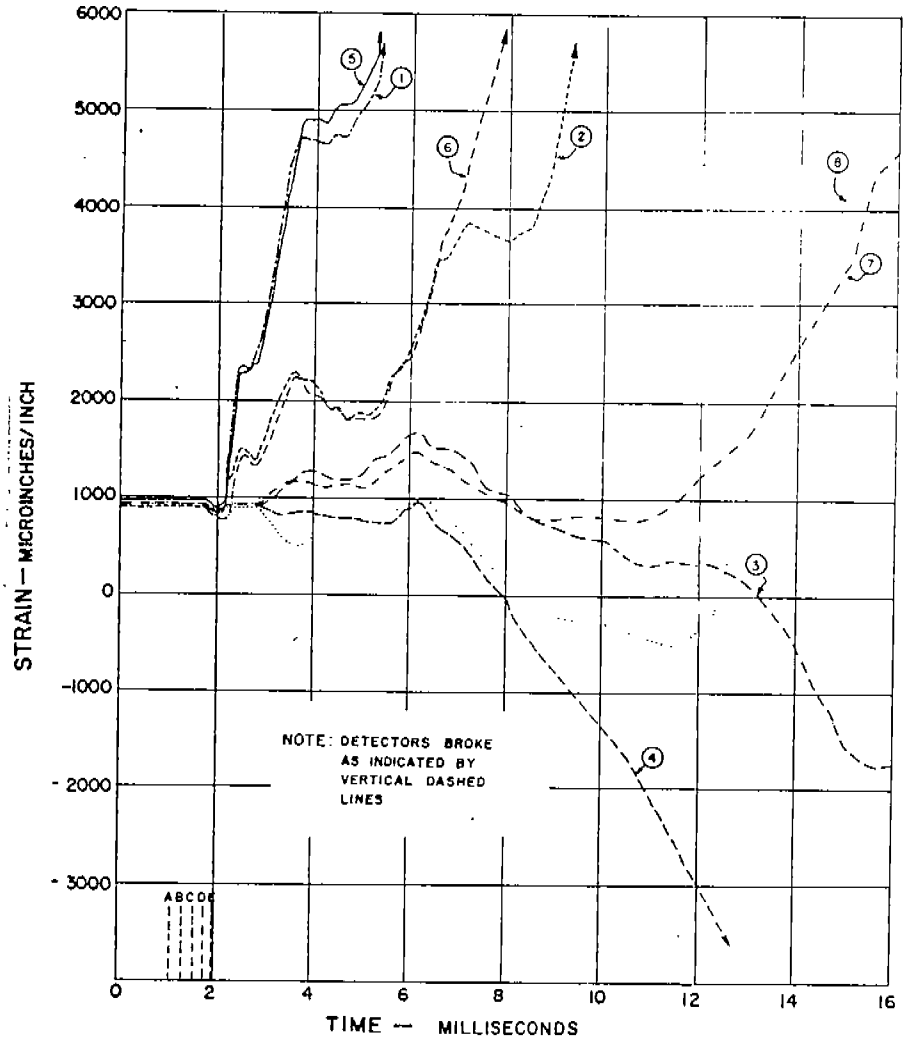

STATIC STRAIN GAGES			
NO.	X in.	Y in.	INITIAL STRAIN
11	50.0	0	+ 960
12	52.5	0	+ 885
13	55.5	0	+ 970
14	59.5	0	+ 900
15	66.0	0	+ 835
16	6.5	0	+ 920
17	50.0	0	+ 985
18	52.5	0	+ 990
19	55.5	0	+ 965
20	59.5	0	+ 930
21	66.0	0	+ 930

DETECTORS		
NO.	X in.	SPEED ft./sec
A	6.0	
B	16.0	3200
C	26.0	3600
D	36.0	3600
E	46.0	4900

Fig. 25. Instrumentation and Record--Test 16.

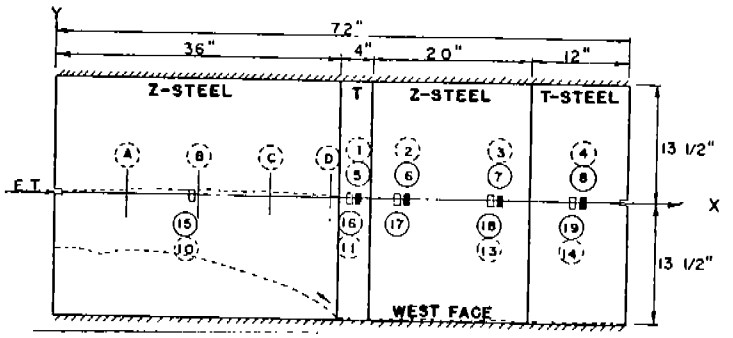

TEST CONDITIONS
AVERAGE STRESS = 28KSI
TEMPERATURE = −20° F.
THEORETICAL IMPACT = 1200 FT. LB.
◌ GAGES ON EAST FACE
○ GAGES ON WEST FACE

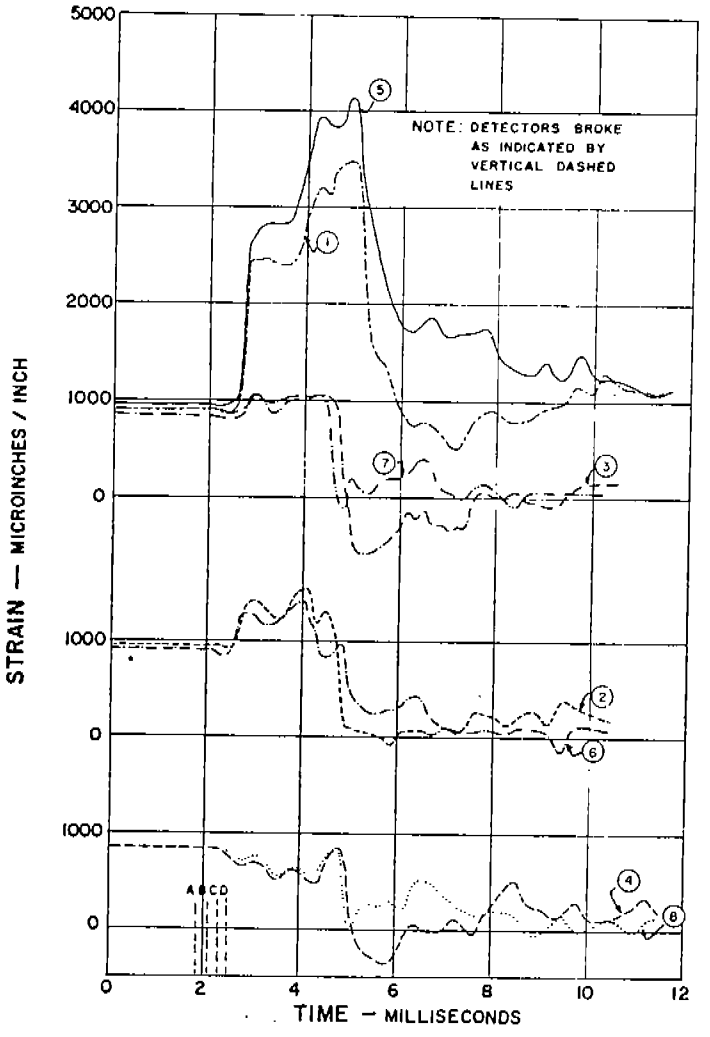

DYNAMIC STRAIN GAGES			
NO.	X in.	Y in.	INITIAL STRAIN
1	38.0	0	+900
2	44.0	0	+950
3	56.0	0	+895
4	66.0	0	+840
5	38.0	0	+960
6	44.0	0	+910
7	56.0	0	+835
8	66.0	0	+840

STATIC STRAIN GAGES			
NO.	X in.	Y in	INITIAL STRAIN
10	17.0	0	+910
11	37.5	0	+945
13	55.5	0	+950
14	65.5	0	+900
15	17.0	0	+980
16	37.5	0	+930
17	43.5	0	+930
18	55.5	0	+950
19	65.5	0	+890

DETECTORS		
NO.	X in.	SPEED ft./sec.
A	9.0	
B	18.0	3400
C	27.0	3450
D	35.0	3800

CRACK PATH	
X in	Y in.
6	+0.35
12	+0.70
18	+0.78
24	+0.67
30	+0.52
36	+0.40

Fig. 26. Instrumentation and Record--Test 17.

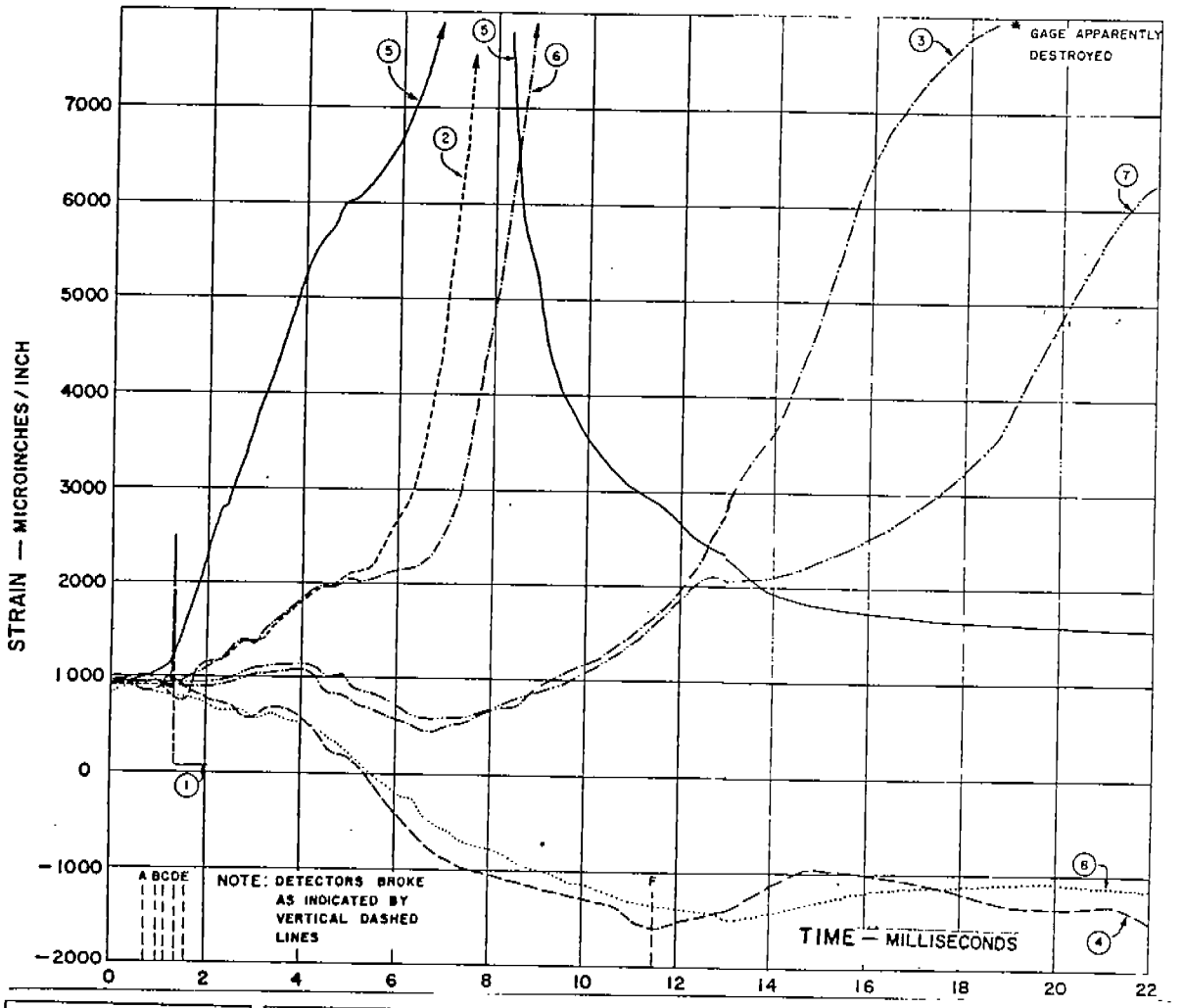

TEST CONDITIONS
AVERAGE STRESS = 2.8 KSI
TEMPERATURE = -13°F
THEORETICAL IMPACT = 1200 FT. LB
◯ GAGES ON EAST FACE
○ GAGES ON WEST FACE

DYNAMIC STRAIN GAGES			
NO.	X in.	Y In.	INITIAL STRAIN
1	23.0	0	+ 930
3	55.5	0	+ 920
4	66.0	0	+ 955
5	37.5	0	+ 940
6	44.0	0	+ 925
7	55.5	0	+ 945
8	66.0	0	+ 825

STATIC STRAIN GAGES			
NO.	X in	Y in	INITIAL STRAIN
10	16.5	0	+ 880
14	65.5	0	+ 800
15	16.5	0	+ 910
16	38.0	0	+ 900
17	43.5	0	+ 860
18	56.0	0	+ 880
19	65.5	0	+ 810

DETECTORS		
NO.	X in	SPEED ft./sec.
A	3.0	
B	11.0	2900
C	19.0	4750
D	27.0	2800
E	35.0	3350
F	45.0	
G	50.0	50
H	55.0	50
I	59.0	3350

CRACK PATH	
X in	Y in
11	-0.14
23	-0.74
35	-1.10
40.3	-0.84
48.5	0
53	+0.28
57	0
60	-1.40
61.5	-1.80

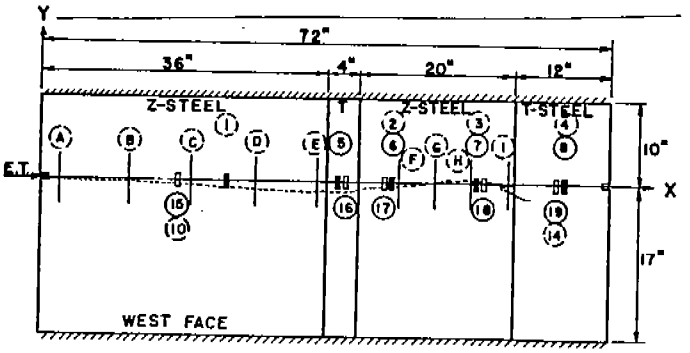

Fig. 27. Instrumentation and Record--Test 18.

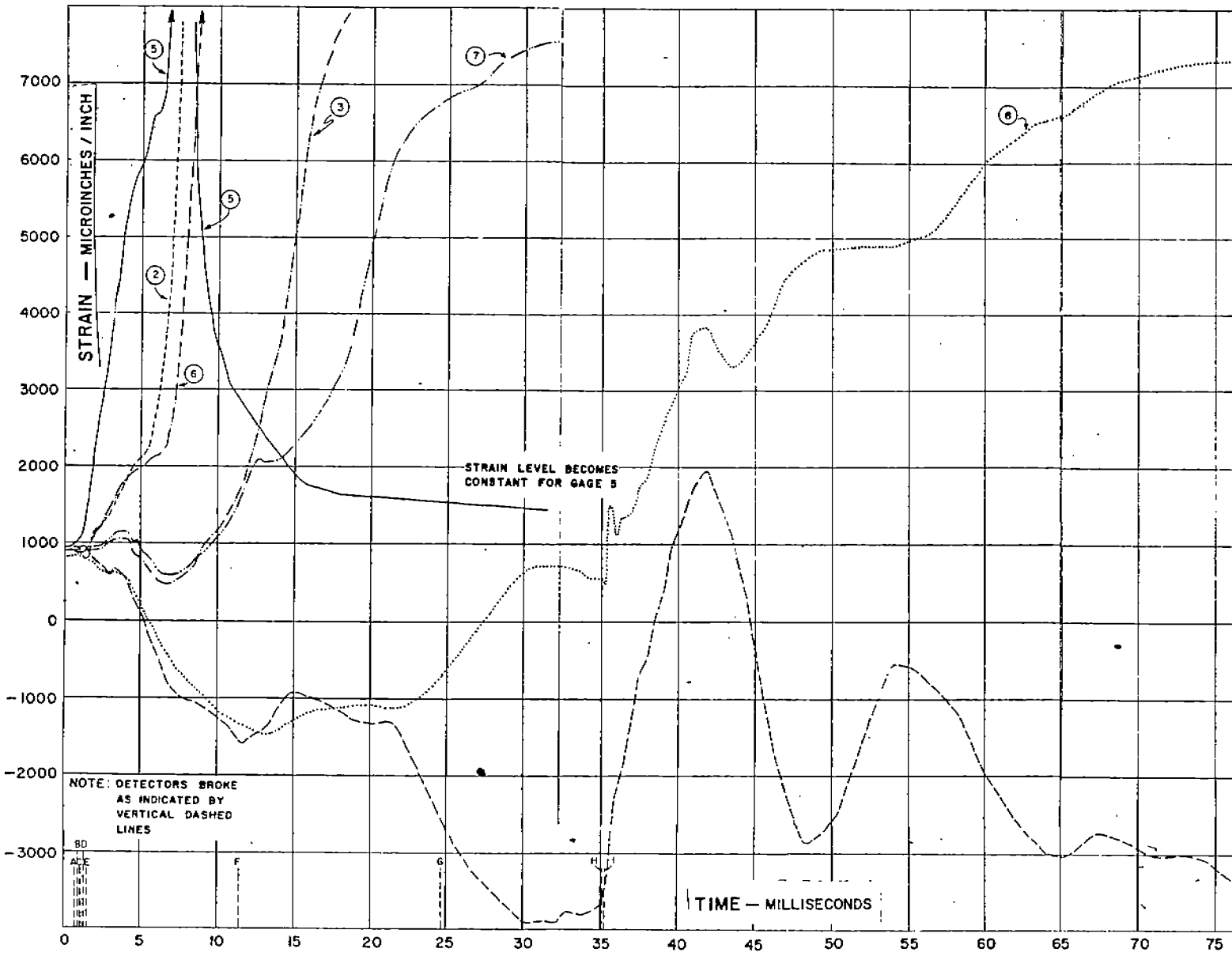

Fig. 28. Dynamic Strain Record--Test 18.

TABLE 3

SUMMARY OF TESTS ON 6-FT WIDE WELDED ARRESTOR SPECIMENS CONTAINING T-1 STEEL STRAKES

Test (Plate No.)	Width of Starter Material (in.)	Initial Load (kips)	Avg. Stress on Net Section (ksi)	Avg. Temp. (°F)
These tests were conducted on 6-ft wide specimens in a 3,000,000 lb hydraulic testing machine. The test specimen is an insert 3/4 in. thick x 72 in. wide with the depth varying from 18 to 58 in. The insert is welded to 1 in. pull-plates (each pull-plate was approximately 6 3/4 ft long for Tests 4-14 and 3 1/2 ft long for Tests 15-18) using double "V" butt welds - E7016 electrodes. All vertical welds within the specimen are double "V" butt welds made with E12015 electrodes. A theoretical impact of 1200 ft-lb was used in all tests. Notch length was 1 in. in Tests 4-10 (see Table 1) and 1 1/8 in. for Tests 11-18. Following the first fracture test on a given specimen, the fracture is generally cut out and the remaining portion of the insert used for a second or third test. The initial test on an insert is designated by an (A), the second test by a (B), and the third test by a (C) in the "Remarks" section. Strain gages and/or crack detectors were mounted on all specimens in this series.				
The 3/4 x 56 x 72 in. insert consisted of 12 in. of rimmed E-steel, 12 in. of T-steel, and 48 in. of semikilled X-steel. This insert was cut and rewelded for three tests.				
4 (STE-1)	12	1310	25.0	-35
Remarks: (A) Final load - 1290 kips. Crack propagated 12 in. to near side of weld. Entire record lost.				
5 (STE-2)	12	1310	25.0	10
Remarks: (B) Final load - 1290 kips. Crack propagated 12 in. to near side of weld. Partial record, good quality.				
6 (STE-3)	12	1750	33.0	-13
Remarks: (C) Final load - 1735 kips. Crack propagated 12 in. to near side of weld. Complete record, good quality.				
The 3/4 x 18 x 72 in. insert consisted of 28 in. of Z-steel and 44 in. of X-steel.				
7 (RRS-1)	12	1600	30.0	-10
Remarks: (A) Complete fracture. Secondary crack initiation at welded-over notch 1 ft from far edge. Partial record, poor quality.				

TABLE 3 (Continued)

Test (Plate No.)	Width of Starter Material (in.)	Initial Load (kips)	Avg. Stress on Net Section (ksi)	Avg. Temp. (°F)
The 3/4 x 58 x 72 in. insert consisted of 12 in. of Z-steel, 4 in. of T-steel, 12 in. of Z-steel, and 44 in. of X-steel. This insert was cut and rewelded for three tests.				
8 (RTRS-1)	12	1750	33.0	-5
Remarks: (A) Final load - 1730 kips. Crack propagated 12 in. to near side of weld. Complete record, good quality.				
9 (RTRS-2)	12	1575	30.0	-54
Remarks: (B) Final load - 1550 kips. Crack propagated 12 in. to weld and penetrated 0.85 in. into T-steel on east side. Complete record, good quality.				
10 (RTRS-3)	56	1415	27.0	-39
Remarks: (C) Complete fracture. Fracture surface on 45° plane through T-steel. Far side slightly buckled. Complete record, fair quality.				
Notch length changed from 1 in. to 1 1/8 in. The notch now consists of a slot which is four hacksaw blades wide (approx. 0.141 in.) for the first one inch, one hacksaw blade wide (approx. 0.034 in.) for the next 1/16 in., and one jeweler's-saw cut wide (approx. 0.012 in.) for the remaining 1/16 in.				
The 3/4 x 54 x 72 in. insert consisted of 24 in. of Z-steel, 4 in. of T-steel, 4 in. of Z-steel, 4 in. of T-steel, and 36 in. of Z-steel. This insert was cut and rewelded for two tests.				
11 (RTRT-1)	24	1475	28.0	-25
Remarks: (A) Final load - 1320 kips. Crack propagated 24 in. to near side of weld. Complete record, good quality.				
12 (RTRT-2)	36	1475	28.0	-18
Remarks: (B) Complete fracture in about ten seconds. Extreme buckling on far side. Fracture surface on 45° plane through T-steel. Complete record, good quality.				

TABLE 3 (Continued)

Test (Plate No.)	Width of Starter Material (in.)	Initial Load (kips)	Avg. Stress on Net Section (ksi)	Avg. Temp. (°F)
	The 3/4 x 54 x 72 in. insert consisted of 36 in. of Z-steel and 36 in. of T-steel. This insert was cut and rewelded for two tests.			
13 (RT-1)	36	1475	28.0	8
Remarks: (A) Final load - 860 kips. Crack propagated 36 in. to weld and penetrated 1.5 in. into T-steel. No visible buckling. Entire record lost because of severe condensation.				
14 (RT-2)	36	1475	28.0	-21
Remarks: (B) Final load - 800 kips. Crack propagated 36 in. to weld and then along the weld for about 1 in. No visible buckling. Partial record, good quality.				
	The 3/4 x 34 x 72 in. insert consisted of 36 in. of Z-steel, 12 in. of T-steel, and 24 in. of Z-steel.			
15 (RTR-1)	36	1475	28.0	-24
Remarks: (C) Final load - 900 kips. Crack propagated 36 in. to weld and penetrated 1 in. into T-steel. Extreme buckling occurred on far side. Complete record, good quality.				
	The 3/4 x 27 x 72 in. insert consisted of 48 in. of Z-steel and 24 in. of T-steel.			
16 (RT-3)	48	1475	28.0	-22
Remarks: (A) Final load - 260 kips. Crack propagated 48 in. to weld and penetrated 6 in. into T-steel. Severe buckling occurred in the remaining 18 in. of T-steel. Complete record, good quality.				
	The 3/4 x 27 x 72 in. insert consisted of 36 in. of Z-steel, 4 in. of T-steel, 20 in. of Z-steel, and 12 in. of T-steel.			
17 (RTRT-3)	36	1475	28.0	-20
Remarks: (A) Crack propagated 36 in. to weld and stopped. During load redistribution, a secondary crack was initiated at the junction of the insert and lower pull plate, resulting in complete fracture. Complete record, good quality.				

TABLE 3 (Continued)

Test (Plate No.)	Width of Starter Material (in.)	Initial Load (kips)	Avg. Stress on Net Section (ksi)	Avg. Temp. (°F)
The 3/4 x 27 x 72 in. insert consisted of 36 in. of Z-steel, 4 in. of T-steel, 20 in. of Z-steel, and 12 in. of T-steel.				
18 (RTRT-4)	36	1475	28.0	-13
Remarks: (A) Final load - 85 kips. Crack propagated 36 in. to weld, crossed 4 in. strip of T-steel and 20 in. strip of Z-steel, then penetrated 1.5 in. into 12 in. strip of T-steel. Fracture surface on 45° plane in T-steel. Extreme buckling occurred on far side. Complete record, good quality.				

from the dynamic gages. In all cases the strain traces start at a level corresponding to the initial test-load strain so that absolute values of strain variation are shown. For tests where crack detectors were included, the detector breaking time is indicated on the record to designate the approximate location of the crack front.

The quality of the records from the tests varies considerably. Poor records may result from faulty triggering, poor connections, improper focus of camera or oscilloscope, or so much overlapping of the strain traces that individual traces are difficult to follow. In some cases only partial records were obtained--that is, only some of the strain traces were recorded.

An examination of the figures reveals that the duration of the strain records in Tests 5-12 was relatively short, varying from 0.5 to 8 millisec. These strain records are presented in their entirety. The selected record duration (oscilloscope sweep time) for each test was based on the results obtained from previous tests and on what was considered to be a sufficient interval at the time. Unfortunately, some of the selected times appear to have been too short to record the specimen behavior during and after the redistribution of load.

As the length of the starter material was increased, records over a

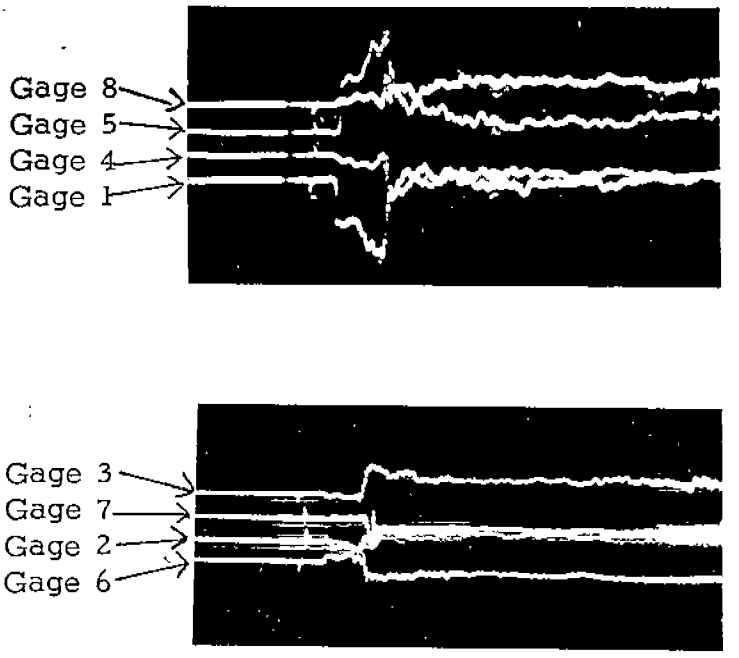

Fig. 29. Photographic Records for Test 17.

longer interval of time became necessary. Moving film was used to record the strain responses for all dynamic gages in Tests 14-18 for relatively long periods of time (355 millisec. in Test 14). Photographs of a typical dynamic record (considered to be of good quality) taken on moving film are presented in Fig. 29.

In many of the dynamic strain records, the plot of one or more strain responses is shown to terminate in an arrowhead. The trace for such a gage generally exhibits an extremely rapid rise and leaves the scope face when it records a magnitude of strain greater than the sensitivity set on the oscilloscope. Once this gage has "peaked out," it usually does not reappear on the scope face within the duration of the record.

Dynamic Strain Measurements. Since a limited number of channels were available for dynamic strain measurements, gages were placed initially at various locations thoughout the plate so that a feeling for the magnitude of strains to be expected in subsequent tests could be developed. As the tests continued and more information became available, it appeared that the most useful strain

measurements would come from gages located on the notch line in what was expected to be unfractured material. It was also found advantageous to place all gages back-to-back, and this was done in Tests 14-18.

In the majority of the tests, the overall quality of the records was good, although occasionally short portions of the traces were not readable because of extreme microphonics or pronounced overlapping. In a few tests, only a partial record was obtained when some of the intended dynamic traces were lost because of condensation and shorting of the circuits. It must be emphasized that the observations that follow represent the general behavior of the majority of gages, and there may be some exceptions that were observed but cannot be satisfactorily explained.

It appears that there are three factors which may contribute to the strain pattern of the dynamic strain gages. The first is the effect of the notch-wedge-impact method of crack initiation on the strain distribution in the specimen. From a series of striking tests,[16] it was found that gages in the general vicinity of the notch recorded strains as high as 220 μ in./in., but, for gages located 8 in. or more from the tip of the notch (on the notch line), a strain response over 50 μ in./in. was not measured for any gage. These results indicate that the effect of impact on the strain pattern of the gages may be neglected.

The second factor is the effect of the large strain increment that accompanies the tip of the crack on the behavior of the strain gages. If the crack detectors locate the approximate position of the propagating crack, the records indicate that there is, in general, little change in strain level in the uncracked portion of the plate that is beyond the sphere of influence of the crack front. This would indicate that even though there is a reduction in the net section as the crack is progressing across the plate the strain and corresponding load on the remaining section do not change during the fracture process.

The third and probably most influential effect on the total strain pattern is the redistribution of load after the fracture has been stopped. In many

of the tests prior to the use of moving film (Tests 5-12), the duration of the record may have been too short for the strain pattern to be influenced by the redistribution of load. Also, three of these specimens (Tests 5, 8, and 9) contained a crack only 12 in. long, and a redistribution of load on the remaining net section (5 ft wide) does not substantially affect the initial strain level in the specimen. In Test 12, the average reading of back-to-back gages 5 and 6 shows a definite reduction in strain level at about 4 millisec.which may indicate the initial influence of a redistribution of load.

In Tests 14-18, four of the dynamic gages (3, 4, 7, and 8) were located on an area of the plate that was not subjected to the sphere of influence of the propagating crack front. Consequently, the major portion of strain pattern may be considered to be the result of the redistribution of load. The remaining gages (1, 2, 5, and 6) were usually placed sufficiently close to the point of initial arrest to ensure that their strain pattern would be affected by both the propagating crack front and the redistribution of load. From a study of the test records, there seems to be a pattern in the strain responses from those gages that is influenced by both the propagating crack front and the redistribution of load. This pattern appears to be composed of three stages which may be described as follows. The first stage is the increase in strain as a result of the influence of the approaching crack front. When the crack is stopped at the butt weld, the strain levels off approximately and then starts to increase again. This second increase in strain is probably caused by the beginning of the load redistribution. Once again the strain levels off and then may increase either gradually or suddenly. This last stage of increasing strain could be the result of either the transfer of load because of inelastic buckling at the far side of the plate or the extension of the crack into the T-steel because of the redistribution of load, or a combination of both effects.

An examination of the strain records from Tests 14-18 clearly shows a similarity in strain pattern for the gages located back-to-back. However, this similarity does not usually prevail throughout the entire duration of the

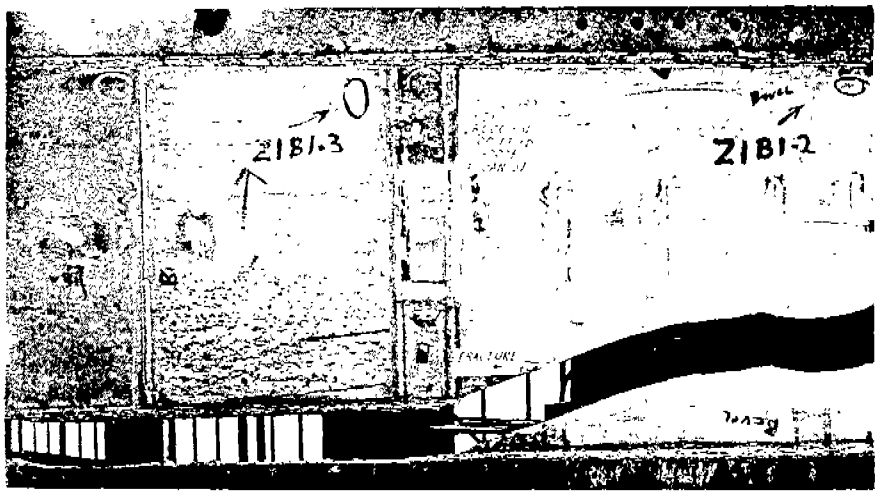

(a) Crack Path of Initial and Secondary Fracture

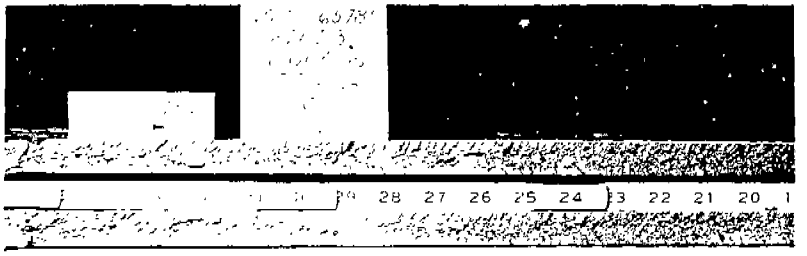

(b) Crack Texture of Secondary Fracture in Z-Steel

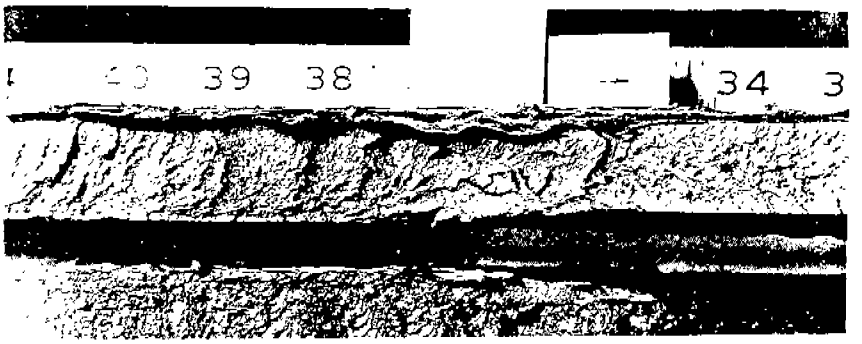

(c) Fractured Surface at Possible Source of Secondary Fracture

Fig. 30. Initial and Secondary Fracture in Test 17.

strain record. In Tests 14, 15, and 16, the strain responses of gages 4 and 8 diverge markedly between 4 and 12 millisec. indicating the beginning of buckling on the far side of the plate. In Test 18, gages 4 and 8 indicate the beginning of buckling at approximately 23 millisec. This time variation in the first indication of buckling may be attributed to variation in the alignment of the pull-plates, difference in the geometry of the specimen, or difference in

the resistance of Z- and T-steel to inelastic buckling. When the area of buckling was extensive (Tests 15 and 16), the strain pattern of gages 3 and 7 also diverged eventually.

In Test 17, an unusual strain pattern developed because of an unexpected occurrence after the fracture was initiated and propagated to the arrestor material. Apparently, during the initial stage of load redistribution, a secondary crack initiated in the butt weld joining the insert plate to the bottom pull-plate. This secondary crack caused a complete fracture in the specimen on a section approximately 1 ft below the notch line, as shown in Fig. 30. The chevron pattern in the 36-in. strip of Z-steel shows that the secondary fracture propagated from the center to the edge of the plate. However, the fracture surface in the weld between the insert and pull-plate offers no information on the direction of crack propagation. In Fig. 26 it can be seen that all the gages on this specimen start to decrease in strain between 4.5 and 5.0 millisec. This probably represents the time that the fracture propagated along the weld between the insert and pull-plate. All gages except 1 and 5 decrease to strains that correspond fairly well to the initial values at zero load. The strains from gages 1 and 5 show some permanent set, probably because they experienced high magnitudes of strain for about 2 millisec.

With the introduction of moving film (Test 14), the strain history of a gage could be obtained for several hundred millisec. if the gage did not "peak out" or fail in some other manner. This relatively long strain record presented an opportunity to determine the time required for the gage responses to reach a relatively stationary level of strain. Figures 23 and 24 present the strain levels measured at time intervals of 355 and 160 millisec. in Tests 14 and 15 respectively. Within minor deviations, the values at 18 to 20 millisec. are in good agreement with the last readings plotted. Actually, there are mild oscillations between these times, but it was found that at a time of approximately 100 millisec. a reasonably constant "final" strain value could be obtained.

The strain distribution across the plate at various times selected during Tests 14, 15, and 17 is shown in Figs. 31—33. These figures illustrate

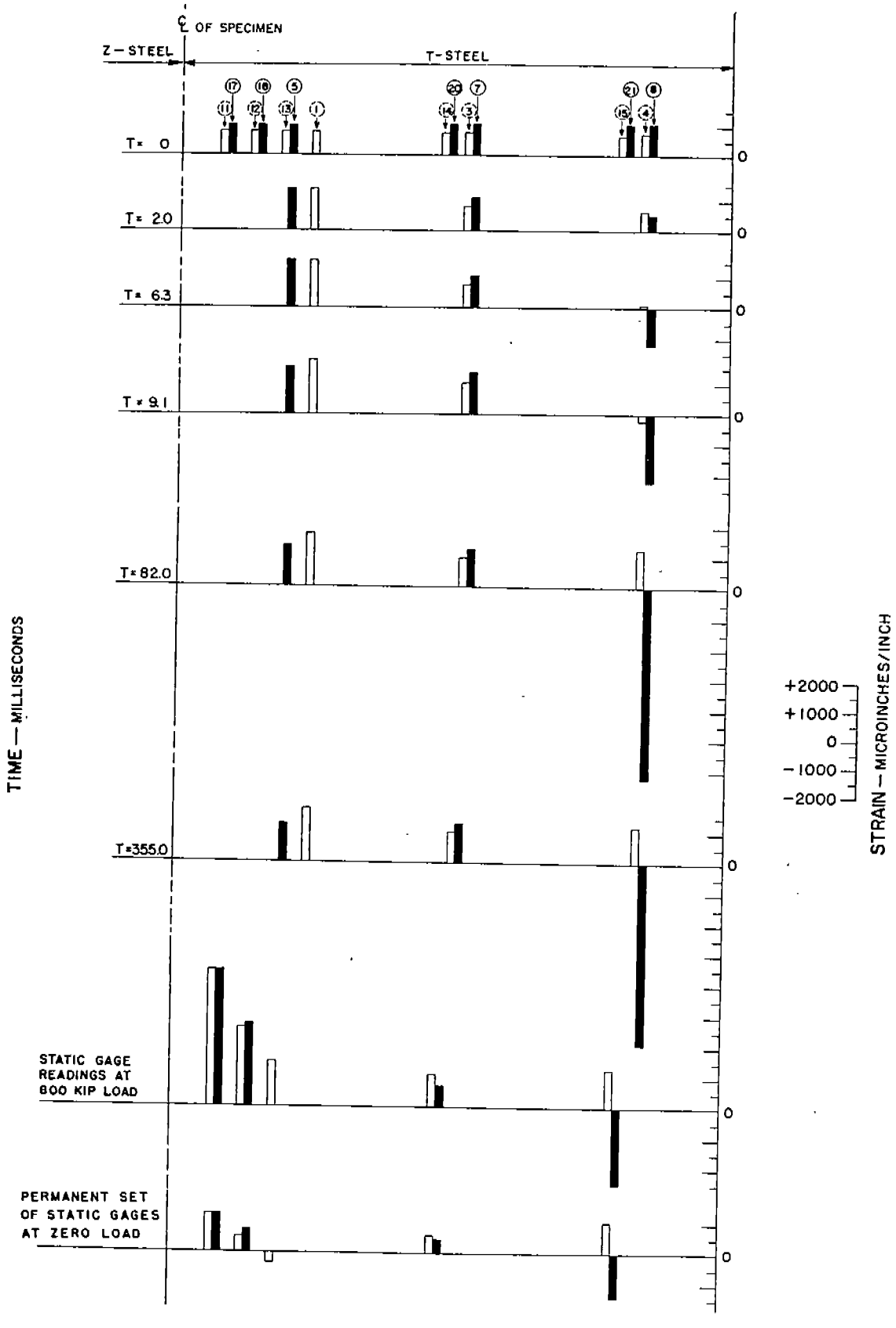

Fig. 31. Strain Distribution at Various Times--Test 14.

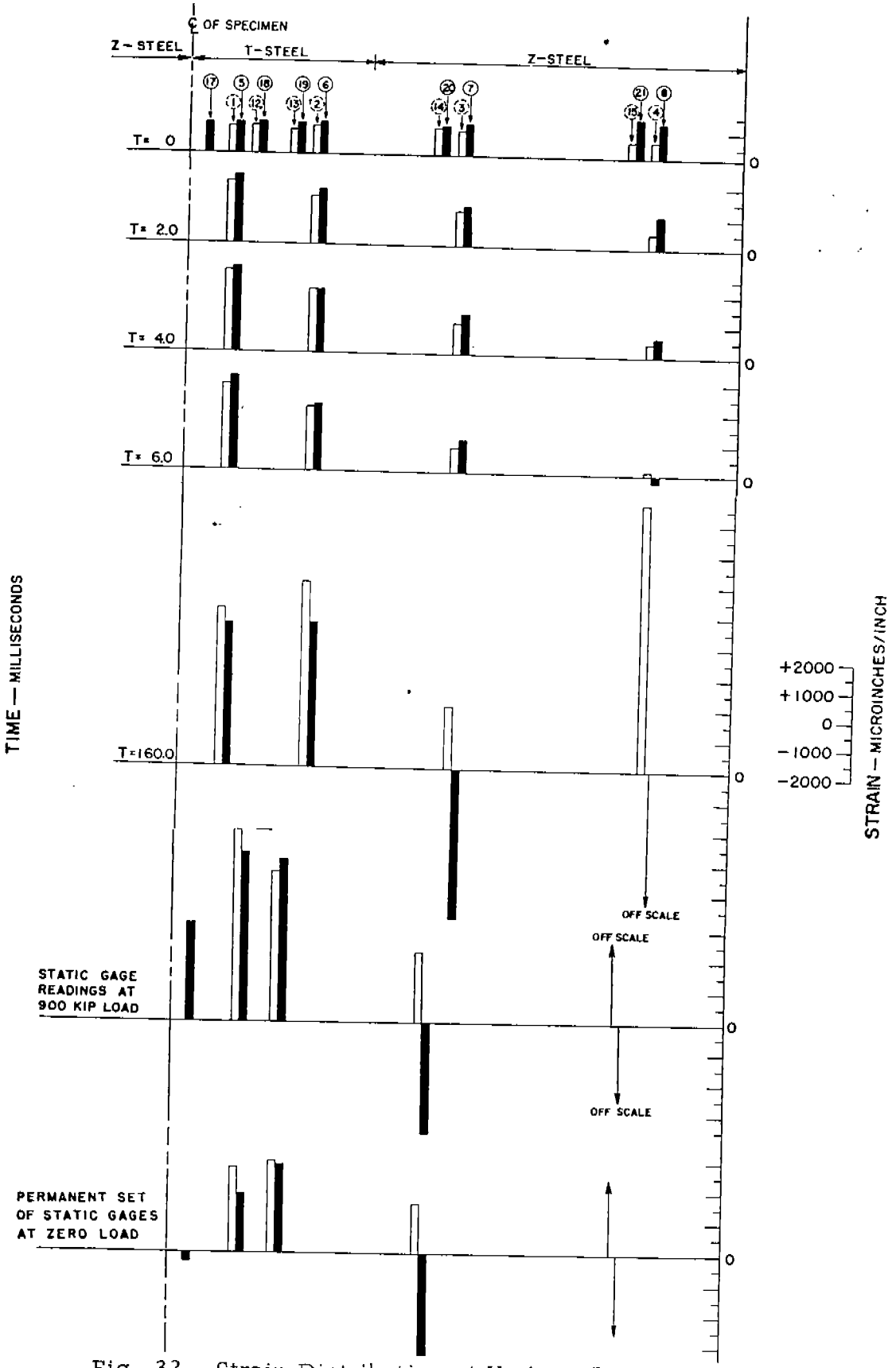

Fig. 32. Strain Distribution at Various Times--Test 15.

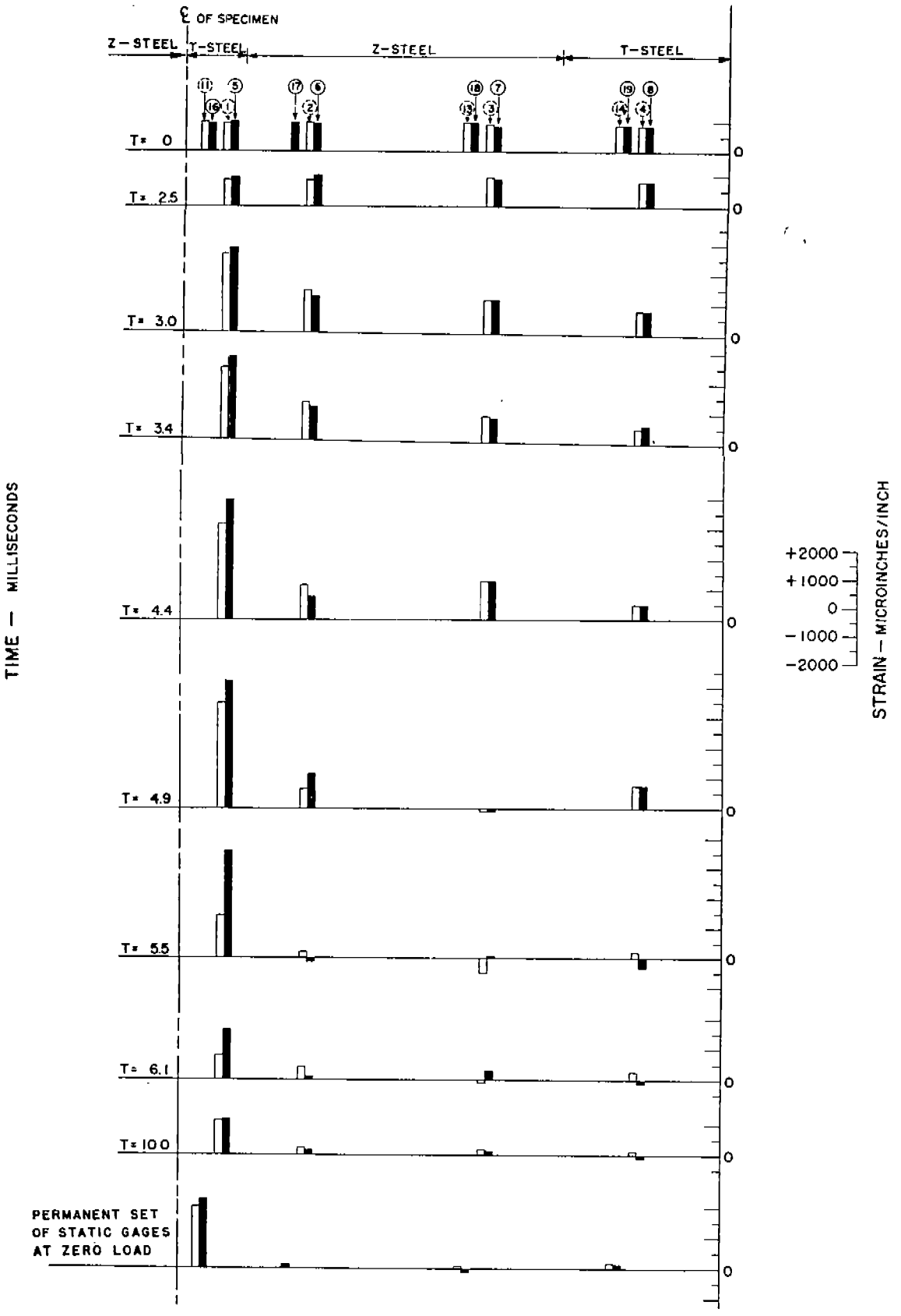

Fig. 33. Strain Distribution at Various Times--Test 17.

more clearly the strain distribution across the remaining net section during the redistribution of load. Also, they permit a convenient comparison between the last dynamic strain readings shown and the static values read after the test. This comparison is discussed in more detail in the section immediately following.

Static Strain Measurements. Early in the testing program, the general purpose of the static strain gages was to measure the strain level across the width of the specimen and the bending developed in the insert plate. In the majority of the specimens tested, the strain level at test load was nearly uniform throughout the plate. However in some tests it was observed that the strain distribution varied considerably across the width of the test piece and through the thickness. In one of these specimens (Test 15), base strains were found to vary by as much as 380 μ in./in. across the width of the plate on one side only (gages 12 and 15). Also, in the thickness direction, a difference as high as 735 μ in./in. was recorded by back-to-back gages 15 and 21. In spite of this large difference in strain, the average of these back-to-back gages is 900 μ in./in., which is in good agreement with the computed strain of 935 μ in./in.

As the testing program advanced, it was found advantageous to place a static gage 1/2 in. from each dynamic gage. This readily provided a replacement for a dynamic gage which may have shorted out during the cooling process or was found to be unsatisfactory during the calibration period immediately before the test (which accounts for the interruptions in consecutive numbering of the static gages that appear on some of the instrumentation drawings). Secondly, the level of strain recorded by the static gages after the test could be compared with the strains recorded by the dynamic gages during the test.

From Figs. 31–33, a comparison can be made between the static strain measurements (taken under the existing load immediately after the test) and the last dynamic strain recorded. In general, the sense and magnitude of strains from static and dynamic readings are in good agreement considering that a comparison is being made of strains measured by gages

1/2 in. apart on the plate. In areas of the plate subjected to high strains or considerable buckling, a marked difference in strain level can exist between two gages located only 1/2 in. apart.

Fracture Speeds. The speeds of brittle fracture propagation measured on the plate surfaces of E-, Z-, and X-steels are summarized in Fig. 34 for these tests. In the majority of tests reported, the speed measurements were restricted to the starter material, and the spacing of the crack detectors was determined to some extent by the width of starter strip available. To examine these results, the fracture speed measurements are divided into the following groups: (1) specimens in which the detectors were spaced approximately 2 in. apart (Tests 5-8); (2) specimens in which the detectors were spaced from 6 to 15 in. apart (Tests 10, 12, and 15-18); and (3) specimens in which the speed was measured across vertical butt welds made with E12015 electrodes (Tests 7 and 10).

In the first group, the fracture speeds varied from 2000 to 5600 fps. However, this wide variation represents the two extremes of calculated speed, and, except for three values, most of the speeds are in the 2000 to 4100 fps range. For the tests in this group, the average net stress varied from 25 to 33 ksi; the temperature ranged from 10 to -13 F; and either E- or Z-steel was used for the starter material. Because of the variation in measurements obtained for each individual specimen, no effect of any of these variables on crack speed can be observed.

As wider starter strips were used, the detector spacing was increased, and for Tests 10, 12, and 15-18 the spacing between most detectors varied from 6 to 15 in., although for any individual specimen the spacing was approximately constant. In all cases but one (discussed in the following paragraph), the speed measured over these distances ranged from 2800 to 4900 fps. However, this range is not representative of the majority of the speed measurements, because, with the exception of 4750 and 4900 fps, the speeds range from 2800 to 3800 fps. All of the speeds in this group were measured on Z-steel at an average net stress of 28 ksi and a temperature around -20 F, except for Test 10 where measurements

TEST NO.	AVERAGE STRESS, KSI.	TEMP. DEGREES F.	DISTANCE FROM INITIATION EDGE — FEET (0 1 2 3 4 5 6)
5	25	+10	2000 4050 2700 (A B C D)
6	33	-13	2350 2600 2100 2400 (A B C D E)
7	30	-10	2150 2300 3150 2550 5200 4600 500 (A B C D E F G H I)
8	33	-5	5600 3050 3600 (A B D E)
10	27	-39	1900 3300 3200 1800 700 100 (A B C D E T_2 F G)
12	28	-18	3300 3350 2950 (A B D E)
15	28	-24	3600 3450 3500 (A B C D)
16	28	-22	3200 3600 3600 4900 (A B C D E)
17	28	-20	3400 3450 3800 (A B C D)
18	28	-13	2900 4750 2800 3350 (A B C D E); 50 50 3350 (F G H I)
19	26.8	+1	2450 4950 4600 (B C D E)
20	26.8	-19	4100 (A); 2650 3450 (B C D)
22	26.8	-20	750 (A B)

Fig. 34. Summary of Fracture Speeds in Six-Foot Wide Arrestor Specimens.

were made on X-steel at a slightly lower stress and temperature. Neglecting the slight differences in stress and temperature, the speeds of crack propagation in the two different steels are in agreement.

In Test 10, a substantially lower crack speed (700 fps) is evident in the Z-steel between the second trigger T_2 and detector F. The reason for this reduced crack speed is not clear, but there is evidence from the response of the dynamic gages that there was some delay in the breaking time recorded for detector F.

In Test 18, the reliability of the speeds recorded by the detectors in the 20-in. wide strip of Z-steel is highly questionable for several reasons. First, there was extremely high strain in the area of detector F because of the redistribution of load, and it is quite possible that this strain may have stretched the detector a sufficient amount to break it prematurely before the actual crack was present. Also, there is some doubt as to the reliability of the breaking time of detector I because the fracture path branched slightly near detector I, as shown in Fig. 35(b). However, because of the greater reduction in plate thickness measured across the major portion of this 20-in. strip of Z-steel (see Fig. 36), it seems reasonable to expect a somewhat slower speed in this material.

In Tests 7 and 10, the average speed measured across the vertical butt welds and short segments of the plate material ranged from 500 to 2550 fps. A reduced speed through the welds seems reasonable since a close inspection of the fractured surfaces usually indicated some ductility in the weld. In Test 10, the substantially lower fracture speed of 100 fps between detectors F and G is highly questionable since, in another specimen (Test 13), a detector placed on T-steel was found broken as a result of the high strain and not the presence of an actual fracture in that area. Since T-steel exhibits considerably more strain before fracturing than either E-, X-, or Z-steels, results from detectors mounted on T-steel should not be combined with data from detectors mounted on other steels to compute average crack speeds.

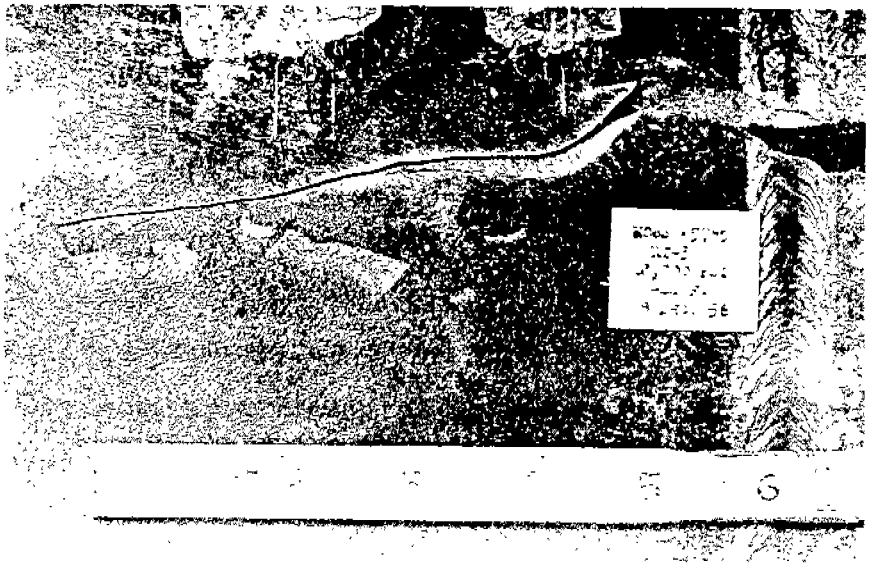

(a) Test 16, 24 in. T-Steel Strake

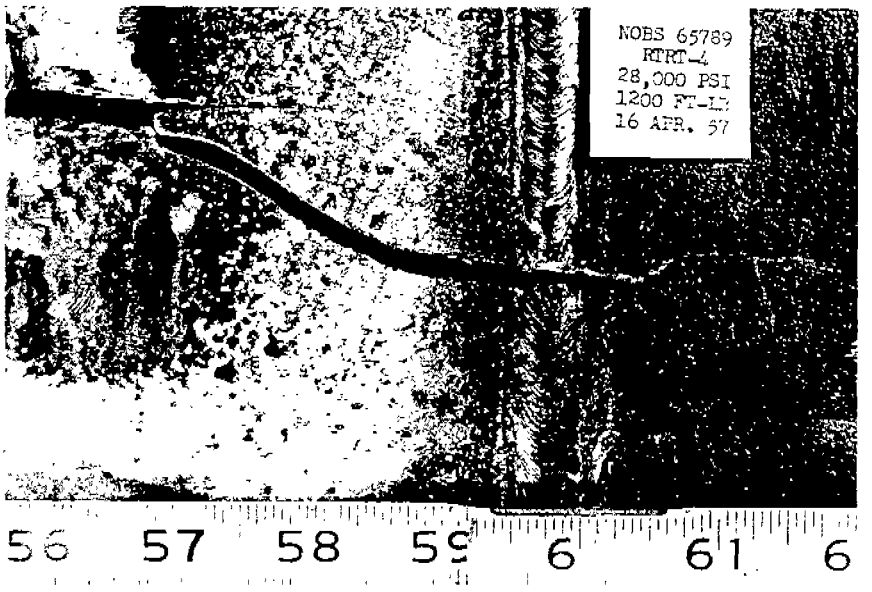

(b) Test 18, 12 in. T-Steel Strake

Fig. 35. Arrest of 48 and 60 in. Long Cracks--Tests 16 and 18.

In conclusion, the speeds measured between the more widely spaced detectors are more uniform and, for the most part, fall within the range of 2800 to 3800 fps. In most cases the speed measurements made on plain plate specimens of Z-steel (Project SR-137) were of about the same magnitude when determined from detectors. Variation in speed is more apparent between closely spaced detectors, and this may be further evidence that the fracture progresses across the plate in an irregular manner.[16]

Reduction in Plate Thickness. The reduction in plate thickness along the crack path for eight specimens (Tests 4, 9, 10, 11, 12, 13, 16, and 18) is presented in Figs. 36 and 37. These values were obtained at various points by careful measurements with a pair of micrometer calipers.

In all of these tests, the reduction in thickness in the starter material (E, Z, or X) varied from approximately 1/2 to 2 per cent. However, in Tests 10, 12, and 18, a reduction in plate thickness as high as 10 per cent was measured in those sections of Z-steel that experienced high strains prior to fracture. The fractured surfaces in these strips of Z-steel still exhibited the familiar chevron pattern which was prevalent in the starter strips. An illustration of this can be seen in Fig. 38 (Test 12).

Reduction in plate thickness as high as 11.5 per cent was measured in the strakes of T-steel where the fracture had crossed or partially penetrated this material. For those fractures that had partially penetrated the T-steel, the reduction in thickness at the point of arrest varied from about 7.5 to 11 per cent, except for Test 9, where the crack penetrated approximately 0.85 in. on one side of the plate and the reduction in thickness at the point of arrest was slightly less than one per cent.

For strakes of T-steel not penetrated by a propagating crack, the measured reduction in thickness was about one per cent in Test 4, although in similar specimens (Tests 5 and 6), no reduction in thickness could be measured. In Test 11, a reduction of plate thickness of 4.5 per cent was measured in the first 4-in. strake of T-steel, clearly indicating the presence of very high strains in that area.

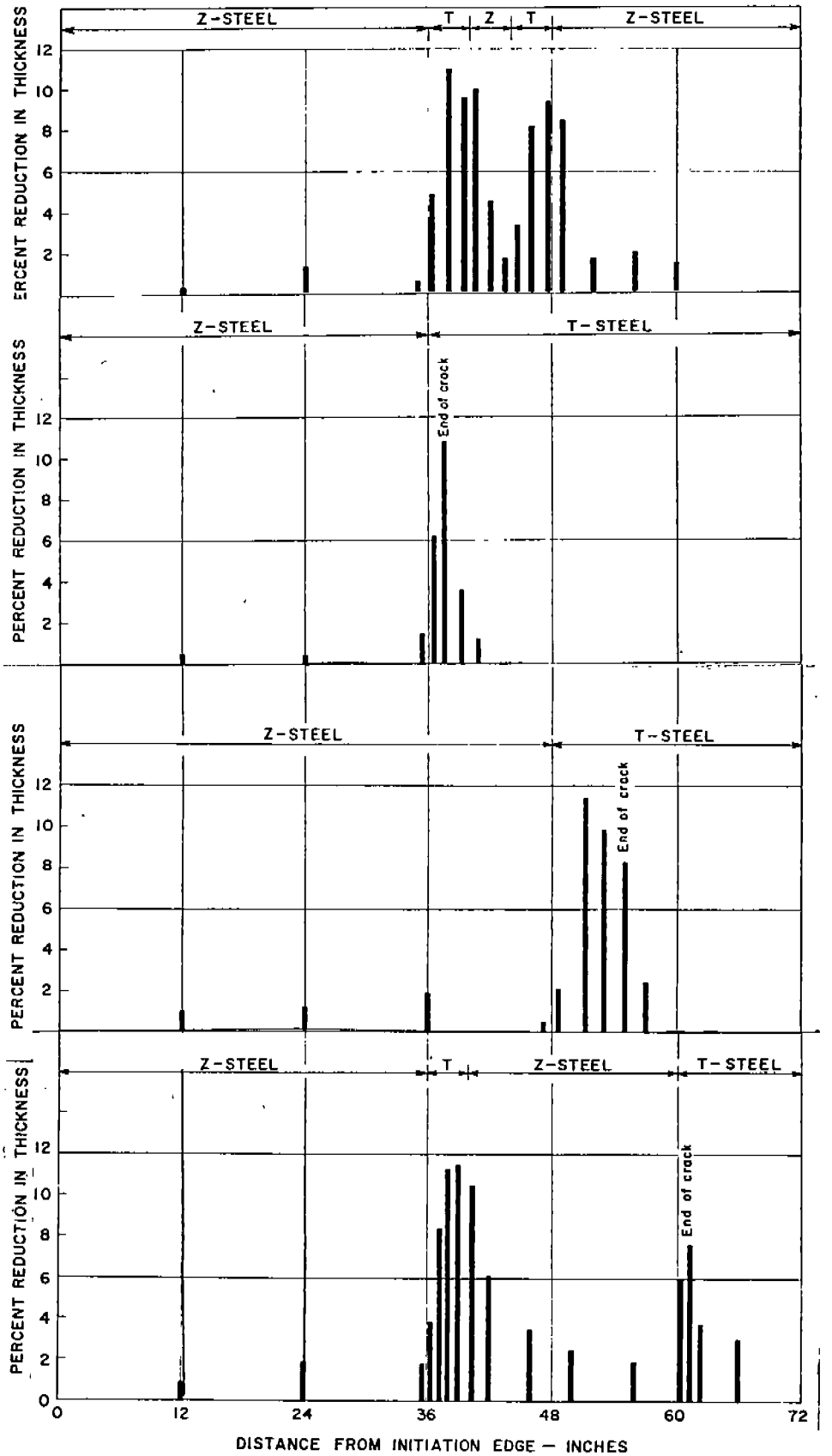

Fig. 36. Reduction in Plate Thickness along the Crack Path--Tests 12, 13, 16, 18.

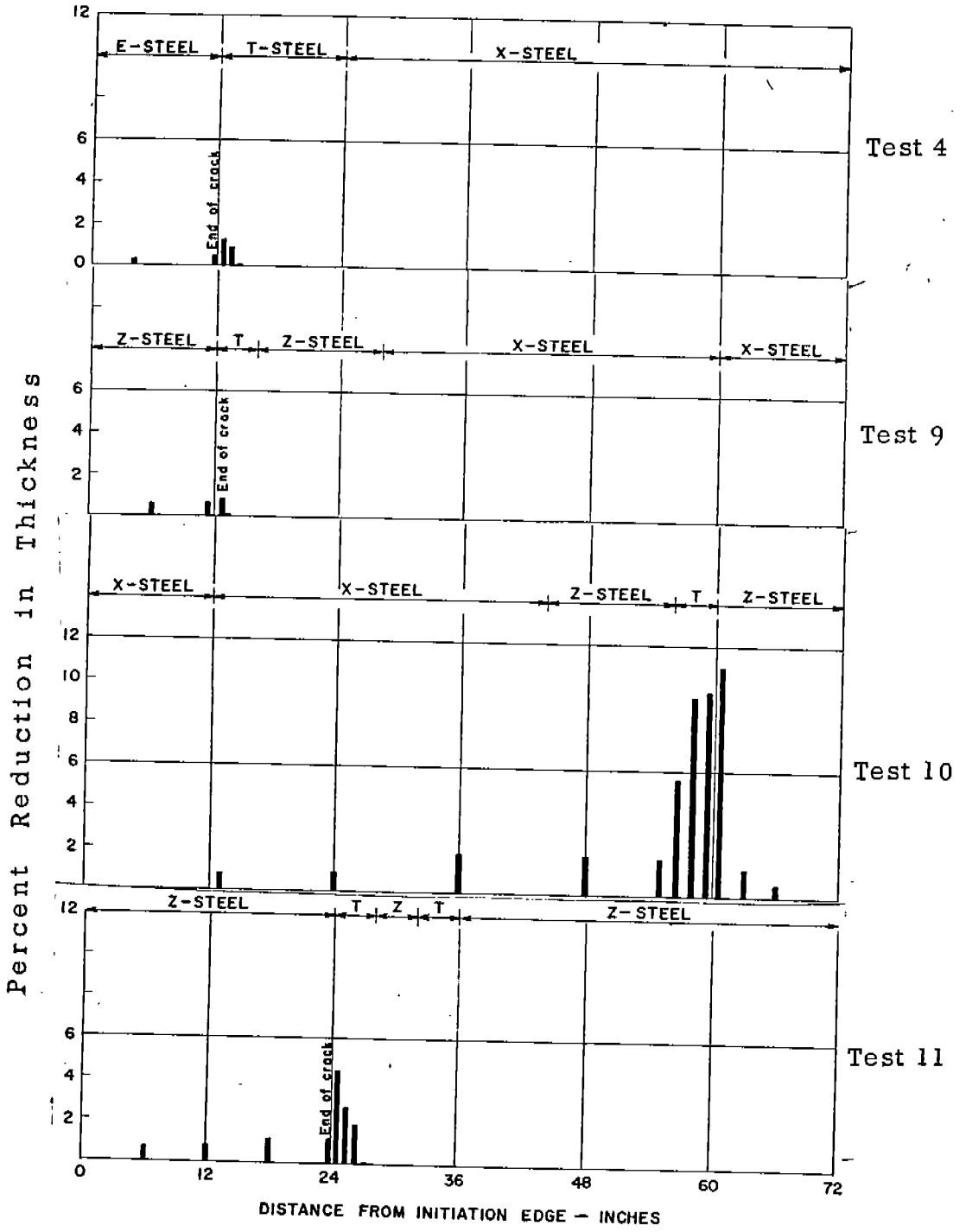

Fig. 37. Reduction in Plate Thickness along the Crack Path--Tests 4, 9, 10, 11.

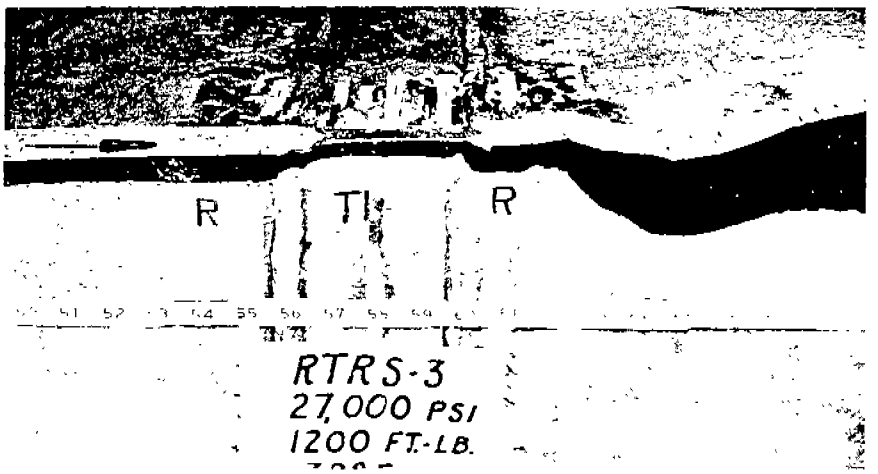

Test 10

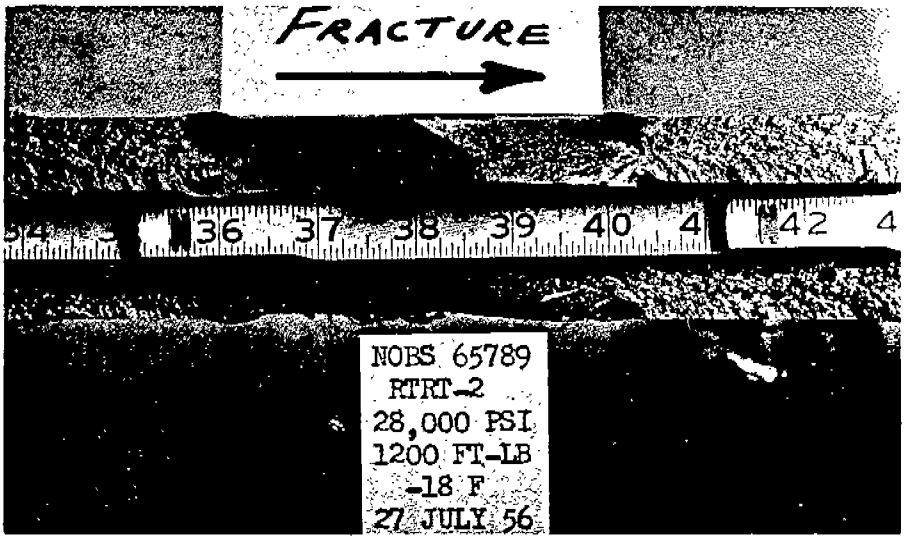

Test 12

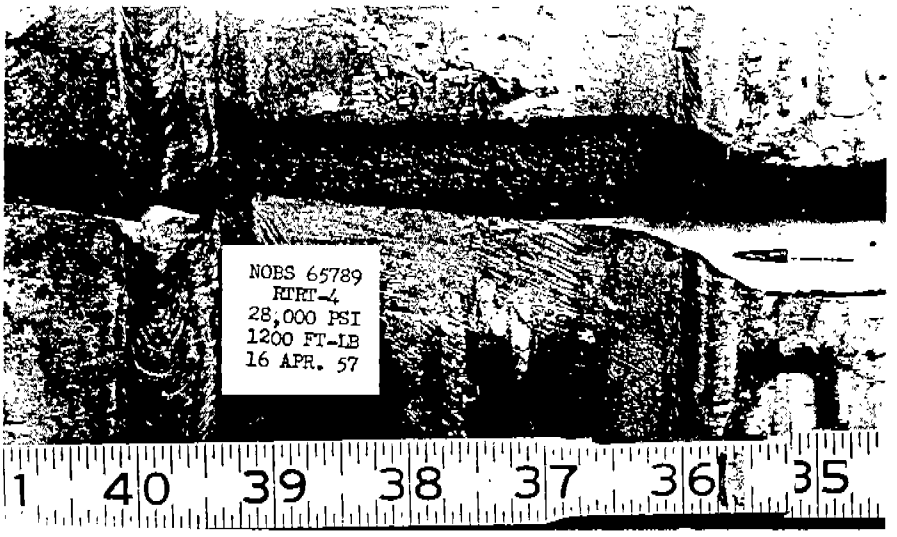

Test 18

Fig. 38. Typical Fracture Surfaces in 4 in. T-Steel Strakes.

Test 7

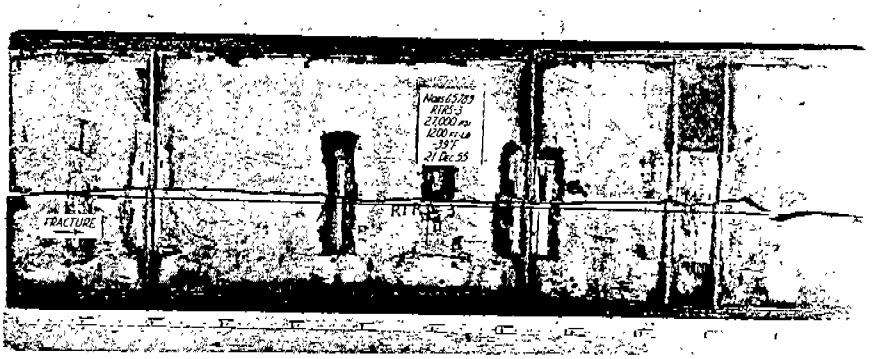

Test 10

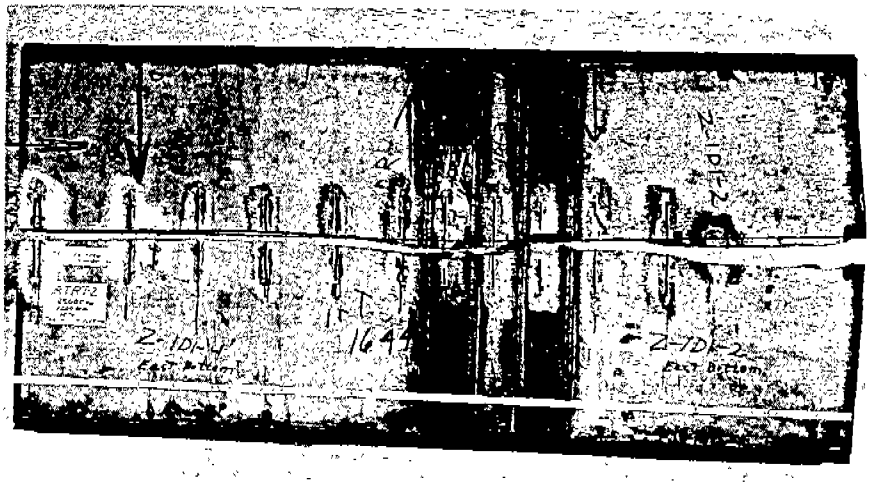

Test 12

Fig. 39. Views of Completely Fractured Inserts--
Tests 7, 10, and 12.

Crack Path and Texture. The fracture has not shown any tendency to follow a particular crack path, although the majority of fractures slope upward from the point of initiation and then level off somewhat. The crack paths for completely and partially fractured specimens are shown in Figs. 39 and 40 respectively. The maximum deviation of a crack path from the notch line was 4.90 in. for a 36-in. crack length in Test 15.

For all of the specimens in this series, the fracture surface in the E-, X-, and Z-steels had a typical brittle appearance. The texture of the fracture surface varied intermittently from smooth to coarse in all these steels and could not be correlated with calculated crack speeds. Photographs of the fractured surfaces of specimens that fractured completely (Tests 7, 10, and 12) are shown in Fig. 41.

In contrast to the brittle appearance of the fractured surface of the rimmed and semikilled steels, the fractured surface of the T-steel was always on a 45° plane, indicating a shear-type mode of failure. The surface texture of three 4-in. strakes of T-steel, which were completely fractured, is shown in Fig. 38. Partial fractures into T-steel occurred in several specimens, and photographs showing their surface appearance are presented in Fig. 42.

Figures 35 and 43–45 are photographs of the surface of the T-steel in the region around the end of the arrested crack. In Figs. 43 and 44 it is evident that a 4-in. wide strake of T-steel completely arrested 12- and 24-in. long cracks and that only in Test 9, where the testing temperature was extremely low, is there visible evidence of the crack beyond the butt weld in the T-steel. In specimens containing a 36-in. width of starter material, the arrested crack penetrated 12- and 36-in. wide strakes of T-steel as shown in Fig. 45. The penetration of cracks that had propagated 48 and 60 in. and then been arrested can be seen in Fig. 35. Inelastic buckling usually occurred at the far edge of the specimens in which these long crack lengths were developed.

In the specimen of Test 17, the brittle crack propagated 36 in. to the 4-in. strake of T-steel. It is believed that, during the initial stage of

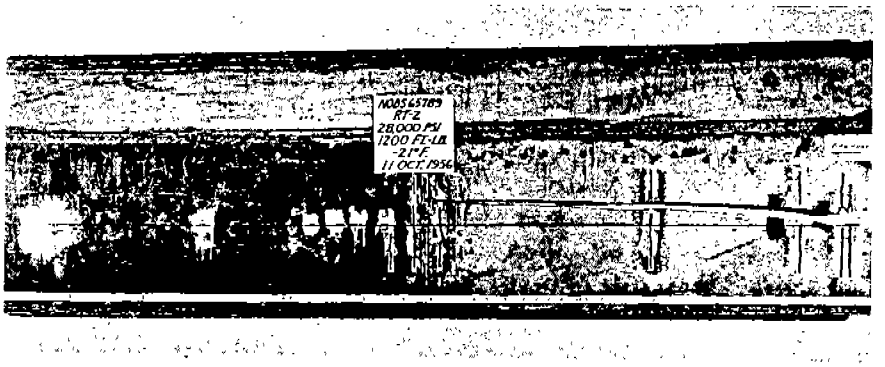

Test 14, 36 in. Crack Length

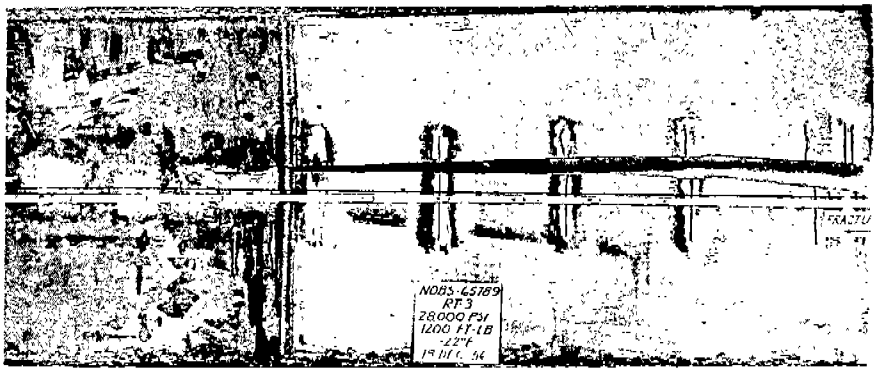

Test 16, 48 in. Crack Length

Test 18, 60 in. Crack Length

Fig. 40. Views of Partially Fractured Inserts--
Tests 14, 16, and 18.

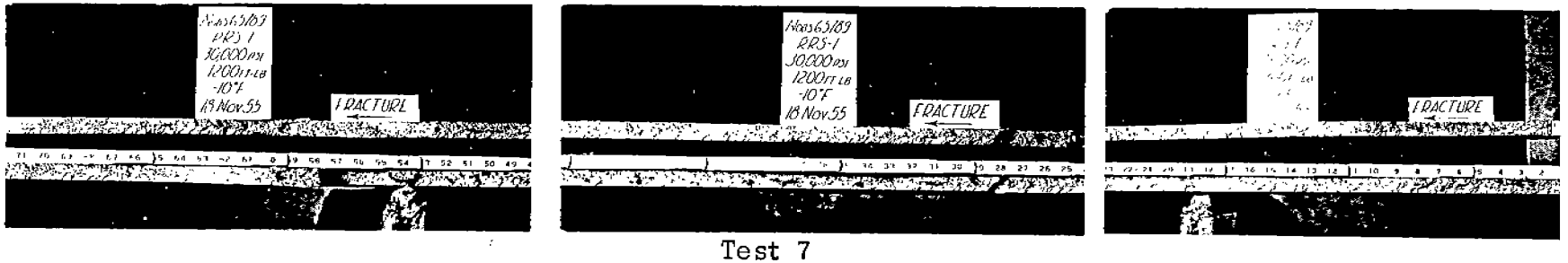

Test 7

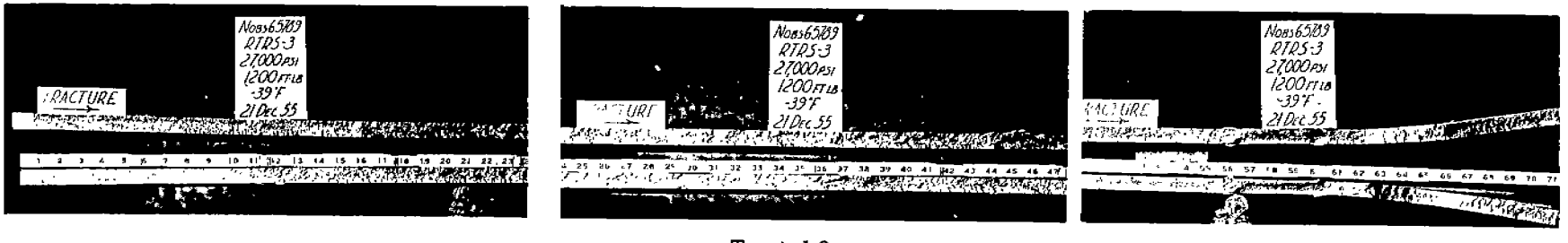

Test 10

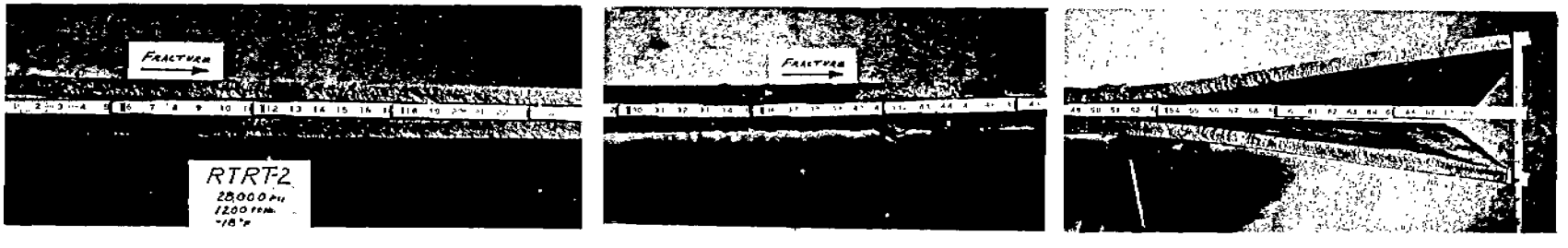

Test 12

Fig. 41. Crack Textures of Completely Fractured Specimens--Tests 7, 10, and 12.

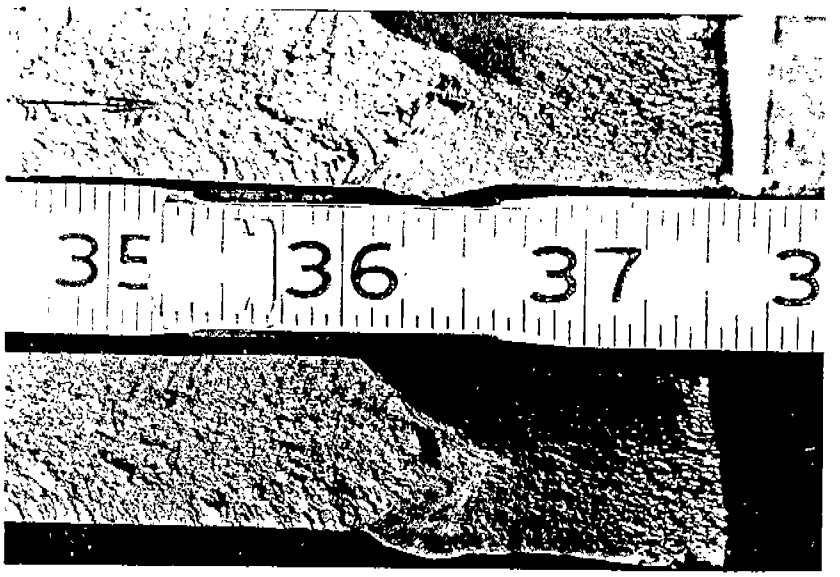

Test 13

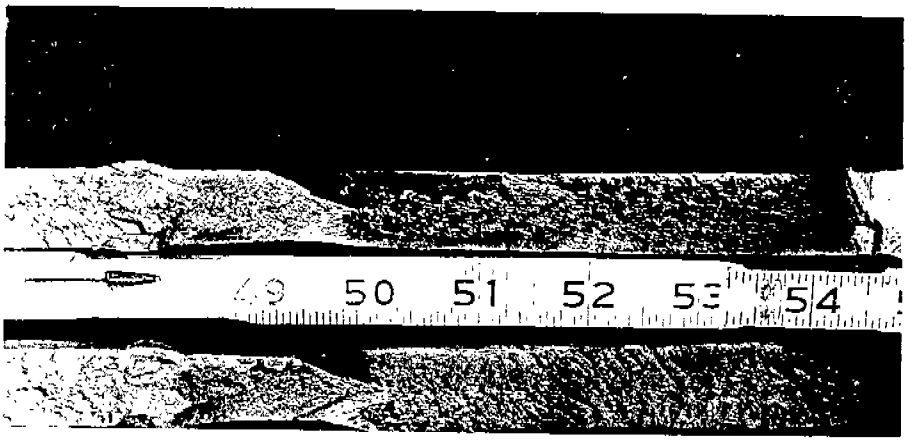

Test 16

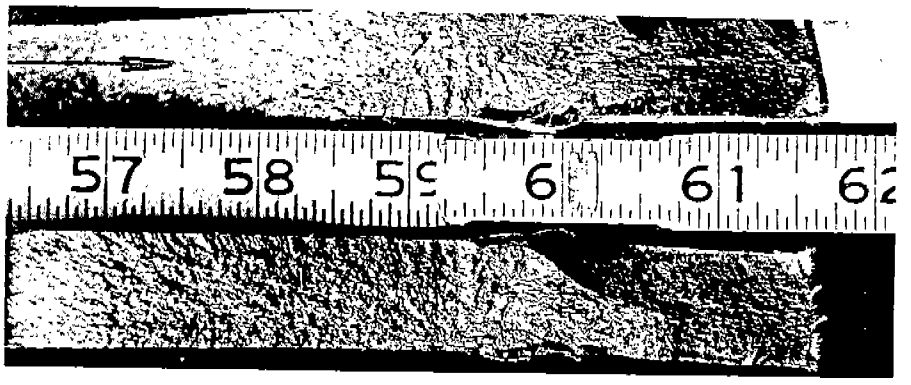

Test 18

Fig. 42. Typical Fracture Surfaces in Partially Fractured T-Steel Strakes.

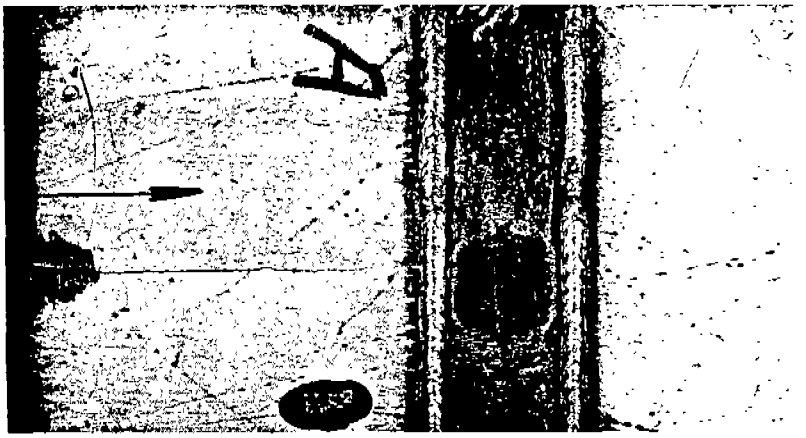

(a) Test 8, 4 in. T-Steel Strake

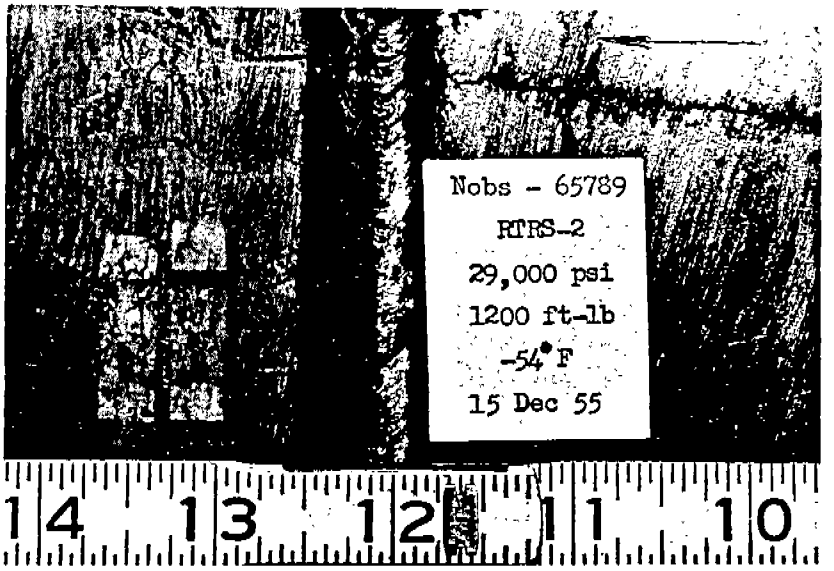

(b) Test 9, 4 in. T-Steel Strake

Fig. 43. Arrest of a 12 in. Long Crack--Tests 8 and 9.

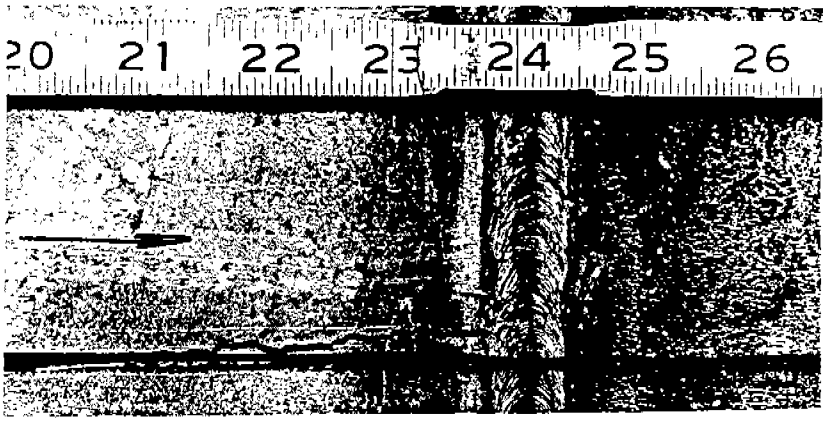

Test 11, 4 in. T-Steel Strake

Fig. 44. Arrest of a 24 in. Long Crack--Test 11.

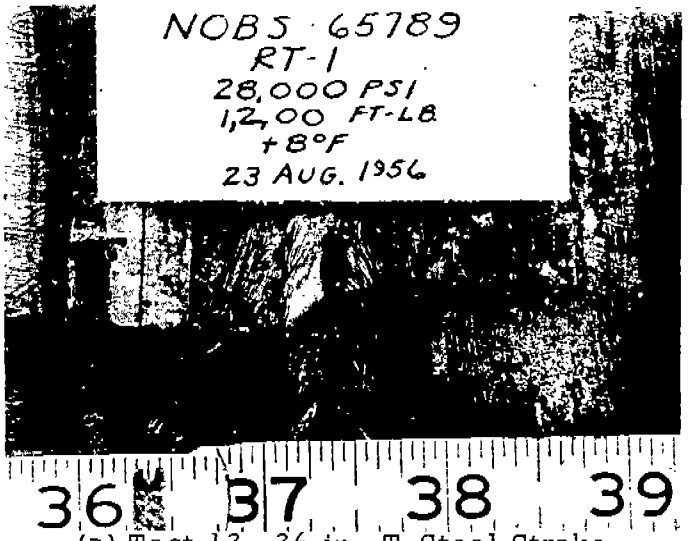

(a) Test 13, 36 in. T-Steel Strake

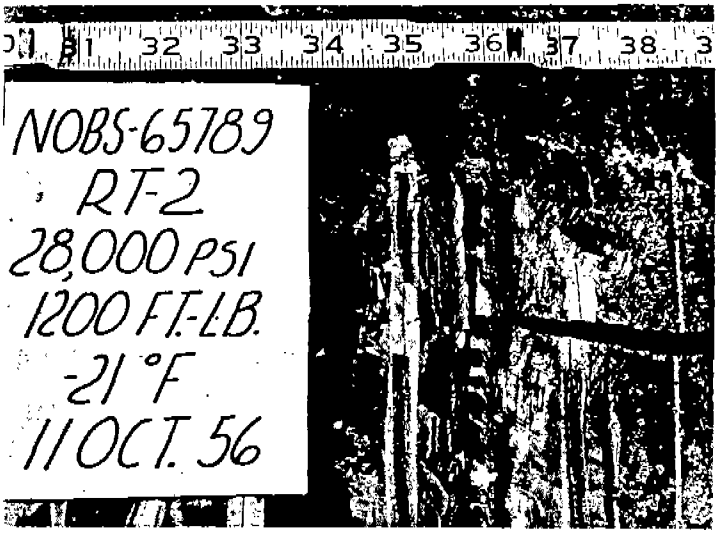

(b) Test 14, 36 in. T-Steel Strake

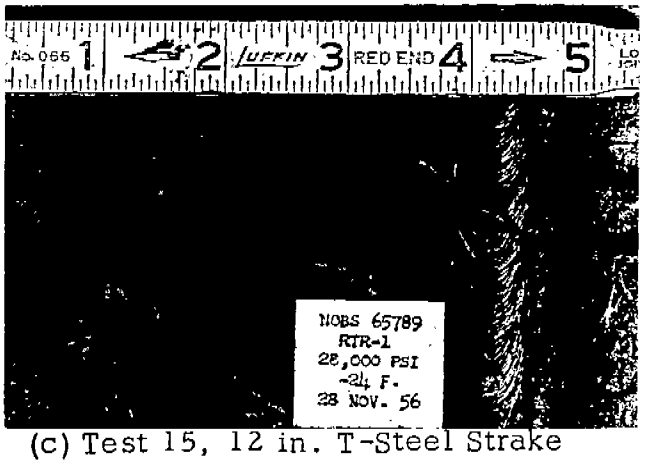

(c) Test 15, 12 in. T-Steel Strake

Fig. 45. Arrest of a 36 in. Long Crack--Tests 13, 14, and 15.

load redistribution, a secondary crack was initiated and resulted in the complete fracture of the specimen, as shown in Fig. 30. Referring to the dynamic strain records in Fig. 26, it appears that the arrestor strake of T-steel was not subjected to a major redistribution of load. This also seems reasonable because the arrested crack in this specimen was visible across the surface of the plate to the butt weld only, whereas in other cases where a 36-in. long crack was developed (Tests 13, 14, and 15), penetration of the T-steel strake was always evident after the test was completed (Fig. 45).

It seemed that the butt weld and 4-in. T-steel strake in this specimen (Test 17) contained an arrested crack which had been relatively unaffected by a redistribution of load and which should be examined further. A radiograph of the arrest region showed that the point of deepest penetration of the crack was the heat-affected zone of the T-steel. A metallographic examination of this region revealed that the contour of the arrested crack front was a thumbnail-type shape.

6-Ft Wide Riveted Arrestor Specimens

To provide a basis for comparison of the tests of welded arrestor specimens, it was felt that a few riveted crack arrestor specimens should be fabricated, according to a detail for which there was a great deal of service information, and tested under laboratory conditions. The arrestor detail in these specimens was the same as a design used on ships in service and consisted of a doubler plate riveted to one side of a slotted main insert plate. The doubler plate was extended above and below the insert plate so that it could be bolted to each pull-plate and thus more fully develop the desired load in the doubler. For comparative purposes in the test program, a few specimens were fabricated without a slot beneath the doubler. All of the riveted arrestor specimens in this series were fabricated by a qualified shipbuilder to insure that the laboratory specimens were typical of those used in actual practice.

In the riveted arrestor specimens, the arresting device consisted of a 16-in. wide by 3/4-in. thick doubler plate riveted to one side of the main

TABLE 4

SUMMARY OF TESTS ON 6-FT WIDE RIVETED ARRESTOR SPECIMENS

Test (Plate No.)	Width of Starter Material (in.)	Initial Load (kips)	Avg. Stress on Net Section (ksi)	Avg. Temp. (°F)
These tests were conducted on 6-ft wide specimens in a 3,000,000 lb hydraulic testing machine. The test specimen consists of a 3/4 x 54 x 73 1/4 in. Z-steel main plate (welded to 1 in. pull plates using double "V" butt welds - E7016 electrodes) with a 3/4 x 99 x 16 in. Z-steel doubler plate (riveted with 1 in. dia., countersunk pan-head rivets to the insert and bolted with 1 in. dia. tight-fitting bolts to the pull-plates) located on one side and centered approximately 19 in. from one edge of the insert. Each pull-plate was approximately 6 3/4 ft long for Tests 19-23. The main plate of the specimen for Tests 19 and 20 contains a longitudinal flame-cut slot, which was located along the centerline of the doubler plate; the main plate of the specimen for Tests 21-23 does not have a flame-cut slot. The notch length was 1 in. for Tests 19-21 and 1 1/8 in. for Tests 22 and 23. A theoretical impact of 1200 ft-lb was used in all these tests. Following the first fracture test on a given specimen, the partial fracture is gouged out and the specimen rewelded for a second or third test. The initial test on an insert is designated by an (A), the second test by a (B), and the third test by a (C) in the "Remarks" section. Strain gages and/or crack detectors were mounted on all specimens in this series.				
This insert, with a flame-cut slot beneath the doubler, was rewelded for 2 tests.				
19 (RIVS-1)	~11	1600	26.8	1
Remarks: (A) Final load - 1485 kips. Crack propagated between horizontal rivet rows to slot (~19 in.). No fracture in doubler. Complete record, good quality.				
20 (RIVS-2)	~45	1600	26.9	-19
Remarks: (B) Final load - 40 kips. Crack propagated between horizontal rivet rows to slot (~54 in.). Doubler fractured from south edge to third vertical rivet line. Severe buckling occurred at far side. Complete record, good quality.				
This insert, without a flame-cut slot beneath the doubler, was rewelded for 3 tests.				
21 (RIV-1)	~11	1600	26.8	-13
Remarks: (A) Final load - 1570 kips. Crack propagated to rivet in first vertical line (~12 in.). No fracture in doubler. Complete record, good quality.				

TABLE 4 (Continued)

Test (Plate No.)	Width of Starter Material (in.)	Initial Load (kips)	Avg. Stress on Net Section (ksi)	Avg. Temp. (°F)
22 (RIV-2)	~11	1600	26.8	-20
Remarks: (B) Final load - 1505 kips. Crack propagated between horizontal rivet rows to rivet in third vertical line (~20 in.). No fracture in doubler. Complete record, good quality.				
23 (RIV-3)	~11	1600	26.8	-16
Remarks: (C) Complete fracture of main plate with crack propagating between horizontal rivet rows. Doubler fractured from south edge to second vertical rivet line. Complete record, good quality.				

insert plate with four vertical lines of 1-in. diameter, countersunk, pan-head rivets. The rivet holes were drilled in the main plate, and those in the doubler were subpunched and reamed. In one case, the insert plate contained a longitudinal slot centered beneath the doubler plate, while in the other case it did not. While only the slotted specimen is typical of the type of arrestor in general use, it was felt that similar tests of an unslotted specimen would provide an opportunity to compare the effectiveness of the two details.

Table 4 summarizes the tests conducted on 6-ft wide specimens containing a riveted doubler plate. In these tests, the average stress on the net section was 26.8 ksi, the theoretical lateral impact was 1200 ft-lb, and the testing temperature varied from 1 to -20 F.

Test Records. Dynamic records were obtained in each of the five tests on riveted arrestor specimens; these are shown in Figs. 46-50. These figures have been made up in the same manner as that previously described. It can be seen that the duration of the strain records from Tests 19-23 varies from 4 to 10 millisec.

Slotted Insert with Doubler. In both tests on this insert, the brittle crack was initiated from a notch that was on a line with a horizontal row of

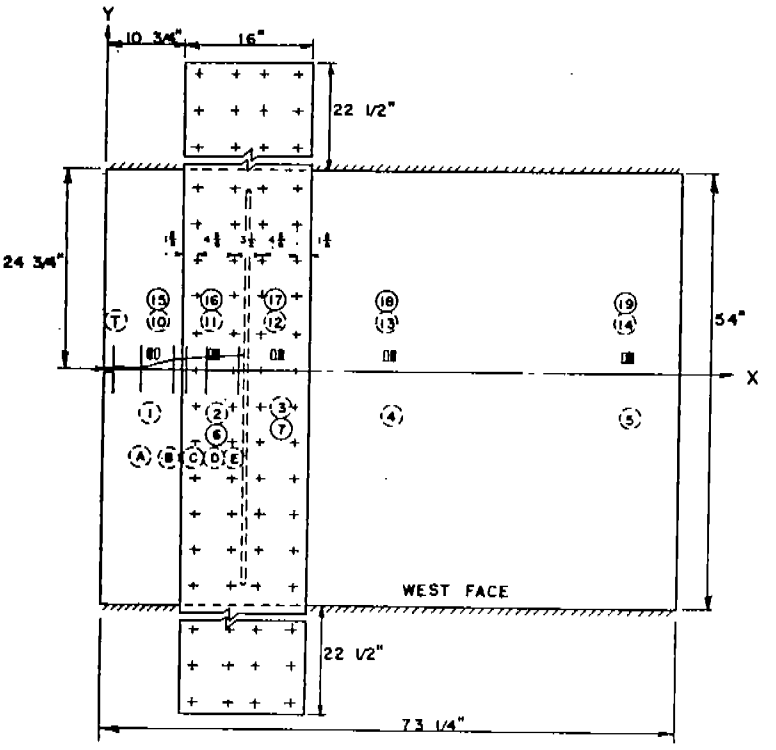

TEST CONDITIONS
AVERAGE STRESS=26.8KSI
TEMPERATURE =+1° F.
THEORETICAL IMPACT =1200 FT. LB.
○ GAGES ON EAST FACE ○ GAGES ON WEST FACE

STATIC STRAIN GAGES			
NO.	X in.	Y in.	INITIAL STRAIN
10	6.5	+2.0	+ 680
11	14.5	+2.0	+ 730
12	22.0	+2.0	+ 600
13	36.5	+2.0	+ 910
14	66.7	+2.0	+1020
15	6.5	+2.0	+ 580
16	14.5	+2.0	+ 480
17	22.0	+2.0	+ 600
18	36.5	+2.0	+ 860
19	66.7	+2.0	+ 980

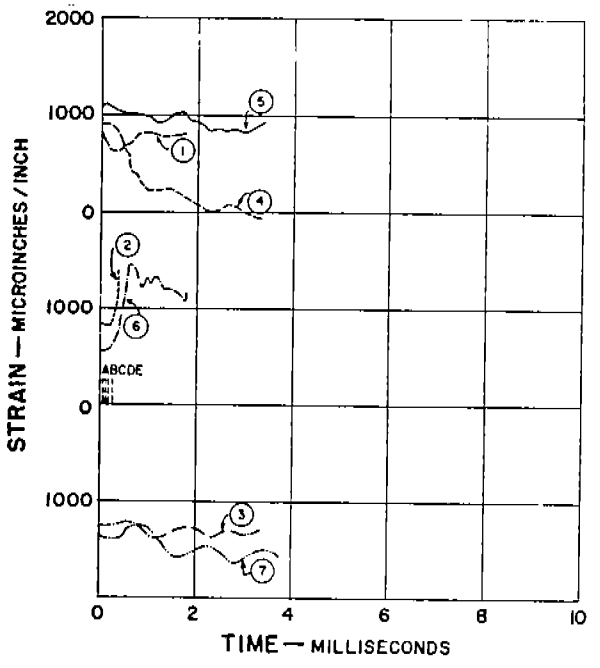

DYNAMIC STRAIN GAGES			
NO	X in	Y in	INITIAL STRAIN
1	6.0	+2.0	+ 820
2	15.0	+2.0	+ 840
3	22.5	+2.0	+ 750
4	37.0	+2.0	+ 900
5	67.2	+2.0	+1080
6	15.0	+2.0	+ 560
7	22.5	+2.0	+ 640

DETECTORS		
NO.	X in.	SPEED ft./sec.
A	5.0	
B	9.6	2450
C	11.1	4950
D	14.0	4600
E	18.5	

CRACK PATH	
X in	Y in.
1.8	+0.2
2.5	+0.1
7.5	+0.9
11.0	+1.3
14.0	+1.8
19.0	+1.9

Fig. 46. Instrumentation and Record--Test 19.

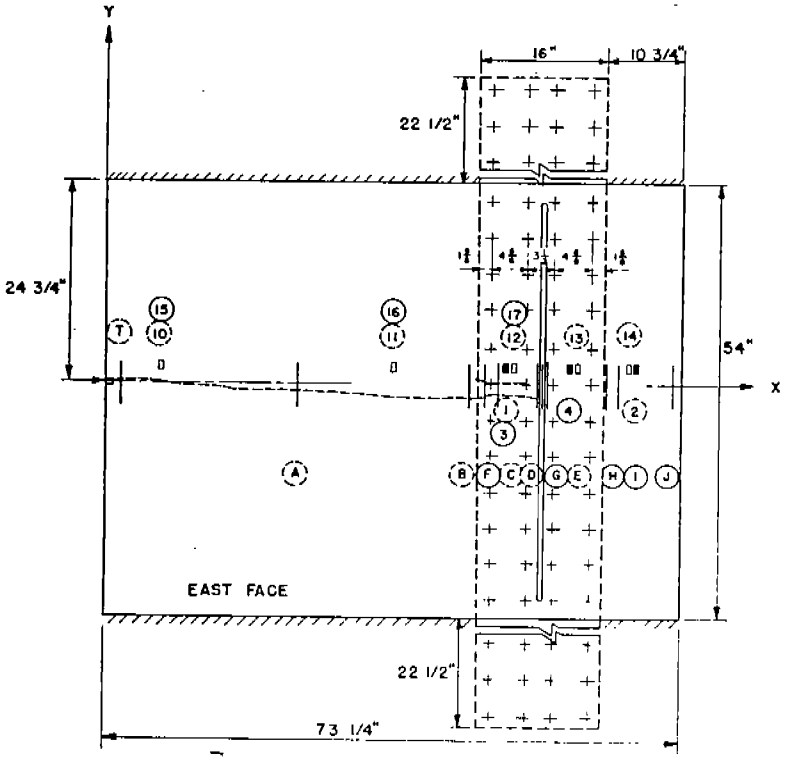

TEST CONDITIONS
AVERAGE STRESS=26.8 KSI
TEMPERATURE = -19°F
THEORETICAL IMPACT = 1200 FT.LB.
○ GAGES ON EAST FACE ○ GAGES ON WEST FACE

DYNAMIC STRAIN GAGES			
NO.	X in.	Y in.	INITIAL STRAIN
1	50.7	+2.0	+780
2	67.2	+2.0	+740
3	50.7	+2.0	+670
4	58.2	+2.0	+670
8	54.0	-95.0	+740
9	18.0	-95.0	+750

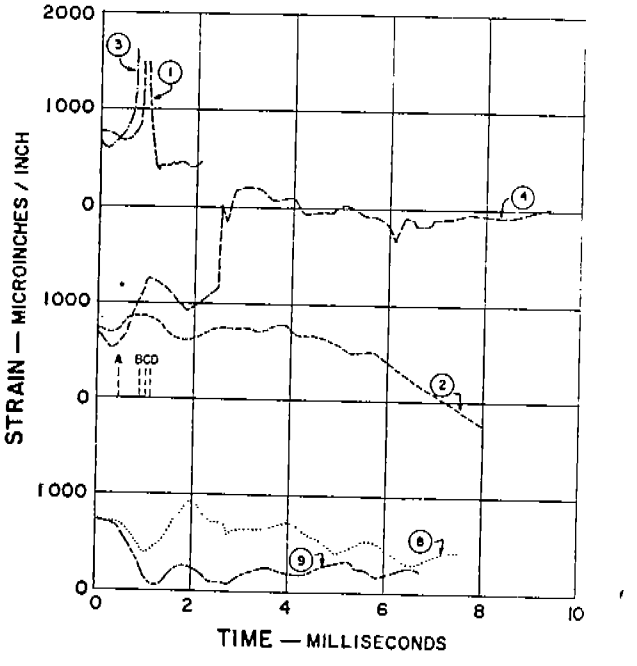

STATIC STRAIN GAGES			
NO.	X in.	Y in.	INITIAL STRAIN
10	6.5	+2.0	+1080
11	36.5	+2.0	+ 990
12	51.2	+2.0	+ 670
13	58.7	+2.0	+ 680
14	66.7	+2.0	+ 700
15	6.5	+2.0	+ 940
16	36.5	+2.0	+ 850
17	51.2	+2.0	+ 630

DETECTORS		
NO	X in.	SPEED ft./sec.
A	24.1	4100
B	45.3	2650
C	49.8	3450
D	53.9	
E	54.9	
F	46.9	
G	54.6	
H	62.0	
I	63.7	
J	70.7	

CRACK PATH	
X in.	Y in.
7.0	0.0
12.0	-0.4
25.0	-1.0
36.0	-1.5
48.0	-1.2
54.0	-1.8

Fig. 47. Instrumentation and Record--Test 20.

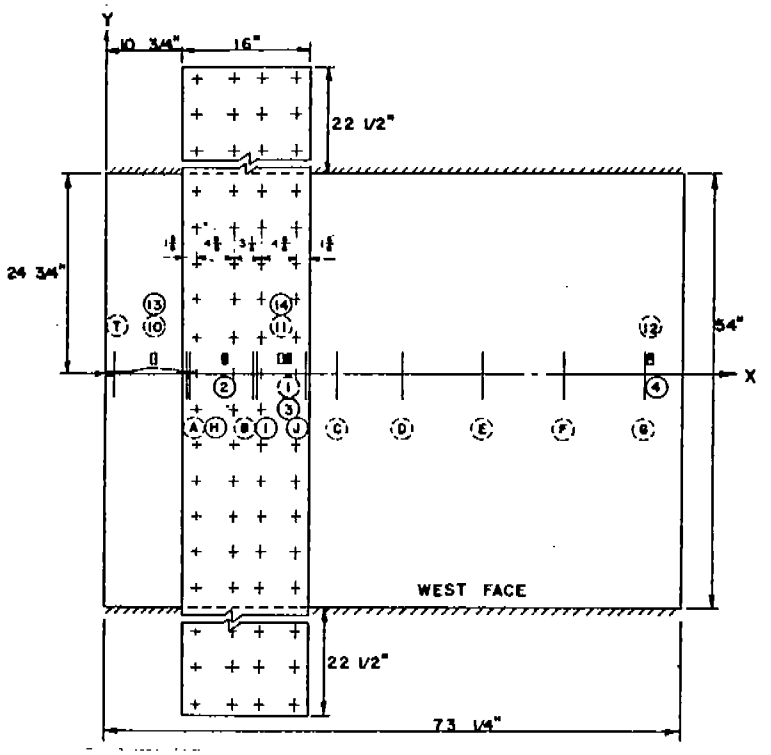

TEST CONDITIONS
AVERAGE STRESS = 26.8 KSI
TEMPERATURE = −13° F.
THEORETICAL IMPACT = 1200 FT. LB.
◯ GAGES ON EAST FACE
◯ GAGES ON WEST FACE

DYNAMIC STRAIN GAGES			
NO.	X in.	Y in.	INITIAL STRAIN
1	22.5	+2.0	+ 950
2	15.0	+2.0	+ 740
3	22.5	+2.0	+ 730
4	67.8	+2.0	+ 940
8	18.0	−95.0	+ 740
9	54.0	−95.0	+ 740

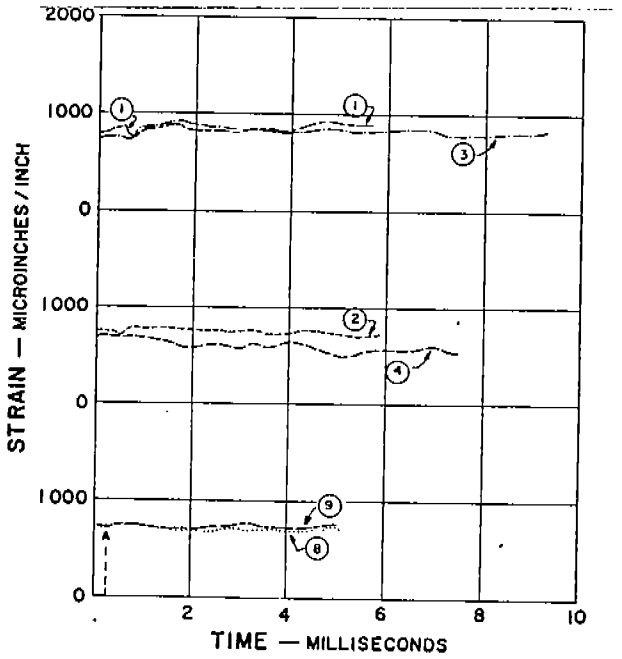

STATIC STRAIN GAGES			
NO.	X in.	Y in.	INITIAL STRAIN
10	6.0	+2.0	+ 820
11	22.0	+2.0	+ 830
12	67.8	+2.0	+1120
13	6.0	+2.0	+ 830
14	22.0	+2.0	+ 610

DETECTORS		
NO.	X in.	SPEED ft./sec.
A	11.0	
B	18.5	
C	29.0	
D	37.5	
E	47.0	
F	57.0	
G	67.0	
H	11.2	
I	18.8	
J	26.2	

CRACK PATH	
X in.	Y in.
3.0	+0.5
4.2	+0.6
6.0	+0.5
9.0	+0.4
11.6	+0.3

Fig. 48. Instrumentation and Record--Test 21.

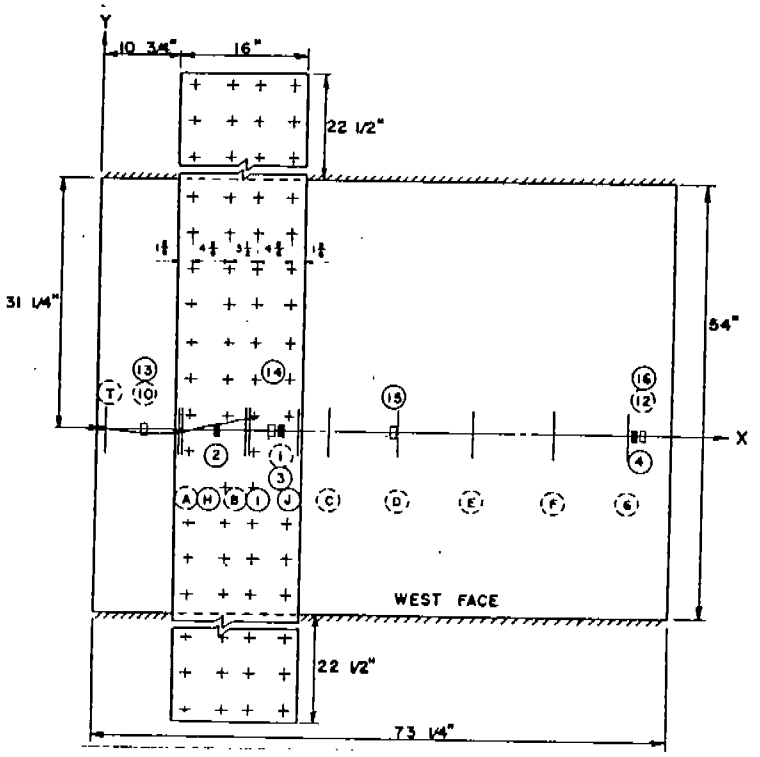

TEST CONDITIONS
AVERAGE STRESS = 26.8 KSI
TEMPERATURE = −20° F
THEORETICAL IMPACT = 1200 FT. LB.
○ GAGES ON EAST FACE
○ GAGES ON WEST FACE

DYNAMIC STRAIN GAGES			
NO.	X in	Y in	INITIAL STRAIN
1	22.5	0	+ 935
2	15.0	0	+ 650
3	22.5	0	+ 645
4	67.3	0	+ 645
8	18.0	-88.8	+ 740
9	54.0	-88.8	+ 740

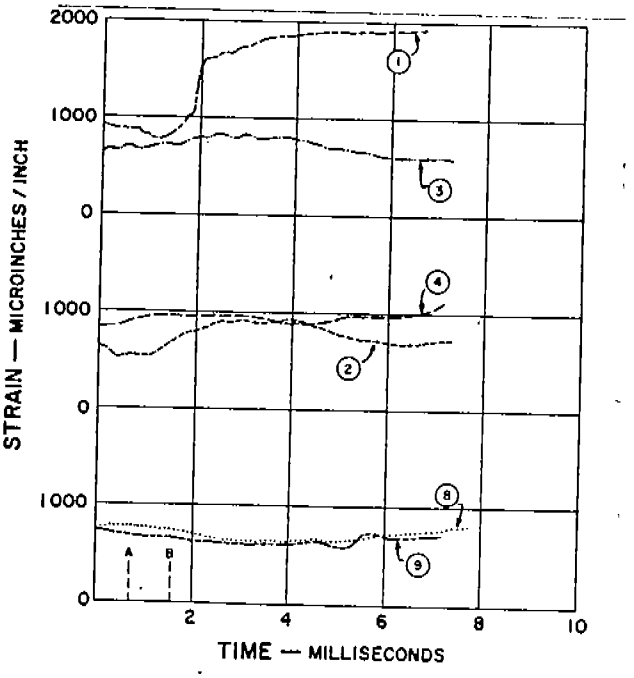

STATIC STRAIN GAGES			
NO.	X in	Y in	INITIAL STRAIN
10	6.0	0	+ 720
12	67.8	0	+ 1065
13	6.0	0	+ 390
14	22.0	0	+ 520
15	37.0	0	+ 795
16	67.8	0	+ 830

DETECTORS		
NO.	X in	SPEED ft./sec.
A	11.0	
B	18.7	750
C	29.0	
D	37.5	
E	47.0	
F	57.0	
G	67.0	
H	11.2	
I	19.0	
J	26.5	

CRACK PATH	
X in.	Y in.
6.0	−0.4
12.0	0.0
18.0	+1.2
20.0	+1.5

Fig. 49. Instrumentation and Record--Test 22.

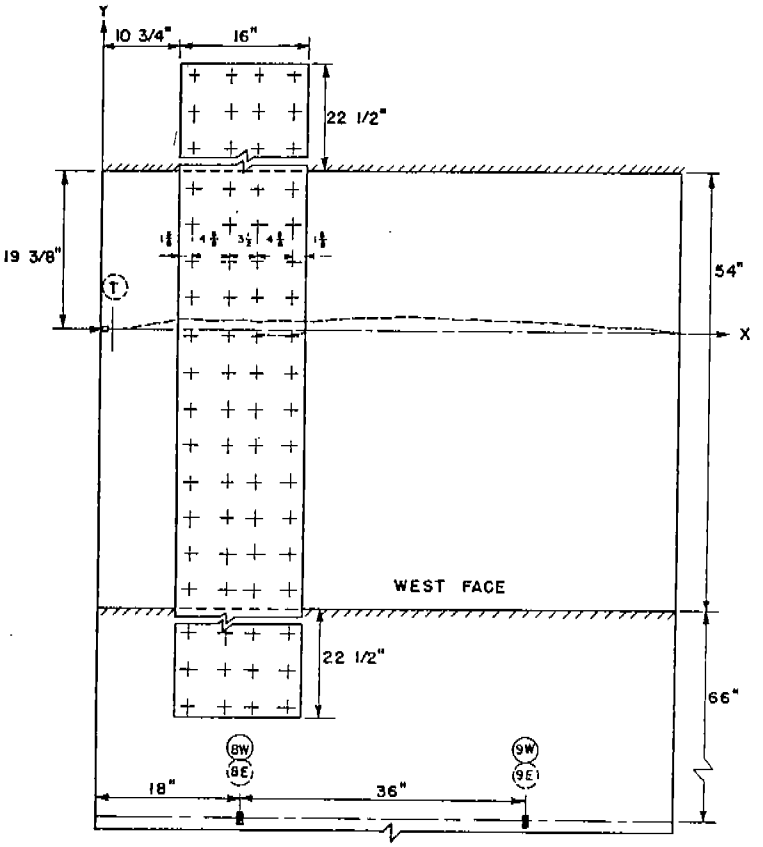

TEST CONDITIONS
AVERAGE STRESS = 26.8 KSI
TEMPERATURE = −16° F.
THEORETICAL IMPACT = 1200 FT. LB.
◌ GAGES ON EAST FACE ○ GAGES ON WEST FACE

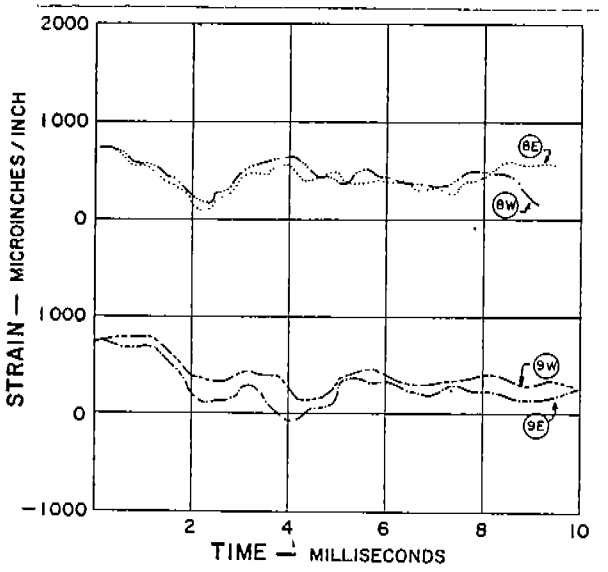

DYNAMIC STRAIN GAGES			
NO.	X in	Y in	INITIAL STRAIN
8E	18.0	-100.6	+ 740
8W	18.0	-100.6	+ 740
9E	54.0	-100.6	+ 740
9W	54.0	-100.6	+ 740

CRACK PATH	
X in	Y in
6.0	+0.4
10.8	+1.0
26.8	+0.9
30.0	+1.0
36.6	+1.2
43.2	+1.2
49.2	+1.1
55.2	+0.9
61.2	+0.3
67.2	0.0
73.2	−0.3

Fig. 50. Instrumentation and Record--Test 23.

rivets connecting the doubler to the main plate. In Test 19 the notch was at the edge of the specimen near the doubler, while in Test 20 the notch was at the opposite edge of the specimen.

Under an average stress on the net section of 26.8 ksi and an average temperature of 1°F (Test 19), the brittle crack traveled slightly upward, passing between the horizontal rivet rows to the flame-cut slot in the main plate. There was no indication of fracture in the main-plate material beyond the slot (Fig. 51) or in the doubler plate.

The partial fracture from Test 19 was rewelded. In the next test on this specimen (Test 20), where the crack was initiated from the opposite edge, an average stress of 26.8 ksi, an average temperature of -19 F, and a theoretical impact of 1200 ft-lb were combined to produce a crack that propagated 54 in. across the main plate to the flame-cut slot. In addition, the doubler plate fractured across two lines of rivets, as shown in Fig. 51.

The dynamic strain gage record from Test 20 (Fig. 47) shows the rapid development of large strain peaks in the main plate (gage 1) and in the doubler (gage 3) as the crack approaches. In addition, gage 4 on the far side of the doubler plate also shows a sudden large increment of strain approximately 2 millisec. later, which might be indicative of a major redistribution of load and/or buckling of the remaining portion of the main plate.

Measurements on the plate surface give fracture speeds from 2650 to 4950 fps. These speeds are within the range of values obtained from other tests in this investigation (Fig. 34). The texture of the fractured surface of the specimen from Test 20 is shown in Fig. 52.

From these tests it is evident that an abrupt discontinuity, such as that provided by a flame-cut slot, is a satisfactory form of crack-arresting device, if the redistribution of load is not too great. It also appears that rivet holes do not necessarily attract propagating brittle cracks.

Unslotted Insert with Doubler. In all three tests on this specimen (Tests 21, 22 and 23), the brittle crack was initiated from a notch at the edge of the main plate near the doubler plate. The location of the notch with respect to the horizontal rows of rivets connecting the doubler to the

Test 20

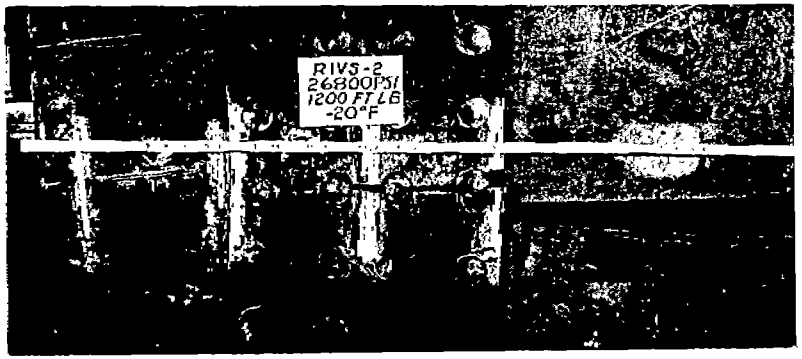

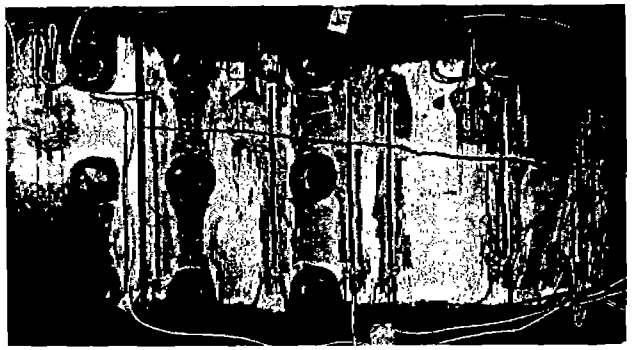

Test 19

Fig. 51. Views of Fractured Inserts--Tests 19 and 20.

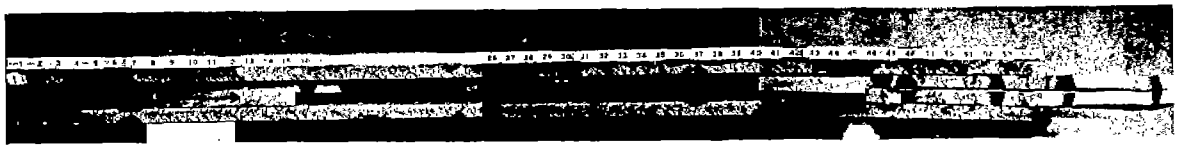

Test 20

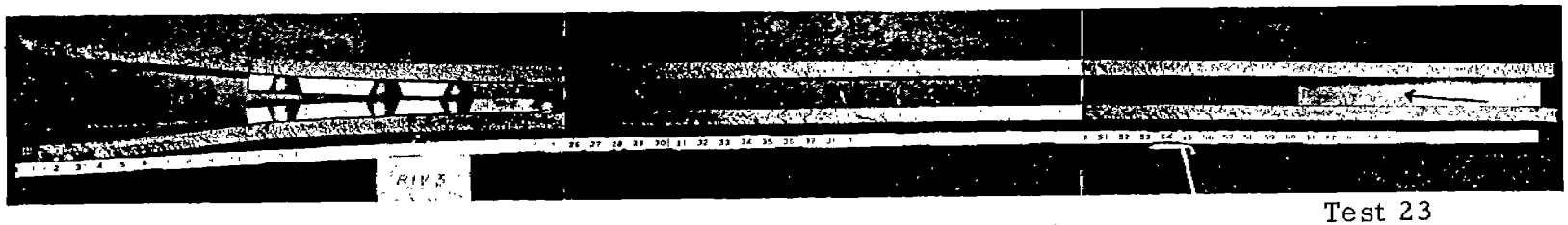

Test 23

Fig. 52. Crack Textures of Fractured Specimens--Tests 20 and 23.

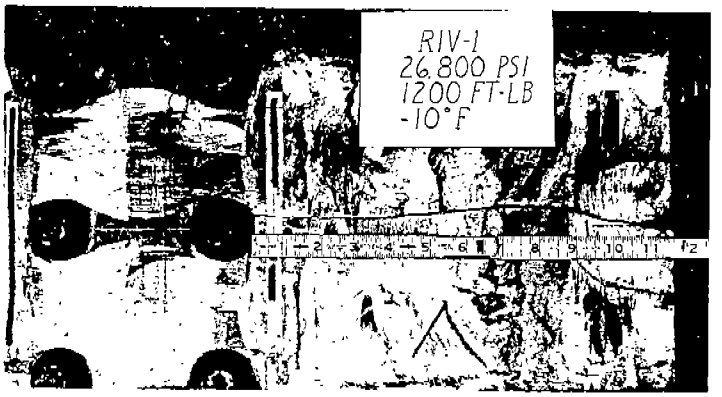

Test 21

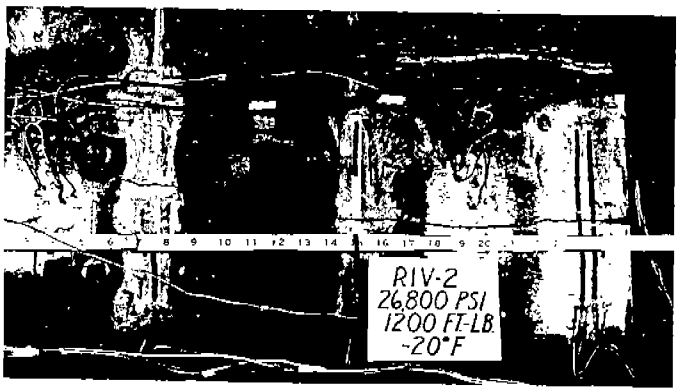

Test 22

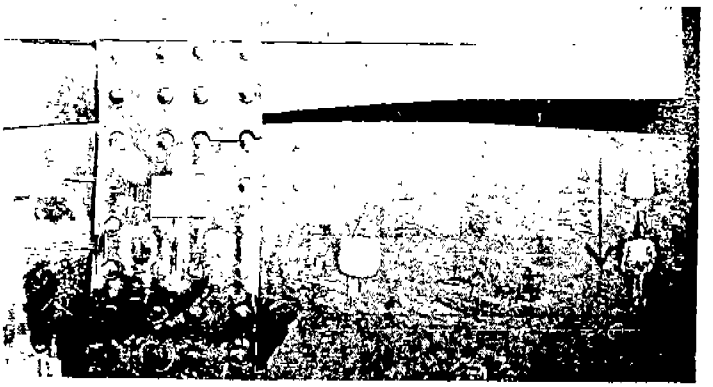

Test 23

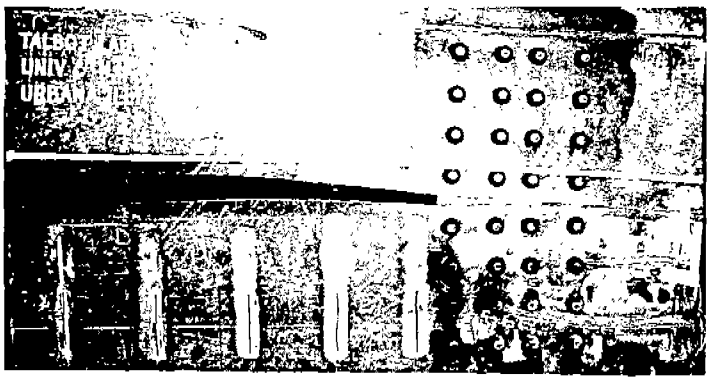

Test 23

Fig. 53. Views of Fractured Inserts--Tests 21, 22, and 23.

main plate was varied in each test. After each test, the fractured portion of the specimen was rewelded for the next test.

In Test 21 the crack was initiated from a notch in line with a horizontal row of rivets. At a stress of 26.8 ksi and a temperature of -13 F, the crack propagated in the main plate to a rivet hole in the first vertical line of rivets (Fig. 53).

In Test 22 the crack was initiated from a notch located midway between two horizontal rows of rivets. In this case, at the same stress and slightly lower temperature, the crack propagated slightly upward and between two horizontal rows of rivets to a rivet hole in the third vertical line (Fig. 53). There was no evidence of fracture in the doubler plate in this test.

In Test 23 the notch was located just slightly above a horizontal row of rivets so that the best opportunity for uninterrupted crack propagation would prevail. In this test, at the same stress and approximately the same temperature, the brittle crack propagated completely across the main plate of the specimen, passing approximately midway between two horizontal rows of rivets in the region where the doubler plate was connected to the main plate. In addition, the doubler plate was fractured from the far edge to the second vertical line of rivets (Fig. 53).

The fractured surface of the specimen used in these tests, with its characteristic chevron pattern, can be seen in Fig. 52.

Since Tests 21 and 22 did not result in complete fracture, full instrumentation was not used on the specimen for Test 23. Instead, dynamic records were taken on the individual gages mounted on the lower pull-plate only, since, up to that time, only an average reading of these back-to-back gages had been recorded and no information was available on the individual behavior of these gages. These individual records, plotted in Fig. 50, indicate good agreement between these back-to-back gages during the brittle-fracture propagation. They also indicate a substantial drop in strain after about 2 millisec., which was about the time required for complete fracture of the insert.

6-Ft Wide Welded Arrestor Specimens with C-Steel

The purpose of this series of tests was to study the behavior of crack-

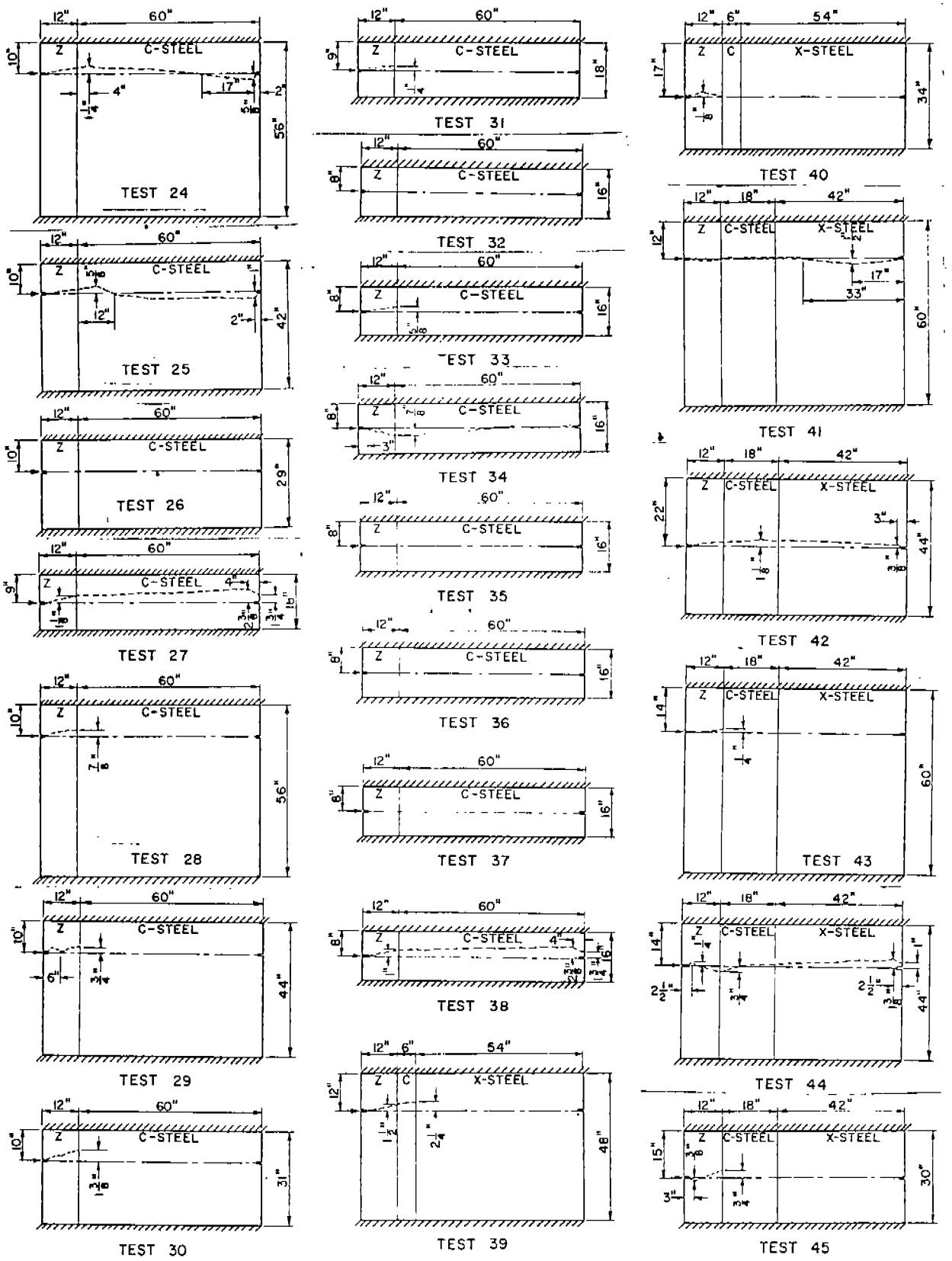

Fig. 54. Specimen Inserts and Crack Paths--Tests 24--45.

arrestor specimens containing a strake of C-steel as the arresting material. In all 22 tests the specimen insert was 3/4 in. thick, 6 ft wide, and contained a 12-in. wide starter strip of Z-steel. This width of starter material was chosen in order to minimize the effects of redistribution and drop-off of load that are associated with the development of longer crack lengths in this type of specimen. From Table 3 it is evident that, for the hydraulic testing machine used, approximately 97 per cent of the initial load remains on a 72-in. wide specimen after a brittle crack has propagated 12 in. and arrested. Crack-speed measurements from this program and also from the closely allied Brittle Fracture Mechanics Study (Project SR-137) have shown that the speed of fracture propagation appears to reach a constant value during the first 6 in. of propagation.[16]

In this series of tests the length of the insert varied from 16 to 60 in., and the overall length of the specimen varied from 8.1 to 19.0 ft. The width of the strake of C-steel was 6, 18, or 60 in. The makeup of the inserts for the various tests is shown in Fig. 54.

The average stress on the net section of the specimen was generally either 20.0 ksi (close to typical design stresses) or 28.0 ksi (a 40-per cent increase over the former). Except for a few tests, the testing temperature varied from 10 to 39 F. At some of the combinations of temperature and stress in this series of tests, the originally adopted theoretical lateral impact of 1200 ft-lb was not sufficient to initiate and propagate a brittle crack. Therefore, the stroke and/or pressure in the impact device were increased in order to provide a larger value of lateral impact for many of the tests in this series. Consequently, another calibration of the impact device was made at that particular time (between Tests 31 and 32) in the manner described earlier in this report. This calibration, made for several combinations of stroke and pressure, provided the values of actual impact given in Table 5, which summarizes the tests conducted on 6-ft wide specimens containing a strake of C-steel.

Initiation and Propagation. The testing temperature used in this series

TABLE 5
SUMMARY OF TESTS ON 6-FT WIDE WELDED ARRESTOR SPECIMENS CONTAINING ABS-C STEEL STRAKES

Test (Plate No.)	Overall Specimen Length (ft)	Initial Load (kips)	Avg. Stress on Net Section (ksi)	Avg. Temp. (°F)	Remarks
These tests were conducted on 6-ft wide specimens in a 3,000,000 lb hydraulic testing machine. The test specimen is an insert 3/4 in. thick x 72 in. wide with the depth varying from 16 to 60 in. The insert is welded to pull-plates (1 in. thick for Tests 24-31 and 3/4 in. thick for Tests 32-45) using double "V" butt welds - E7016 electrodes. All vertical welds within the specimen were also double "V" butt welds made with E7016 electrodes. The length of each pull plate varied from 3 1/4 ft to almost 9 ft in this series of tests. All inserts contained a 12 in. width of rimmed Z-steel starter material and a 1 1/8 in. deep notch (see Table 3). The stroke, pressure, theoretical impact, and actual impact of the piston device varied for the different tests as follows: 5 in., 280 psi, 1200 ft-lb, and 990 ft-lb for Tests 24-27; 7 in., 280 psi, 1600 ft-lb, and 1380 ft-lb for Tests 28-32; and 5 in., 370 psi, 1530 ft-lb, and 1480 ft-lb for Tests 33-45. Following the first fracture test on a given specimen, the fracture is generally cut out and the remaining portion of the insert used for subsequent tests. The initial test on an insert is designated by (A), the second test by a (B), the third test by a (C), and the fourth test by a (D) in the "Remarks" column. Successive trials for each test as indicated by the additional initial load values, however, were made on the same notch. No strain gages or crack detectors were mounted on any of the specimens in this series.					
The 3/4 x 56 x 72 in. insert consisted of 12 in. of Z-steel and 60 in. of C-steel. This insert was cut and rewelded for four tests.					
24 (RCN-1)	11.3	1330	25.0	-22	(A) Complete brittle fracture.
25 (RCN-2)	10.1	980 1070	18.7 20.4	0 1	(B) 1/2 in. crack in Z-steel. Complete brittle fracture.
26 (RCN-3)	9.0	1050 1050 1330	20.0 20.0 25.0	35 22 20	(C) No initiation. No initiation. No initiation.
27 (RCN-4)	8.1	1050 1470 1680	20.0 28.0 32.0	20 18 12	(D) No initiation. 1/2 in. crack in Z-steel. Complete brittle fracture.
28 (RCN-5)	11.3	1050	20.0	16	(A) Final load - 1010 kips. Crack propagated 12 in. to weld (3 in. submerged crack visible in C-steel).
29 (RCN-6)	10.3	1050	20.0	33	(B) Final load - 1010 kips. Crack propagated 12 in. to weld (4 in. submerged crack visible in C-steel).
30 (RCN-7)	9.2	1470	28.0	33	(C) Final load - 1440 kips. Crack propagated 12 in. to weld and arrested.
31 (RCN-8)	8.1	1470	28.0	17	(D) Final load - 1450 kips. Crack propagated 12 in. to weld and arrested.
The 3/4 x 18 x 72 in. inserts consisted of 12 in. of Z-steel and 60 in. of C-steel. Only one test was made on each insert.					
32 (RCN-9)	19.0	1470 1470	28.0 28.0	14 14	(A) No initiation. No initiation.
33 (RCN-10)	19.0	1470	28.0	14	(B) Final load - 1420 kips. Crack propagated 12 in. to weld and arrested.
34 (RCN-11)	19.0	1470	28.0	2	(A) Complete brittle fracture.
35 (RCN-12)	19.0	1050 1050	20.0 20.0	9 11	(A) No initiation. 3 in. crack in Z-steel.
36 (RCN-13)	19.0	1050 1050	20.0 20.0	7 7	(A) No initiation. 2 in. crack in Z-steel.
37 (RCN-14)	16.0	1050	20.0	7	(A) 1 1/2 in. crack in Z-steel.
38 (RCN-15)	19.0	1260	24.0	8	(A) Complete brittle fracture.
The 3/4 x 48 x 72 in. insert consisted of 12 in. of Z-steel, 6 in. of C-steel, and 54 in. of X-steel. The insert was cut and rewelded for two tests.					
39 (RCN-16)	19.0	1050 1470	20.0 28.0	17 15	(A) 1 in. crack in Z-steel. Final load - 1320 kips. Crack propagated 18 in. (across C-steel) to second weld and arrested.
40 (RCN-17)	17.8	1050	20.0	17	(B) Final load - 1030 kips. Crack propagated 12 in. to weld and arrested.
The 3/4 x 60 x 72 in. inserts consisted of 12 in. of Z-steel, 18 in. of C-steel, and 42 in. of X-steel. One insert was cut and rewelded for two tests; the other insert was cut and rewelded for three tests.					
41 (RCN-18)	19.0	1470	28.0	16	(A) Complete brittle fracture.
42 (RCN-19)	17.7	1470	28.0	26	(B) Complete brittle fracture.
43 (RCN-20)	18.8	1470	28.0	38	(A) Final load - 1420 kips. Crack propagated 12 in. to weld and arrested.
44 (RCN-21)	17.6	1050	20.0	28*	(B) Complete brittle fracture.
45 (RCN-22)	16.3	1050	20.0	39*	(C) Final load - 1040 kips. Crack propagated 12 in. to weld and arrested.

*Liquid nitrogen used to subcool the notch just prior to testing.

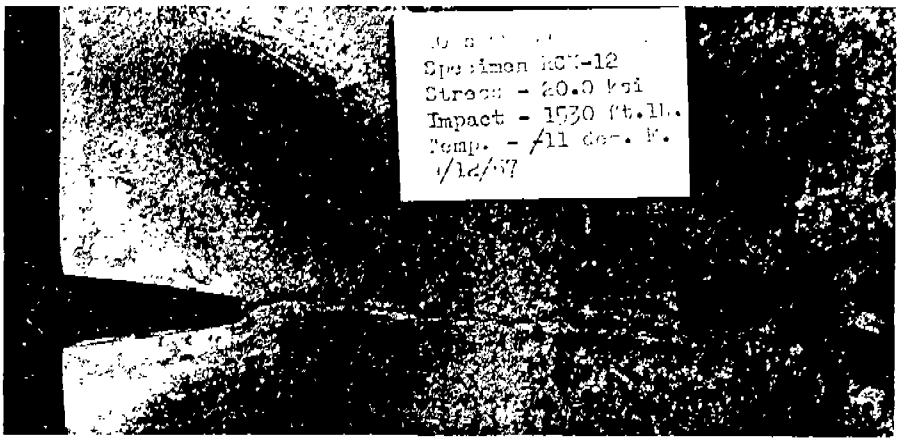

Test 35

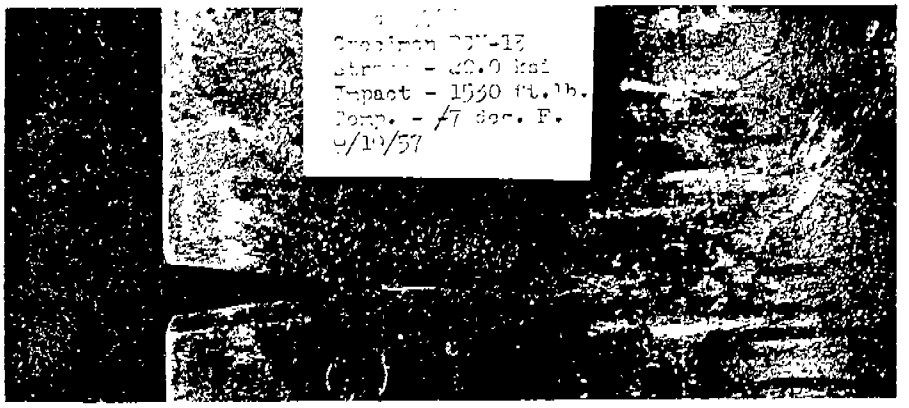

Test 36

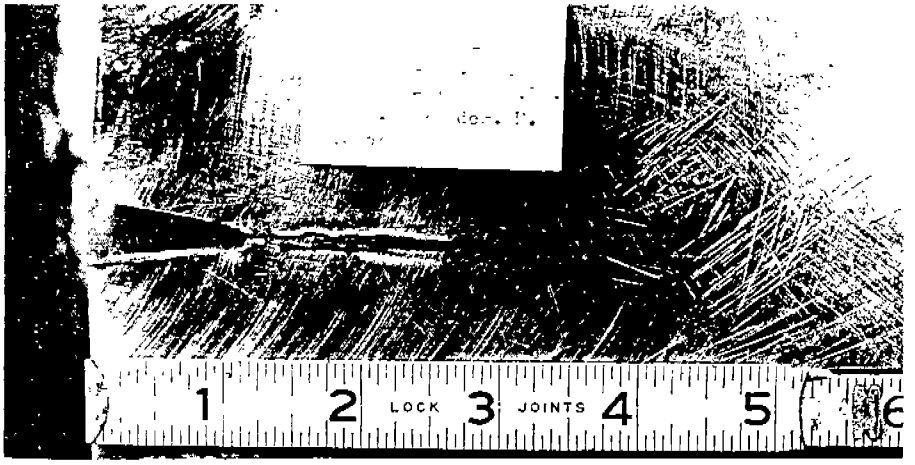

Test 37

Fig. 55. Specimens Failing to Propagate a 12 in. Crack--Tests 35, 36, and 37.

of tests was somewhat warmer than any used previously in the Crack Arrestor Program. Difficulty was encountered in initiating and propagating a brittle crack in the Z-steel starter strip of the specimens in Tests 25, 26, and 27 (Table 5). (In plain plate tests on Z-steel,[14,16] similar test conditions consistently initiated and propagated a brittle crack across the specimen.) Consequently, the lateral impact was increased for Tests 28-31, and brittle cracks were satisfactorily initiated and propagated in each of these specimens. By successively cutting off the tested portion, one insert provided material for a series of four tests. This procedure, however, resulted in a varying overall length of specimen.

After the completion of Test 31, it was thought that it would be desirable to standardize the specimen geometry by adopting a constant insert length of 16 in. and by changing the pull-plate thickness to 3/4 in. so that it would be the same as the insert plate. However, after these changes were made, a brittle crack could not be initiated and propagated (Tests 32, 35, 36, and 37) under test conditions that had previously been sufficient for satisfactory brittle-fracture propagation (Tests 28, 29, 30, and 31). It was concluded that the shorter insert combined with the thinner pull-plate was in some manner hindering the initiation and propagation of a brittle crack in the starter strip of this type of specimen. Photographs of the area around the end of the notch of some of the specimens in which the brittle crack did not propagate across the 12-in. width of starter material are presented in Fig. 55.

It was thought that the variation in residual strain introduced during the preparation of the different sized specimens might have been responsible for some of the difficulty in initiating and propagating a brittle crack. An attempt was made to study these strains, and they were measured in the direction of loading during the fabrication and welding of the specimens for Tests 37 and 38. However, because of the presence of several other possibly significant variables (overall specimen length, pull-plate thickness, and notch location) in this test series and the limited number of specimens that could be examined, no correlation of these variables with the test

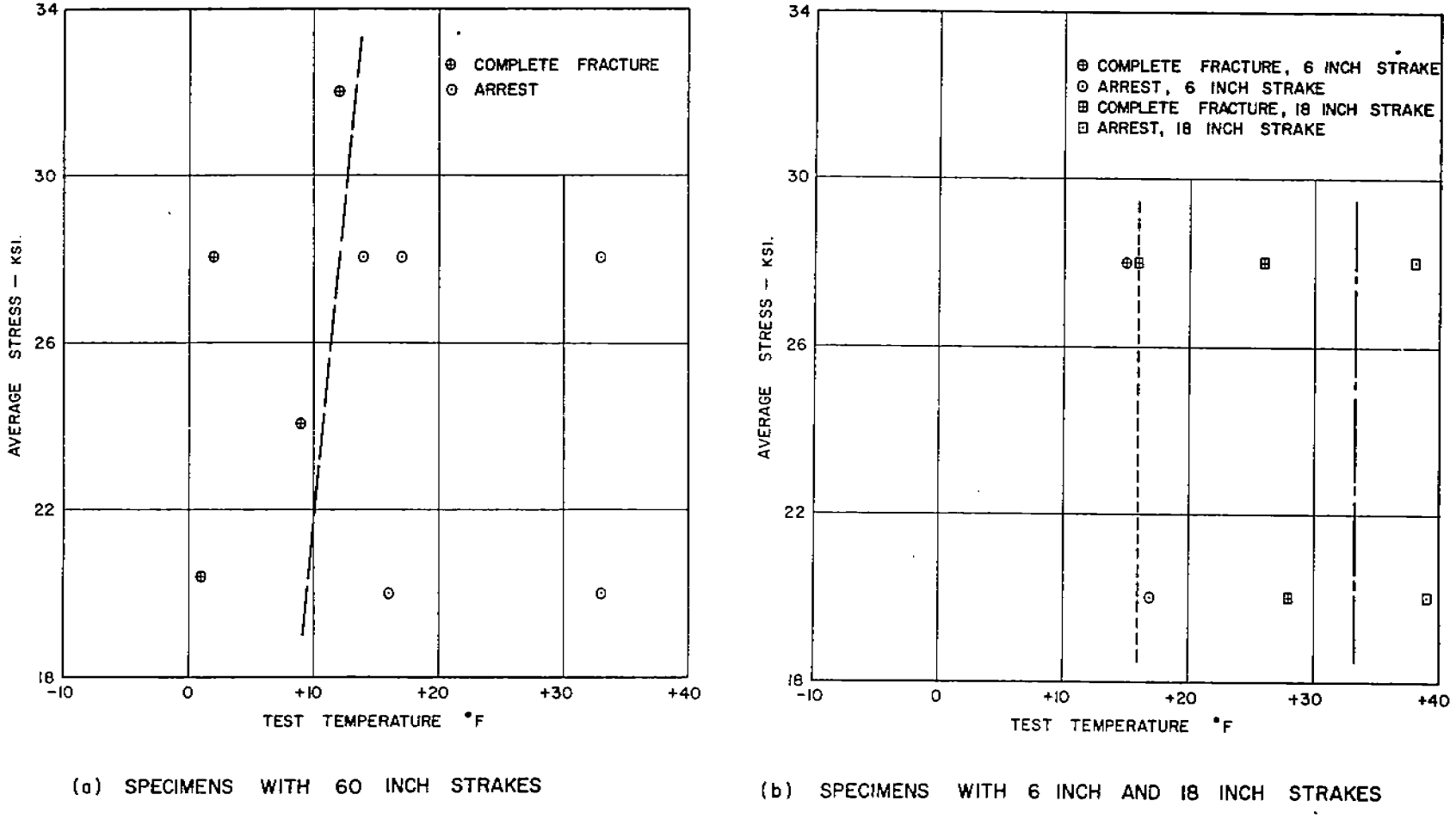

(a) SPECIMENS WITH 60 INCH STRAKES

(b) SPECIMENS WITH 6 INCH AND 18 INCH STRAKES

Fig. 56. Arrest--Transition Plots for ABS-C Steel

results could be obtained.

Arrest. In five of the twenty-two tests in this series, the combination of stress, temperature, and lateral impact was not sufficient to initiate and propagate a brittle crack satisfactorily in the test specimen. Of the seventeen remaining specimens, ten contained a 60-in. width of C-steel, five contained an 18-in. width of C-steel, and two contained a 6-in. width of C-steel. The test results for specimens with these widths of C-steel, under the various combinations of average stress and temperature, are plotted in Fig. 56. Presented in Fig. 57 are photographs of all the specimens in which a 12-in. long crack was arrested by the C-steel strake. In two cases, Tests 40 and 45, incomplete separation of the material on the surface of the plate occurred over part of the length of the crack.

In all specimens except two (Tests 28 and 29--where 3- and 4-in. long submerged cracks in the C-steel were evident), the propagating brittle crack was either entirely accepted or completely refused by the strake of C-steel. There was no other case in which the strake of C-steel was penetrated and partially fractured by the propagating crack. As indicated by the test results plotted in Fig. 56, it appears that the arresting ability of C-steel is not greatly affected by the average applied stress but is very strongly influenced by the temperature of the material.

Referring to Fig. 56, a 60-in. strake of C-steel exhibits a transition in behavior from complete fracture to complete arrest at a temperature around 10 F. After only two tests, it was difficult to define the corresponding temperature for a 6-in. strake of C-steel, but it appeared to be a few degrees higher. However, the temperature range at which an 18-in. width of this material demonstrated this transition in behavior seemed to be about 30-35 F in these specimens.

In tests where an average stress of 20.0 ksi was applied, both 6- and 60-in. wide strakes of C-steel arrested the propagating crack at a temperature of about 16 F. However, when the average stress was increased to 28.0 ksi, neither a 6- nor 18-in. wide strake of C-steel could arrest a crack propagating at this temperature. It is conceivable that the proximity of the

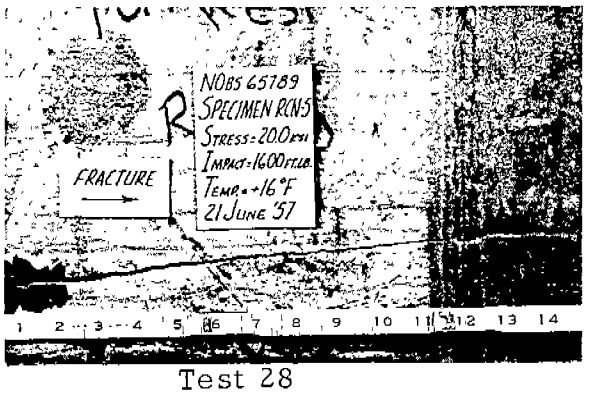

Test 28

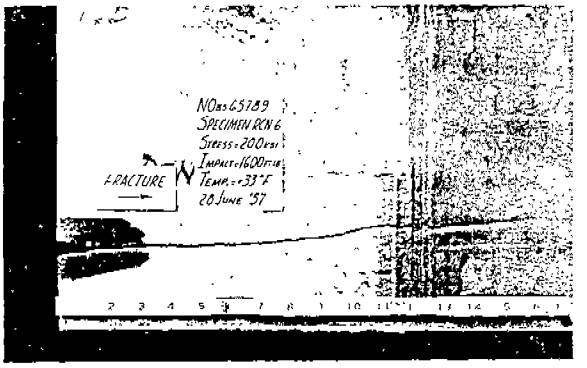

Test 29

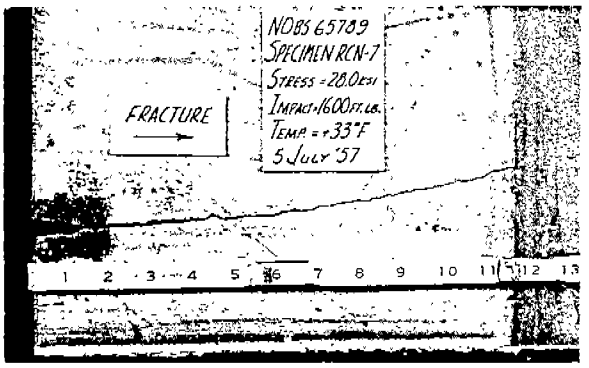

Test 30

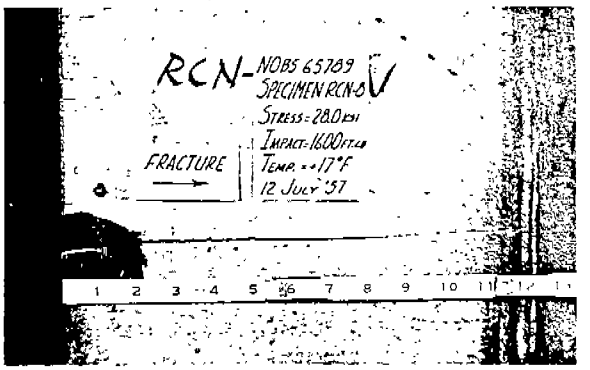

Test 31

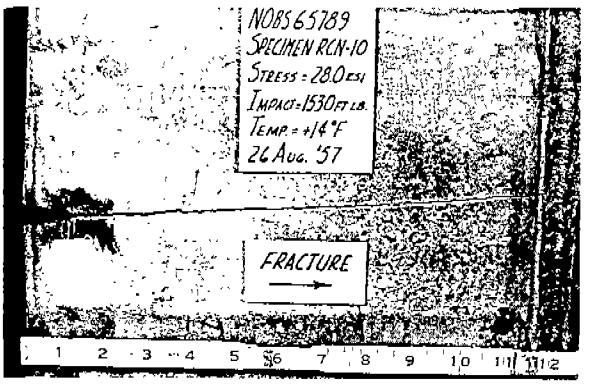

Test 33

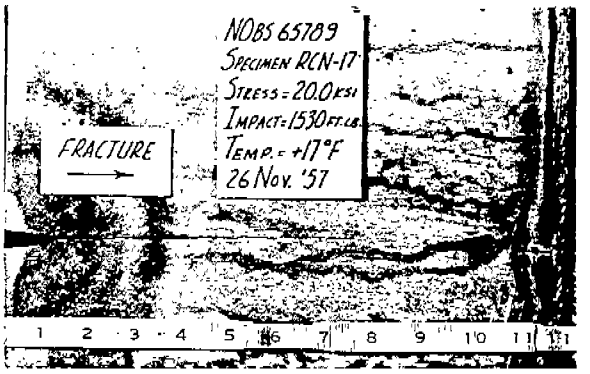

Test 40

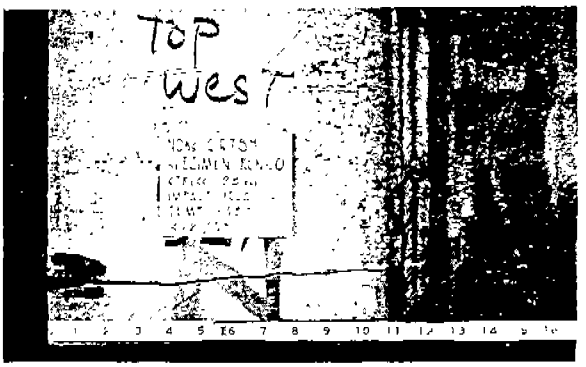

Test 43

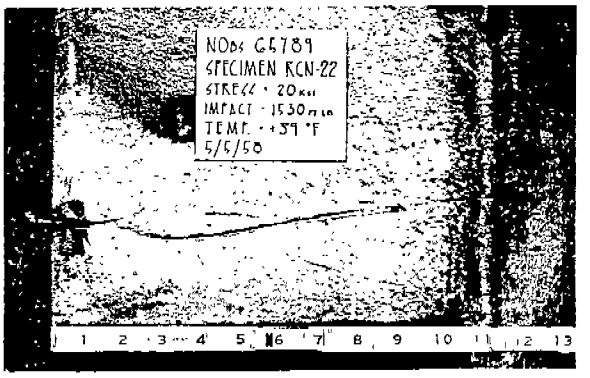

Test 45

Fig. 57. Brittle Cracks Arrested by ABS-C Strakes.

second butt weld in these specimens affects the residual strain pattern in the arrestor strake, thereby influencing the behavior of the specimen. Nevertheless, it should be pointed out that, although a 6-in. wide strake of C-steel did not arrest a crack that had propagated 12 in., this crack was arrested after propagating 18 in. by a 54-in. wide strake of X-steel (Test 39). It is possible that the crack velocity was reduced while crossing the 6-in. width of C-steel and that the butt-weld-X-steel combination offered sufficient resistance to arrest a slower moving crack.

Reduction in Plate Thickness. The reduction in plate thickness along the crack path for the specimens in which a brittle crack was initiated and propagated is presented in Figs. 58 and 59. In general, the reduction in thickness in the Z-steel starter material varied from approximately 1 to 2 per cent. In Tests 43 and 45, where the brittle crack propagated 12 in. and was arrested by an 18-in. width of C-steel, the general level of reduction of plate thickness in the Z-steel starter material seems to be slightly more than the previously mentioned value.

In most cases the reduction in plate thickness measured in the strakes of C-steel varied from about 1 to 3 per cent where the crack had completely fractured the strake. For the specimens where the crack was arrested by the butt-weld and was not visible in the C-steel, the reduction in thickness in the arrestor material was extremely small and measurable only adjacent to the weld. In the two tests (28 and 29) where submerged cracks 3 and 4 in. long were developed in the C-steel, the reduction in plate thickness was as high as 6.5 per cent.

Crack Path and Texture. Again in these tests the fractures have not shown any tendency to follow a particular crack path, although the majority of the fractures slope upward and then level off. The crack paths obtained in the various tests are sketched on the individual inserts in Fig. 54.

For all specimens tested in this series, the fractured surface had a typical brittle appearance and was always on a 90° plane relative to the plane of the plate. The texture of the fractured surface varied intermittently from smooth to coarse in all three steels used and showed no particular pattern.

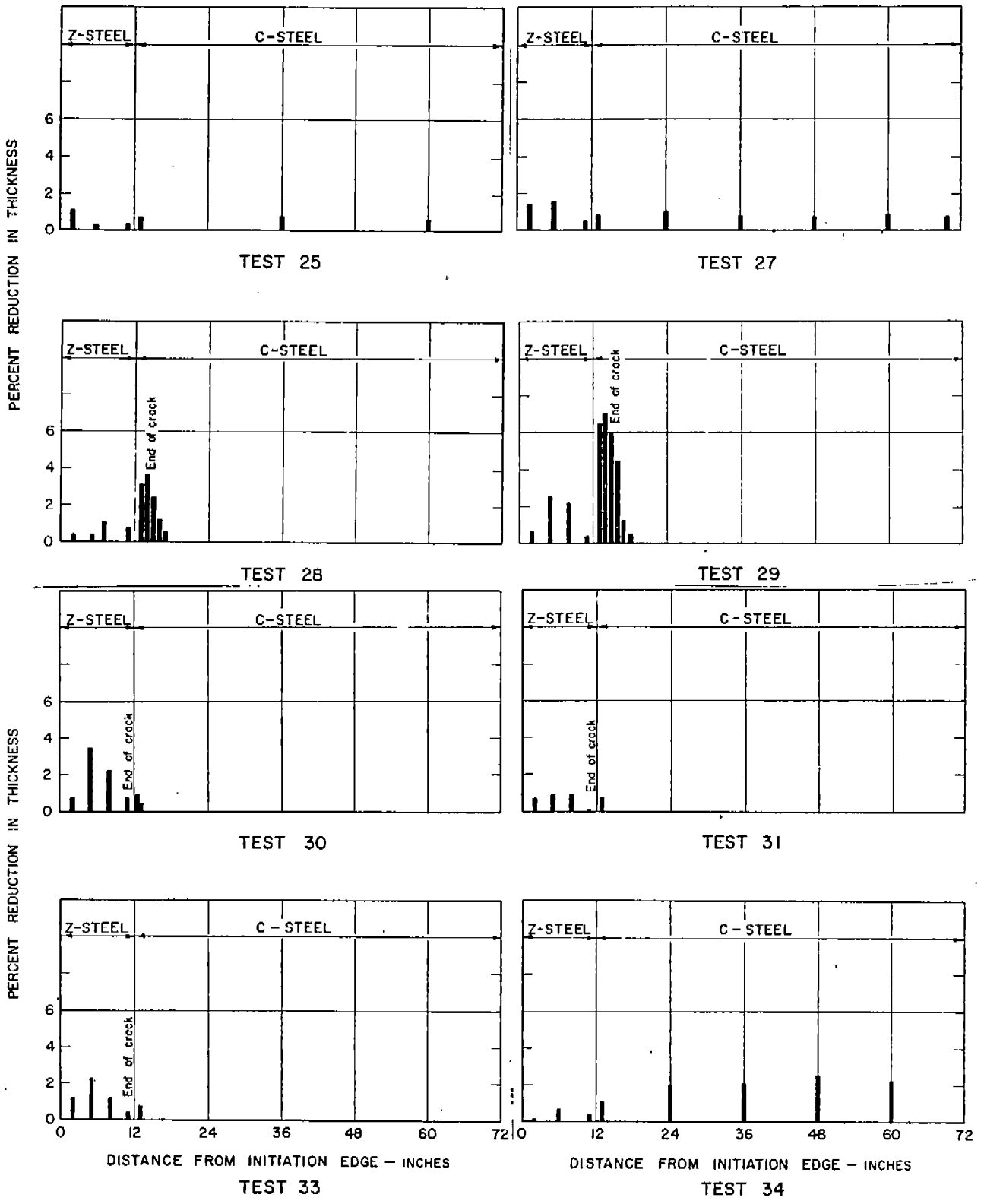

Fig. 58. Reduction in Plate Thickness along the Crack Path--
Tests 25, 27, 28, 29, 30, 31, 33, and 34.

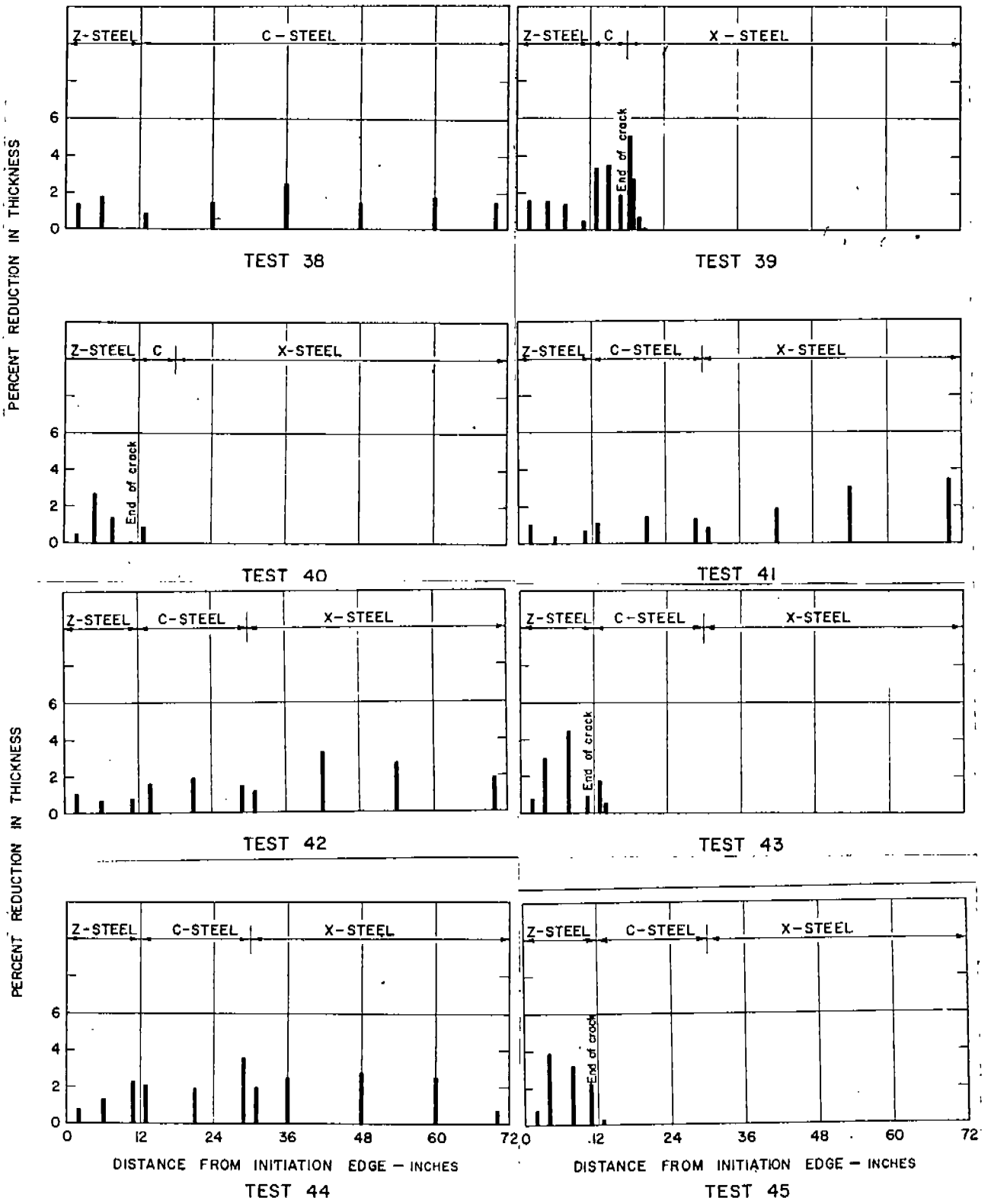

Fig. 59. Reduction in Plate Thickness along the Crack Path--Tests 38, 39, 40, 41, 42, 43, 44, and 45.

The chevron markings, characteristic of brittle fractures, can be seen on the surfaces of the completely fractured specimens shown in Figs. 60 and 61.

Comparison with Various Charpy V-Notch Criteria. Service data from World War II ship plates have demonstrated that the initiation of brittle fractures in welded structures of semikilled and rimmed structural steels is possible only at temperatures where the steel develops less than 10 ft-lb energy in Charpy V-notch tests. Similarly, brittle fractures stopped in these steels at temperatures corresponding to V-notch Charpy energy levels of about 20 ft-lb.

The Naval Research Laboratory developed drop-weight tests (which provide the NDT temperature) and explosion-bulge tests (which provide FTE and FTP temperatures) that were in agreement with the National Bureau of Standards findings.[11] In addition, results from drop-weight and explosion-bulge tests for fully killed steels, high-tensile steels, quenched and tempered steels, and other types of steel have been reported and compared with Charpy V-notch test results on the same materials.[12] For fully killed ABS-Class C normalized steel, the NDT temperature was found to correlate with a Charpy V-notch impact range of 15-24 ft-lb, with a usual value of 17 ft-lb and a conservative (high end of the range) value of 20 ft-lb. The NDT reported for ABS-Class C steel from a limited number of tests was -20 F. The reported FTE and FTP temperatures were 20 and 80 F respectively.[12]

All of the ABS-Class C normalized steel used in this series of tests was taken from three different plates of the same heat. The absorbed energies from tests of Charpy V-notch impact specimens from each plate (plates 12-1, 12-2, and 12-3) have been reported in Fig. 9. These energies, together with the accompanying shear and lateral expansion, are summarized in Table 6 (Charpy specimen axis is parallel to the direction of rolling of the plate and the V-notch axis is normal to the plate surface). In addition, drop-weight specimens from each of these plates, taken from the parent plate as shown in Fig. 62, were tested by the U. S. Steel Corporation and NDT's of -20, -30, and -20 F were obtained for plates 12-1, 12-2, 12-3 respectively. These results are in good agreement with the previously

TABLE 6

SUMMARY OF DATA FOR TESTS OF CHARPY SPECIMENS
TAKEN FROM PLATES 12-1, 12-2 AND 12-3

Temp. °F	Absorbed Energy, ft-lb			Percent of Fracture Surface in Shear			Lateral Expansion, Mils		
	12-1	12-2	12-3	12-1	12-2	12-3	12-1	12-2	12-3
160		92			100			85	
		90			100			85	
		94			100			83	
120		83	88		100	100		81	72
		86	92		100	100		82	78
		92			100			79	
100			96			100			77
			92			100			77
80			74			100			73
			78			83			66
78	88			100			78		
77		83			99			79	
		82			97			80	
		87			92			77	
72			92			83			68
			84			86			69
60			86			87			69
			70			80			63
			96			84			71
50			64			66			58
			58			62			56
			68			70			65
40	62	62	68	67	63	71	59	59	57
	64	62	64	70	58	61	58	56	57
	60	82	74	65	72	64	51	64	60
30			70			62			58
			68			61			58
			58			61			53
20	45	54	52	47	51	50	43	46	48
	--	61	48	57	51	50	50	51	44
	54	56	58	55	48	54	51	48	51
	60	59		59	57		56	50	
		69			67			63	
		67			57			53	
10			41			50			41
			45			44			43
			42			44			40
0	42	45	55	37	44	45	39	39	49
	38	52	46	40	44	43	38	43	42
	35	55	42	42	46	37	36	45	38
		68			50			53	
		60			46			47	
-10			45			36			39
			44			34			38
-20	40	42	28	30	33	31	38	34	29
	23	43	32	26	28	30	24	35	28
	22	43		27	35		24	35	
-30	24			20			25		
	20			22			22		
	32			28			32		
-40	21	27	18	17	18	19	20	21	17
	19	35	23	18	26	21	19	28	23
	16	26	24	17	24	25	16	20	22
-60	15	29	10	16	15	12	15	21	8
	16	22	22	13	14	16	16	15	20
	16	22		13	13		16	16	
	19			14			18		
-80	11	17	10	7	10	7	9	10	6
	11	12	9	9	6	8	10	9	6
		15			8			8	
-100		14	8		4	4		5	5
		14	9		5	5		6	5
		15			5			6	
-108	9			7			5		
	7			4			4		

Test 24

Test 25

Test 27

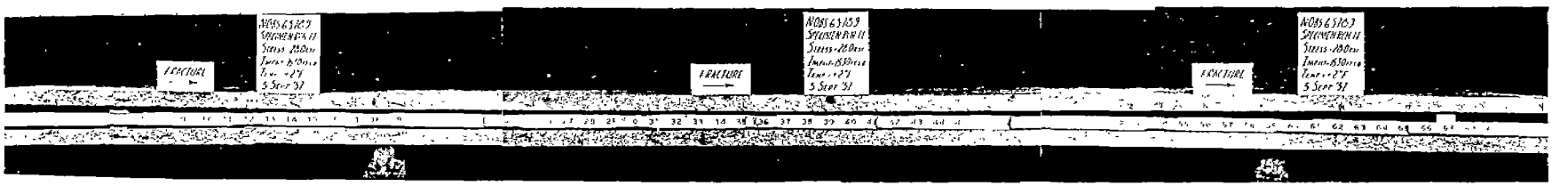

Test 34

Fig. 60. Crack Textures of Completely Fractured Specimens--Tests 24, 25, 27, and 34.

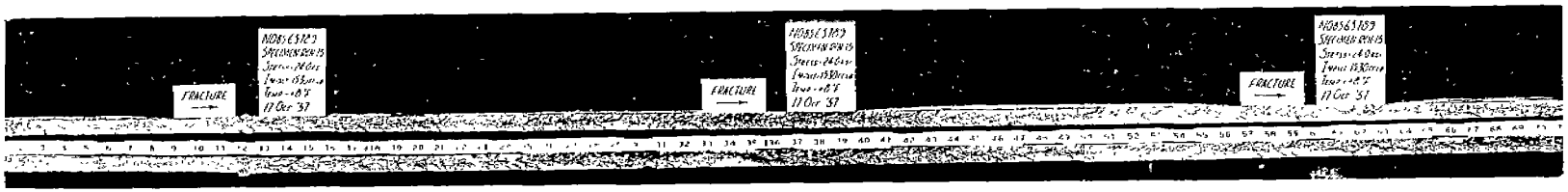

Test 38

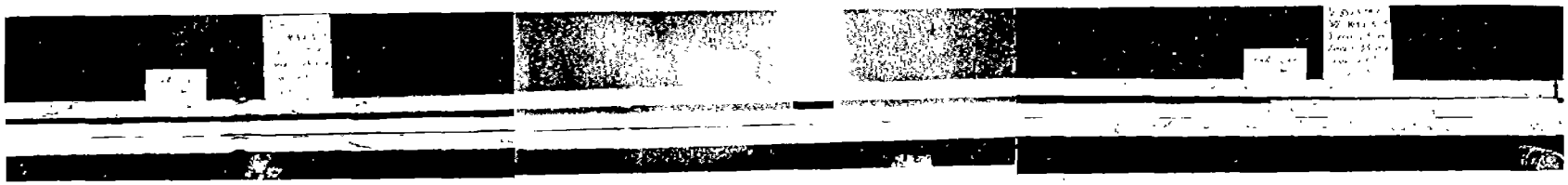

Test 41

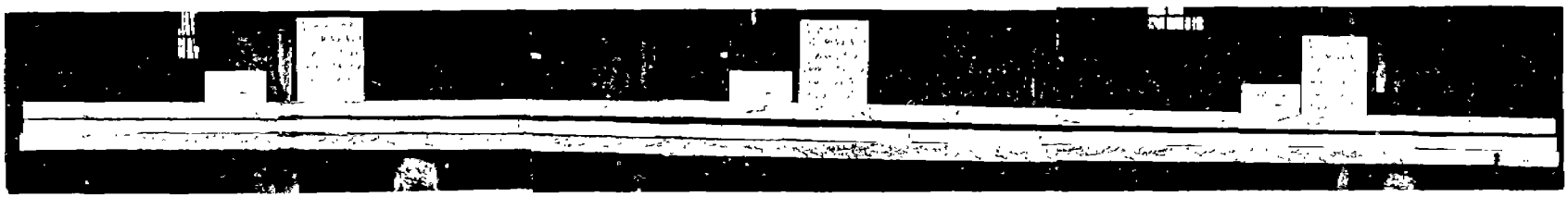

Test 42

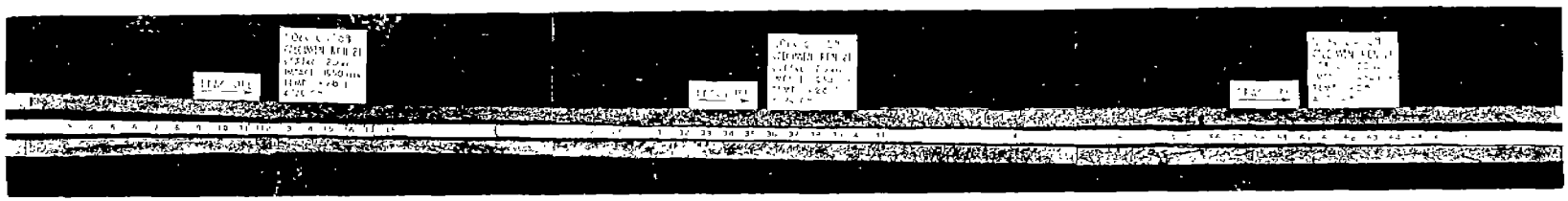

Test 44

Fig. 61. Crack Textures of Completely Fractured Specimens--Tests 38, 41, 42, and 44.

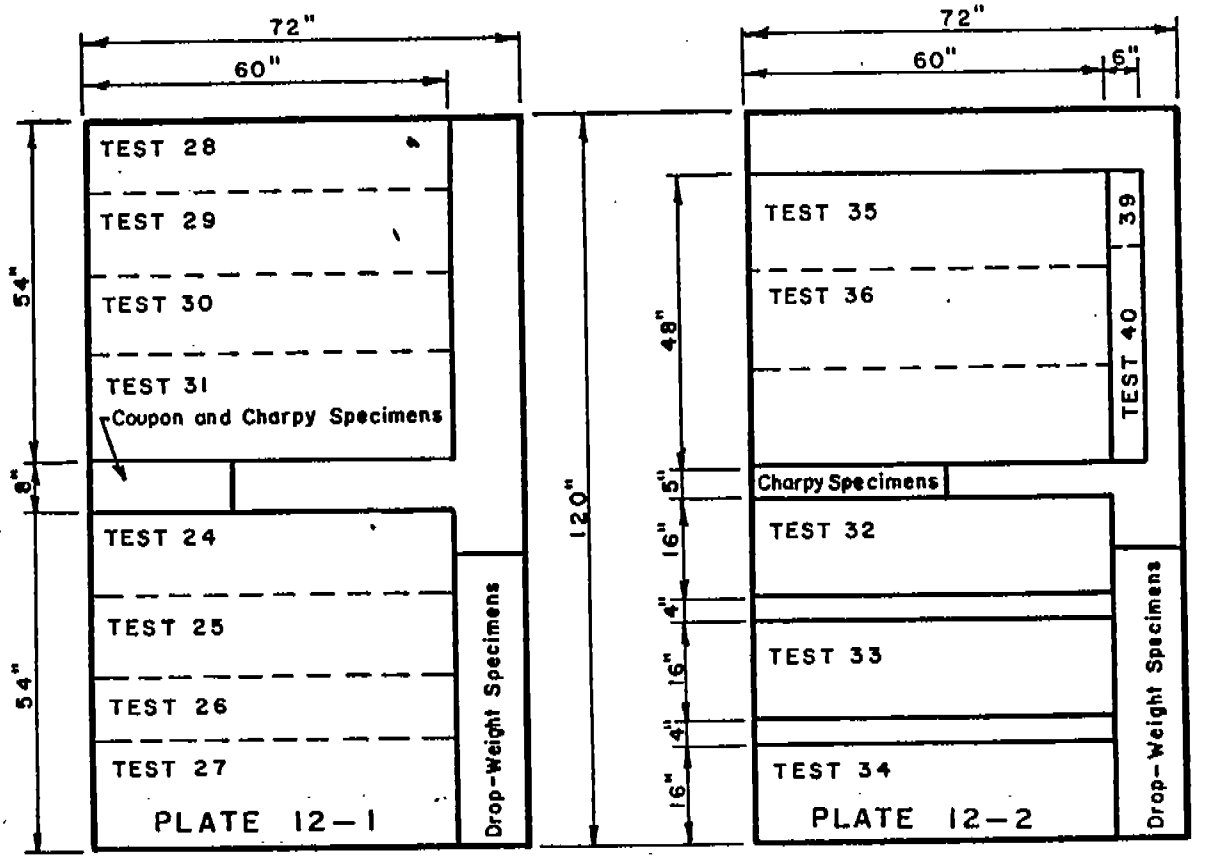

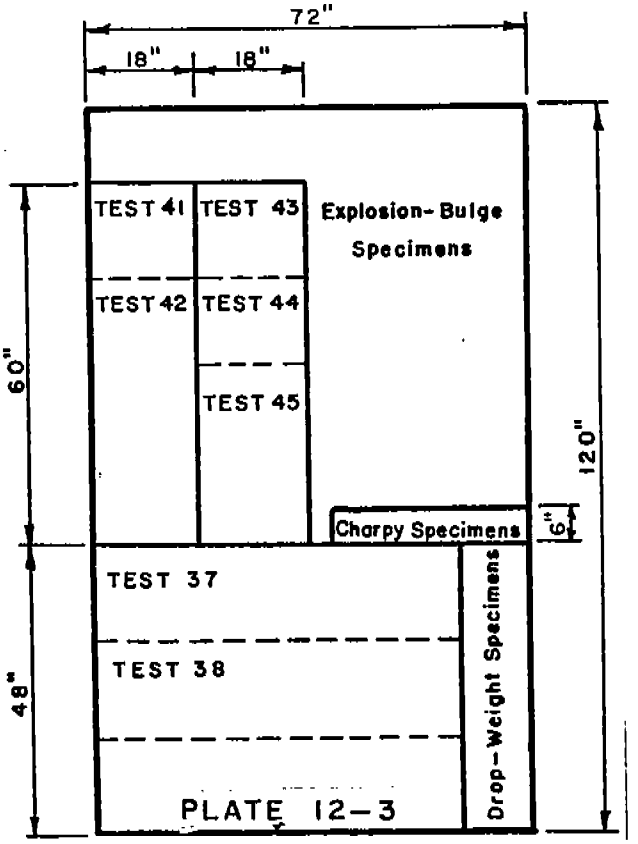

Fig. 62. Cutting Diagram for Various Plates of ABS Class-C Steel.

mentioned NDT of -20 F reported by Puzak for ABS Class-C normalized steel.

The NDT temperatures, together with the Charpy V-notch impact test results, have been plotted in Fig. 63 for each of the three plates of C-steel. It is evident that the NDT for each of these plates corresponds to an energy level of 30-35 ft-lb and thus does not agree with the suggestion that the temperature at the 20 ft-lb Charpy V-notch level gives a conservative value of NDT.

Also shown on Fig. 63 are the FTE range (estimated 30-60 F higher than NDT) and the FTP range (estimated 80-120 F higher than NDT). In addition, explosion-bulge specimens from plate 12-3 were tested by the Naval Research Laboratory, and, as indicated by the results (Fig. 64), an FTE of 25 F was determined for this plate. It is evident that this actual value of FTE falls in the middle of the estimated FTE range.

In Fig. 63, the crack arrestor test results have been plotted according to the plate from which the strake of arrestor material came. It is evident that in each case the transition in behavior observed in the crack arrestor tests occurred within the previously estimated FTE temperature range (determined by adding 30-60 F to the NDT). However, in relation to Charpy V-notch energy level, this transition occurs at about 45 ft-lb in plate 12-1, 55 ft-lb in plate 12-2, and 65 ft-lb in plate 12-3. These data indicate that the transition in behavior for C-steel when used in these crack arrestor specimens does not relate to a closely fixed value of absorbed energy in the Charpy V-notch impact test.

Another suggested index for anticipating the arresting ability of a material is the per cent shear surface exhibited by the broken Charpy V-notch specimens. To investigate this variable, the per cent shear surface of the Charpy V-notch specimens from plates 12-1, 12-2, and 12-3 was obtained with a planimeter accurate to 0.01 sq in. from 3 by 5-in. photographs of the fractured surfaces. The total surface area and the brittle surface area were measured twice on each half of the specimen and the average per cent

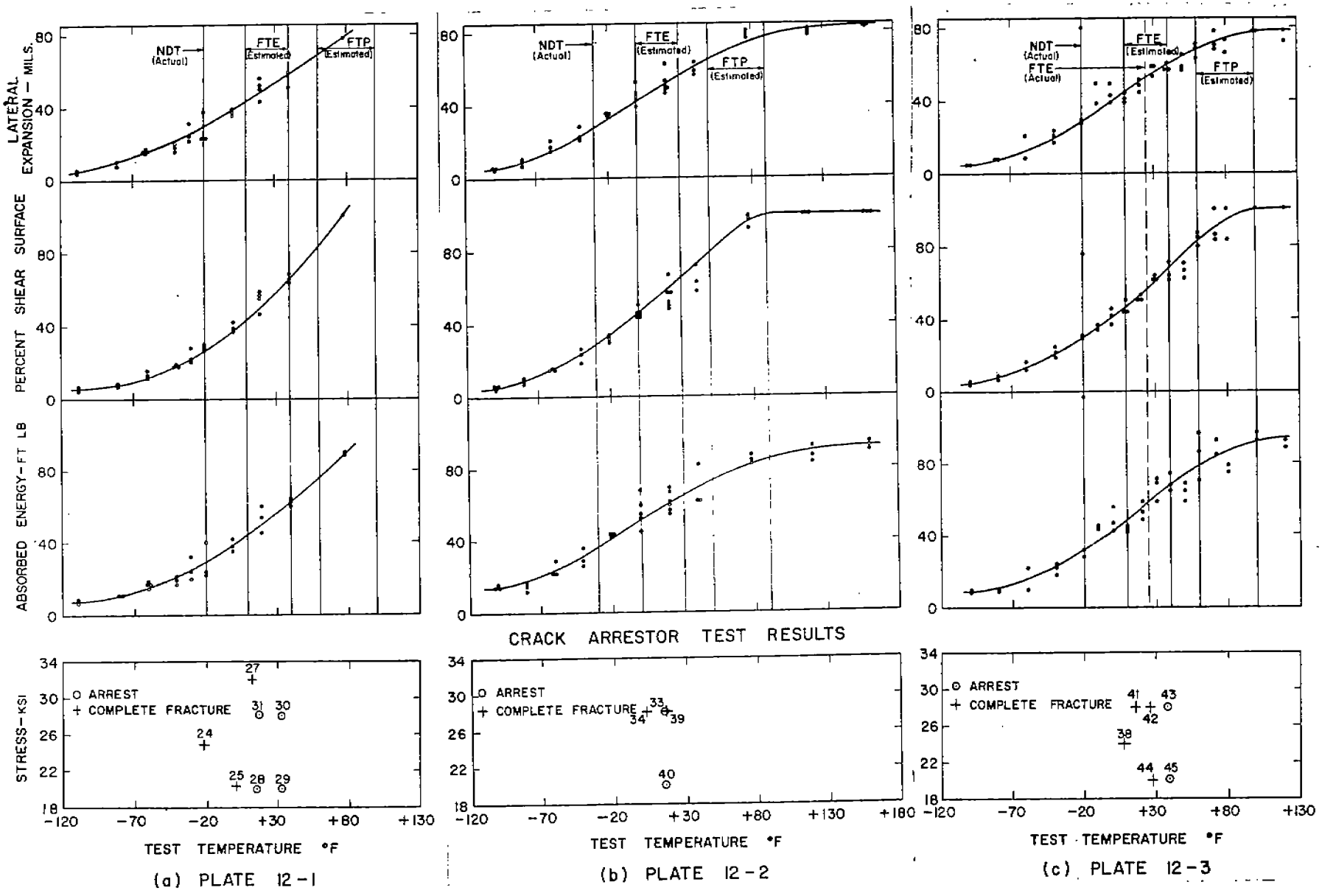

Fig. 63. Charpy V-Notch Criteria and Crack Arrestor Test Results for ABS-Class C Normalized Steel.

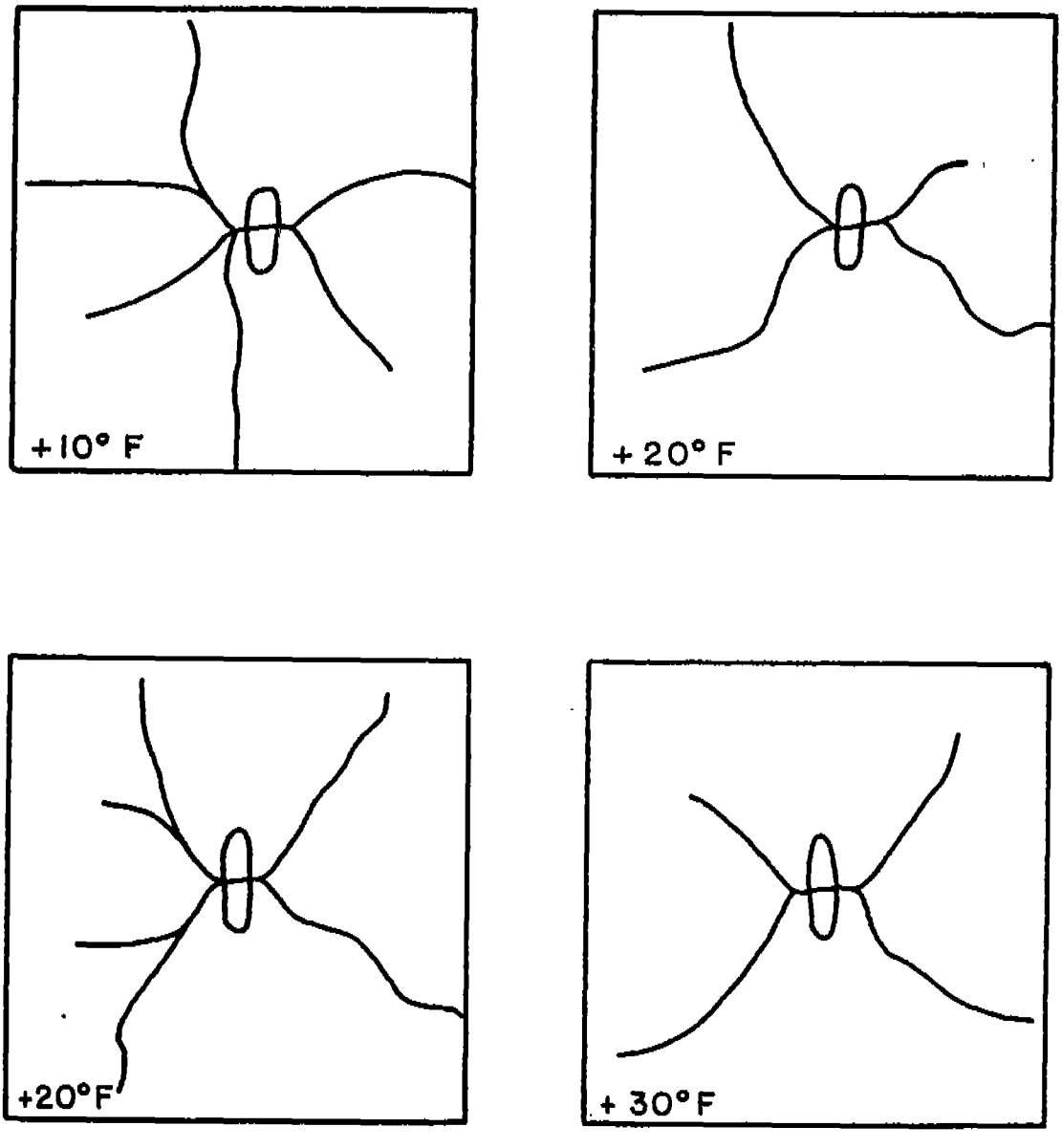

Fig. 64. Explosion Bulge Test Results Obtained by NRL for Plate 12-3 of ABS Class-C Steel.

shear surface was computed from these measurements.* The per cent shear surface has been plotted in Fig. 63. The values of the per cent shear surface that occur at the temperature at which the crack arrestor tests exhibit a transition are approximately 45, 55, and 65 per cent for plates 12-1, 12-2, and 12-3, respectively. It would seem that a particular value of per cent shear would not have predicted the behavior of all specimens tested in this series.

Recently, a comparison was made of the performance of carbon structural steel in welded ships and the lateral expansion of a Charpy specimen, measured on the compression side of the bar directly opposite the notch.[13] The indications from this study are that the temperature at which V-notch Charpy specimens exhibit a 10-mil lateral expansion corresponds closely with the NDT from drop-weight tests and the "source" plate behavior in the NBS ship-plate-fracture correlation (for rimmed and semikilled steels). This study also indicated that a lateral expansion of 15 mils may correlate well with the corresponding energy levels that have been proposed as being significant for killed and low-alloy steels.

The lateral expansion on the compression side of the Charpy V-notch specimens for C-steel was measured with a micrometer accurate to 0.001 in. These data have been plotted on Fig. 63, together with the other Charpy V-notch criteria and the crack-arrestor test results. It can be seen that a lateral expansion of about 30 mils in the Charpy bar was measured at the actual NDT for this fully killed and normalized steel. Furthermore, based on the temperature at which a transition in the crack-arrestor test results occurs, the accompanying lateral expansion in the Charpy bar varies from approximately 45 to 60 mils--substantially more than would be expected by

---

*The method described above to obtain per cent shear from Charpy specimens is related to the deformed cross-sectional area and is similar to the method used by the National Bureau of Standards. Lloyd's Method of determining per cent shear, however, is related to the original cross-sectional area. A check was made on the Charpy specimens in the 50-per cent shear range, and it was found that the use of Lloyd's Method has only a slight effect on the curve.

the proponents of this criterion.

SUMMARY

On the basis of the test results for the specimen geometry selected and the laboratory conditions available, the following observations are made:

1. An E12015 butt weld alone (not followed by a strake of tough material) did not arrest a brittle crack that had propagated 12 in. across a 24-in. wide (Test 3) or 72-in. wide (Test 7) specimen.

2. The brittle-fracture surface in rimmed (E or Z), semikilled (X) or fully killed and normalized (C) steel was always on a plane perpendicular to the plate. However, for a crack that had propagated across or into a strake of tough steel (T), the fracture surface was always on a 45° plane in the tough material.

3. Strain magnitudes of from two to three times the yield strain have been measured on the plate surface in the vicinity of the tip of the propagating crack. However, very little permanent set occurred when these high strains were developed rapidly and existed for an extremely short period of time.

4. During brittle-fracture propagation, little change occurred in the strain level across the uncracked portion of the plate that is beyond the influence of the crack front. This influence appears to precede the propagating crack front by approximately 6 in.

5. From the tests of specimens containing a strake of tough steel (T), it appears that a propagating brittle crack is initially arrested or slowed down in the butt weld joining the starter and arrestor material. Subsequent progress of the crack and the extent of penetration in the T-steel depend primarily on the severity of the resulting eccentric load and the width of the arrestor material. For crack lengths of 24 in. or less, the resulting eccentric load does not create, in the region at the end of the crack, a strain increment sufficient to advance the fracture beyond the initial point of arrest. For crack lengths of 36 in. or greater, the resulting eccentric load creates severe bending (with

corresponding buckling at the far edge) and sufficiently high strain in the region at the end of the crack to extend the crack. Then the ability of the remaining section to absorb high strain depends upon the width and strength of the tough steel available.

6. The speed of the brittle crack appeared to reach an approximately constant value within the first 6 in. of propagation. The average speeds, measured over the distance between widely spaced detectors, were fairly uniform and, for the most part, fell within the 2800 to 3800 fps range.

7. Tests of 6-ft wide specimens containing a riveted arrestor indicated that this is an excellent form of arrestor because of the discontinuity produced by the slot in the main plate. Also, it has been shown that the accompanying rivet holes in this type of specimen do not necessarily attract propagating cracks. If there is no slot beneath the doubler plate, however, it is possible for a brittle crack to pass midway between the horizontal rows of rivets and propagate completely across the main plate of a riveted arrestor specimen.

8. In the tests of specimens containing C-steel as an arrestor material, the brittle crack (which had propagated 12 in.) was either entirely accepted or completely refused by the strakes of C-steel. Apparently, the arresting ability of this steel is not greatly affected by the average applied stress but is quite strongly influenced by the temperature of the material.

9. A transition in behavior from complete fracture to complete arrest occurred between 10 and 35 F in specimens containing 6-, 18-, and 60-in. wide strakes of C-steel. When these data were compared with results from drop-weight and explosion-bulge tests, it was evident that the transition in each case occurred within the estimated FTE temperature range.

10. The results from the tests of crack arrestor specimens containing C-steel were also compared with the values of various criteria that might be obtained from tests of Charpy V-notch specimens. At the transition temperature obtained in the Crack Arrestor Tests, the corresponding values of various Charpy V-notch ciriteria ranged from 45 to 65 ft-lb absorbed energy,

45 to 65 per cent shear, and 45 to 60 mils lateral expansion. The values of these criteria that correspond to the transition in behavior of the arrestor specimens are more than would have heretofore been expected for a fully killed and normalized steel.

REFERENCES

1. Acker, H. G., Review of Welded Ship Failures (Ship Structure Committee Report Serial No. SSC-63), Washington: National Academy of Sciences-National Research Council, December 15, 1953.

2. Minutes of Ship Structure Subcommittee Meeting, February 25, 1953.

3. Wilson, W. M., Hechtman, R. A., and Bruckner, W. H., Cleavage Fractures of Ship Plates (Engineering Experiment Station Bulletin Series No. 388), Urbana: University of Illinois, 1951.

4. Feely, F. J., Jr., Northup, M. S., Kleppe, S. R., and Gensamer, M., "Studies on the Brittle Failure of Tankage Steel Plates," The Welding Journal, 34:12, Research Supplement, 596s-607s (1955).

5. Orowan, Egon, "Fundamentals of Brittle Behavior of Metals" (Paper No. 7), pp. 139-167 in Murray, William MacGregor, ed., Fatigue and Fracture of Metals. New York: John Wiley and Sons, Inc., 1952.

6. Irwin, G. R., "Fracturing and Fracture Dynamics," Transactions of the American Society for Metals, Vol. 40 A, p. 147, 1948.

7. Wells, A. A., The Brittle Fracture Strength of Welded Steel Plates (Paper No. 6), The Institution of Naval Architects, presented at March 22, 1956 meeting.

8. Robertson, T. S., "Propagation of Brittle Fracture in Steel," Journal of the Iron and Steel Institute, vol. 175, pp. 361-374, 1953.

9. Hunter, J., "The Arrest of Brittle Cracks in Ship Plate," The Australasian Engineer, pp. 52-58, February 7, 1957.

10. Wells, A. A., Lane, P. H. R., and Coates, G., "Experiments on the Arrest of Brittle Cracks in 36-In. Wide Steel Plates," British Welding Journal, vol. 3, pp. 554-570 (December 1956).

11. Puzak, P. P., Schuster, M. E., and Pellini, W. S., "Applicability of Charpy Test Data," The Welding Journal, 33:9, Research Supplement, 433s-441s (1954).

12. Puzak, P. P., and Pellini, W. S., "Evaluation of the Significance of Charpy Tests for Quenched and Tempered Steels," The Welding Journal, 35:6, Research Supplement, 275s-290s (1956).

13. Gross, J. H., and Stout, R. D., "Ductility and Energy Relations in Charpy Tests of Structural Steels," The Welding Journal, 37:4, Research Supplement, 151s-155s (1958).

14. Hall, W. J., Godden, W. G., and Fettahlioglu, O. A., Preliminary Studies of Brittle Fracture Propagation in Structural Steel (Ship Structure Committee Report Serial No. SSC-111), Washington: National Academy of Sciences-National Research Council, May 15, 1958. (Basically the same report appeared in the Civil Engineering Studies, Structural Research Series No. 123, published by the University of Illinois (Urbana) in June 1957.)

15. Hall, W. J., Mosborg, R. J., and McDonald, V. J., "Brittle Fracture Propagation in Wide Steel Plates," The Welding Journal, 36:1, Research Supplement, 1s-8s (1957).

16. Lazar, R., and Hall, W. J., Studies of Brittle Fracture Propagation in Six-Foot Wide Structural Steel Plates (Ship Structure Committee Report Serial No. SSC-112), Washington: National Academy of Sciences-National Research Council, September 17, 1959. (Basically the same report appeared in the Civil Engineering Studies, Structural Research Series No. 136, published by the University of Illinois (Urbana) in June 1957.)

17. Mosborg, R. J., Hall, W. J., and Munse, W. H., "Arrest of Brittle Fractures in Wide Steel Plates," The Welding Journal, 36:9, Research Supplement, 393s-400s (1957).

18. Bruckner, W. H., and Robertson, C. A., "Energy Absorption Studies of Welds in Tempered Martensitic Base Metal," The Welding Journal, 37:3, Research Supplement, 97s-100s (1958).

19. Hayashi, K., Preliminary Studies of Welded Crack Arrestors in Structural Steel (M. S. Thesis submitted to the University of Illinois), February 1956.

20. Hall, T. J., Preliminary Investigation of Crack Arrestors in 6-Ft Wide Steel Plates (M. S. Thesis submitted to the University of Illinois), June 1956.

21. Chopy, J. N., An Investigation of the Behavior of Welded T-1 Steel Crack Arrestors in 6-Ft Wide Steel Plates (M. S. Thesis submitted to the University of Illinois), August 1957.

22. Kirk, J. N., An Investigation of the Behavior of Welded ABS-Class C Normalized Steel Crack Arrestors (M. S. Thesis submitted to the University of Illinois), February 1958.

SHIP STRUCTURE SUBCOMMITTEE

Chairman:

J. J. Stilwell, Capt., USN
Head, Hull Design Division
Bureau of Ships

Secretary:

John D. Crowley, LCdr., USCG
Office of the Engineer-in-Chief
U. S. Coast Guard

Members:

E. C. Vicars, Cdr., USN
Head, Metals Fabrication Branch
Bureau of Ships

John Vasta
Chief, Hull Scientific Section
Bureau of Ships

R. D. Karl, Cdr., USN
Director of the Engineering Division
Maintenance and Repair, M.S.T.S.

Hubert Kempel
Head, Technical Branch
Military Sea Transportation Service

J. B. Robertson, Jr.
Deputy Technical Assistant to Chief
Merchant Marine Technical Division, USCG

V. L. Russo
Deputy Chief, Office of Ship Construction
Maritime Administration

W. G. Frederick
Naval Architect (Structural)
Maritime Administration

D. B. Bannerman, Jr.
Chief Surveyor - Hull
American Bureau of Shipping

G. W. Place
Principal Surveyor, Metallurgy - Research
American Bureau of Shipping

J. J. Harwood
Head, Metallurgical Branch
Office of Naval Research